ENEA

ITALIAN NATIONAL AGENCY FOR NEW TECHNOLOGIES,
ENERGY AND SUSTAINABLE ECONOMIC DEVELOPMENT

2011 ACTIVITY REPORT

Unità Tecnica di sviluppo di Applicazioni delle Radiazioni

utaprad

2011 ACTIVITY REPORT

This report was prepared by the Scientific Pubblications and External Relations Office by the scientific and technical staff of ENEA's Technical Unit Development and Applications of Radiation - UTAPRAD

DESIGN AND COMPOSITION

Ilaria Sergi

SCIENTIFIC EDITORS

Antonio Palucci
Rosa Maria Montereali
Giuseppe Dattoli
Gian Piero Gallerano

www.frascati.enea.it/utaprad

Published by:

ENEA
Communications Office
Technical Unit Development
and Applications of Radiation
Research Center

ENEA Frascati
C.P. 65
00044 Frascati, Rome Italy

Phone +39 (06) 94005116
Fax + 39 (06) 94005334
Email **ilaria.sergi@enea.it**

CONTENTS

PREFACE

The second birthday of UTAPRAD is now approaching, so this Report is the first one entirely containing results achieved within the new structure according to the given mission harmonized with the ENEA Agency finalities: to develop applications of radiations in different fields, ranging from environmental protection and sustainable development, to citizen security, safety and health, and finally to assist energy production, store and saving.

It is with an understandable pride that I am presenting here results obtained entirely under my direction. The usual high level of scientific achievements in this case is coupled to a successful effort to match our mission beside the specific project tasks. One year after their foundation new laboratories show significant integration and a balanced mixture among development of new competences and applications, the latter finalized within project activities which ensure the needed funds.

To this respect I wish to mention, beside the outstanding scientific achievements listed in the appendix, that new technology achievements are more and more mature and the respective patents are going to be requested this year.

In 2011 results dissemination and exploitation has been specially considered, in order to support an efficient technology transfer towards national and European industries (with particular care towards SME and micro-SME). Relationships with Italian (in Rome area), European (Spanish) and Mediterranean (Egyptian) universities have been consolidated in order to be best ready to answer new call fro proposals.

Attention has been paid to formation with qualified teaching at university and master courses, and specialized seminars at doctorate courses. Several students graduated at 3 and 5 years university courses, being hosted by our laboratories, where stages have been offered also to foreigner students.

Major results obtained in 2011 are presented in the following, in a such a way to offer a significant overview also to a non specialist reader. Scientifical and technical details can be find in the list of relevant papers reported in the Appendix as major research products.

dr. Roberta Fantoni
UTAPRAD Director

1 DIAGNOSTICS AND METROLOGY LABORATORY

1.1. Mission and infrastructures

The Diagnostics and Laser Metrology Laboratory includes a set of skills available to support various research activities that mainly turn in the support for the development of laser sensors in different application fields of environmental monitoring, safety and health protection of citizens, diagnostics of cultural heritage and energy. The Laboratory, in keeping with its mission, carries on support activities necessary to calibrate, complement and extend the validity of field data during dedicated measurement campaigns.

Specific tasks relevant to the Laboratory concern the development of spectroscopic and optic systems for in-situ or remote sensing and metrological applications, with relevant compact and miniaturized sensors; the development of imaging sensors for in-situ applications in different fields of interest with respective data analysis, images release, and data merging. The competences available at UTAPRAD-DIM are originated from the expertise in different scientific disciplines as laser spectroscopy, optics, active and passive sensors, terrestrial and marine biology, analytical chemistry, biology and data analysis. This know-how is fruitfully devoted to the development of sensors for scientific and industrial applications.

Current main topics deal with:

- development, realization, test and field demonstration of local and remote sensors for Security;
- development and laboratory utilization of methodologies for citizen Safety (food and health);
- development and field utilization of monitoring systems for environmental protection, also related with Climate Changes;
- development and field utilization of innovative diagnostics for Cultural Heritage preservation and fruition;
- development and in situ utilization of industrial diagnostics in hostile environment (e.g. reactors for nuclear fusion).

Available infrastructures include well equipped laboratories and advanced instrumentation with patented prototypes, suitable also to field operation:

- metrology laboratory with 3D laser scanners also for underwater operation:
- active and passive remote sensing laboratory, with facilities for atmospheric and water monitoring and for satellite data processing. A mobile platform (ENVILAB) is available for field campaigns;
- laser spectroscopy laboratory with different analytical facilities (LIF, LIBS, IR spectroscopy, Laser flow cytometer);

- environmental chemistry, bio-electromagnetism and biology laboratories.

Funding and projects

In 2011 the research activities of UTAPRAD-DIM Laboratory were mainly funded within the EC Framework Programmes FP7 Security as coordinator of BONAS project, partner of CUSTOM project, coordinator of the RADEX project (in the frame of the NATO Science for Peace special project STANDEX, and member of the network of excellence NDE).

At national level, the Laboratory participates to MIUR PON projects: BLUARCHEOSYS, IT@CHA and TRAMP, and to MISE Industria 2015 projects, SAL@CQO and MUSS.

The UTAPRAD DIM laboratory has strengthened its commitment for a constructive networking with Large Industries and SMEs both at national and European level. Some personnel are members of European lobby activities as in IMG-S (Industrial and Research Stakeholders Group for Security) or at national level in the Italian technological platform for Security (SERIT) and Photonics. These actions aim at ensuring an high level of cross-fertilization to fully exploit the possibilities arising from European and national funding schemes, as well as to open market channels for the Laboratory scientific achievements.

1.2. Diagnostics for security

Detection of explosives, their precursors and different hazardous substances

The commitment of the Laboratory for the issues of security is strongly continued and has further strengthened, where three current capability projects (CUSTOM, BONAS and RADEX) are starting to see the realization of the first prototypes out of the prior design activity achievements, and a network (NDE) is supporting the EC DG Home Affairs.

The objective of the EC FP7 Security project Drugs And Precursors Sensing By Complementing Low Cost Multiple Techniques (CUSTOM), now entered in its second year of activity, is to develop a portable device capable of detecting traces of precursor chemicals used in the manufacture of the most dangerous drugs on the international market. Selex S.I. is the coordinator. The concept of the sensor is based on a air sampler, feeding two analytical sensor respectively based on Laser Photoacoustic and LED Induced Fluorescence technique. Ultimate sensitivity is reached by additional use of a molecular preconcentrator capable to enrich up 1000 times the drugs concentration in the sampled air flow. Raw signals from analytical sensors are captured

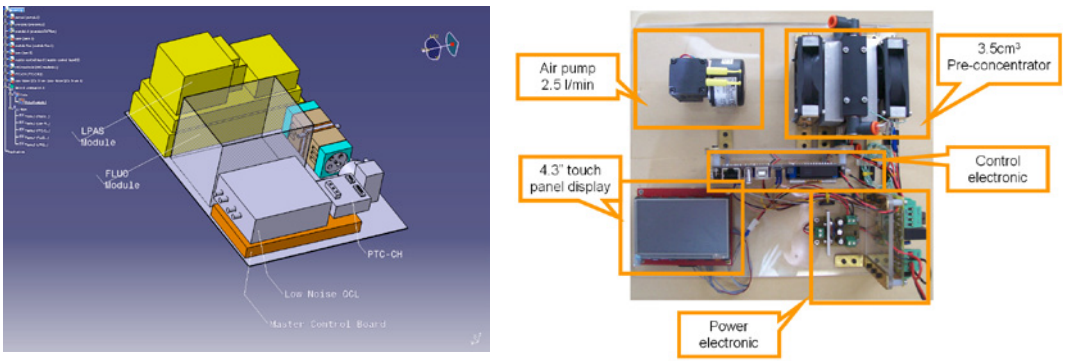

Figure 1 – CUSTOM project: the whole apparatus design (left); the molecular preconcentrator board prototype (right).

by the data acquisition electronics in the control board. Real time signal processing algorithms elaborate the raw signals and compare them to the library data in order to define probability of presence or absence of the considered drug precursors.

ENEA is in charge to design and realize the container for the whole set-up that includes the two instruments, the sampler and the control board (Figure 1 left). The electronic front end of a master board controlling the sensor has been designed according to a proprietary approach in order to guarantee the noise transient suppression of the input signals also in presence of high inductive load (pumping unit) the voltage levels could occasionally have large voltage overshoot/undershoot potentially dangerous for low power devices. Noise reduction on analog signals is then obtained by a careful design of a differential balanced preamplifier, also capable to drive a low impedance Analogue to Digital Converter (ADC).

Recent advances of particular interest successfully, are related to the development of the molecular preconcentrator; its conceptual design has been completed and a prototype has been designed and developed (Figure 1 right) as well as the determination of its optimal use as feeding unit to the analytical sensors. Theoretical considerations of the physical mechanisms involved in the processes of particles capture by the aerogel (absorption) and their successive release (desorption) modulated by temperature changes, suggest the use of large volumes, since in this case the number of capturing micro-cavities is maximized. The limitations concerning the low aerogel thermal conductivity, and its gas permeability have been carefully considered and their practical solution has resulted in a innovative design, worth to start the procedure for patent registration.

The aim of the EC FP7 Security project BONAS (BOmb factory detection by Networks of Advanced Sensors) is to design, develop and test an innovative sensor wireless network, in order to increase citizen protection and homeland security from terrorist attacks, especially against the threat posed by improvised explosive devices, or IEDs.

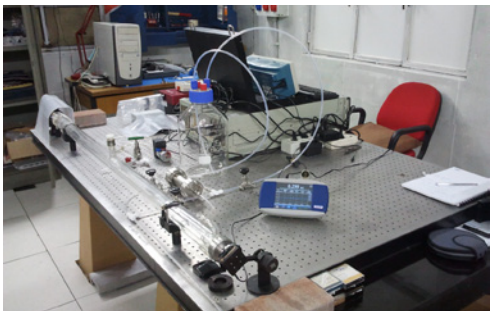

Figure 2 - Spectroscopic system for detection study of explosive precursors in the laboratory assembly.

ENEA is involved in the realization of two instruments: a lidar/DIAL remote and a SERS sensor, respectively. A new state of the art lidar/DIAL is currently under development with the main goal to discovery bomb factories by the detection of gaseous precursors. Core of the system is a OPO laser (Optical Parameter Oscillator) that allows to perform high resolution spectroscopic measurements with high power emission for single line emission. The system has been developed and currently testing in our laboratory (Figure 2).

As second task, ENEA is in charge to support the development of a compact SERS equipment to be realized by the Sersetech company, partner of BONAS project. In particular, we are testing different substrates in order to evaluate their respective amplification factor. The identification of explosive molecules at very low concentrations in different environments is a problem of critical interest for security and forensic diagnostics. To this respect, Raman spectroscopy, due to its inherent ability to distinguish between molecules with great similarity, gained a growing interest. However, due to the intrinsic weakness of Raman scattering (approximately 1 scattered photon for 108 incident photons), the Raman spectroscopy can be used to trace level detection only if coupled to the surface enhancement effect.

The Raman spectra were acquired with an integrated Raman system (BWTEK inc., i-Raman), in the wavelength range 789-1048 nm corresponding to Raman shifts of 75-3200 cm-1 (resolution 3 cm-1). The excitation source was a solid state laser with 785 nm light and a power scalable in the range 30 -180 mW. The near-IR excitation eliminates most of sample fluorescence. The Raman system is equipped with a micropositioning system for fine xyz adjustments and a video camera for sampling viewing. Depending on the

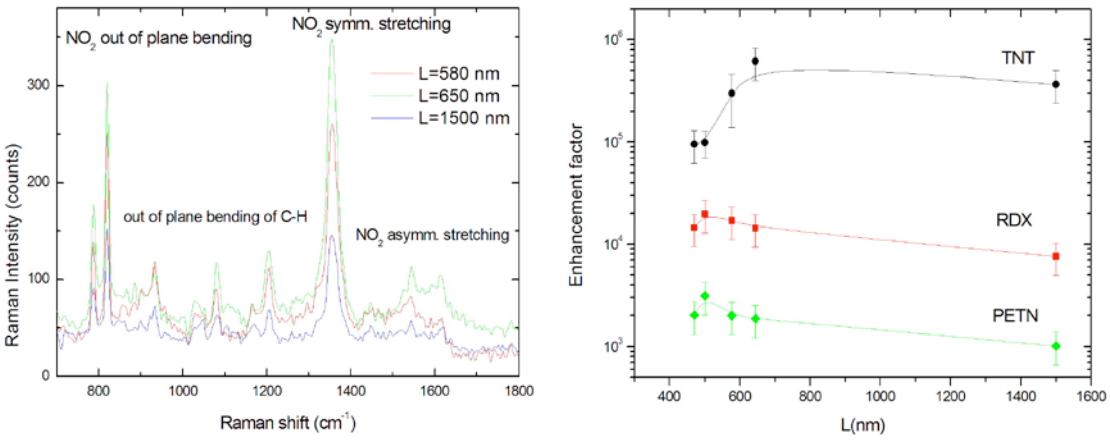

Figure 3 - Surface enhanced Raman effect: left) spectra of TNT adsorbed on pits with different aperture size (L); right) enhancement factors of SERS active substrates with different aperture size of pyramidal voids

mounted microscope objectives, the laser has a diameter of 80 µm or 50 µm.

We analysed the explosive molecules as evaporated films on the SERS substrate. Evaporated films were prepared by dropping a controlled volume of commercially available standard solution of explosive molecules, on the surface.

In Figure 3 left, the Raman spectra of a drop of 0.1 µl of TNT standard solution adsorbed on substrates (Klarite, D3 Technologies Ltd) with different size of pyramidal void are reported. Depending on the substrate, the Raman peaks have different intensities, indicating a different amplification of the Raman signal.

The enhancement factors for each value of L are reported in Figure 3 right. They range from $(6\pm2)\cdot10^{6}$ for TNT to $(3\pm1)\cdot10^{3}$ for PETN. The strong differences between the enhancement factors, confirm that the chemical mechanism plays a role in the amplification of Raman signal.

The NATO Science for Peace and Security (SPS) committee provides fundings to relevant science projects to fight terrorism. Among the various SPS programs, the STANDEX (STANdoff Detection of Explosives) program has the objective of developing a system made of multiple technologies for remote detection of suicide bombers.

In the context of the STANDEX program, a new instrumentation is under development at the Diagnostics and Metrology Laboratory for the stand-off detection of explosives. The RADEX (RAman Detection of EXplosive) system is based on Raman technology to detect trace explosive on fibers with the strong commitment to be complain with the international eye safe regulations in order to avoid damages to human corneas and skin. The choice of an UV excitation laser wavelength for stand-off detection of energetic materials depends not only on the system performance evaluation, but also from eye safety considerations. Figure 4 left shows the maximum permissible exposure (MPE) at the human cornea for a collimated laser beam, as energy density versus exposure time for various wavelengths. For pulse durations from 1 ns to 1 µs the UV MPE

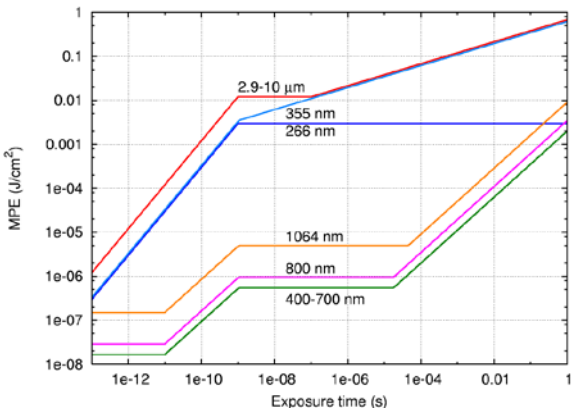

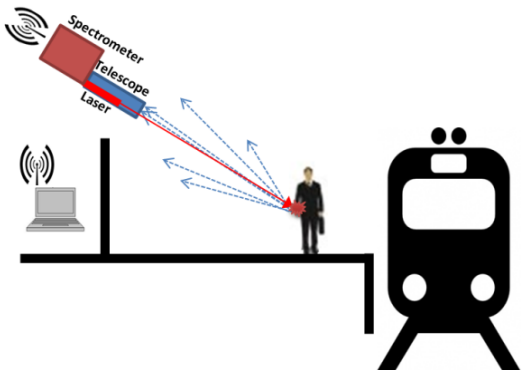

Figure 4 – The RADEX approach: Maximum permissible exposure (MPE) at the cornea for a collimated laser beam according to IEC 60825, as energy density versus exposure time for various wavelengths (left); Schematic representation of the RADEX system (right).

is about 3 orders of magnitude higher than visible or NIR MPE. The operational principle of the RADEX system is the following (Figure 4): an eye-safe laser beam is focussed on the target and the Raman scattered radiation, emitted from the laser illuminated surface, is collected by a telescope and imaged onto the entrance of a Raman spectrometer. The radiation is then analysed giving a spectrum suitable for the explosive detection and identification. Next action will be the test of the whole STANDEX concept in a real metro station.

LIBS measurements were performed on high energetic materials in collaboration with University of Malaga, which sent its PhD student for participating in the work.

An attracting application of artificial intelligence methods in Security is the development of algorithms in neural network in order to obtain an early warning and surveillance continuous process in the frame of "Sistema integrato di gestione e controllo per il TRAsporto in Sicurezza di Merci Pericolose (TRAMP)" MIUR PON Project.

The EC DG HOME AFFAIRS has renewed for the second two-year term the consulting activities of the NDE Network (Network of Explosive Detection), in support of the EC on drafting reports and preparation of the Second European Conference on Explosives to be held in Rome in March 2013. The Laboratory UTAPRAD-DIM participated with its experts and delivered the requested reports.

1.3. Diagnostics for safety

Diagnostics on food and plants

UTAPRAD-DIM holds different activities financed by different agencies and Italian institutions for Food Safety and Health issues.

The Laser Photoacoustic test facility is involved in the development of a sensor for real time detection of adulterants in food products and beverages (MISE National Project MI01_00182 - SAL@ CQO "Development of a Laser system for molecular spectroscopy measurements aimed to the preservation and the control of values concerning organolectic properties of food by means of non invasive techniques against natural or fraudulent degradation". The main aim of the project is to certify the quality of labeled 'Made-in-Italy' agro-alimentary products by means of fast non invasive optical methods based on high resolution spectroscopy.

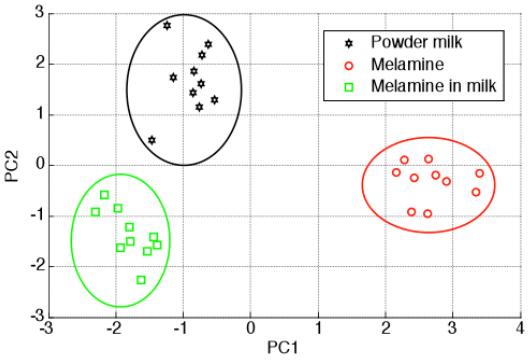

Figure 5 - 2D view of the PCA operated on powder milk (lat), melamine (mel), and milk-melamine mixture (L2-).

The laser photoacustic signal (LPA) processed by PCA (Principal Component Analysis) is shown in figure 5 for melamine, milk and the mixture of both. The presence of melamine in milk is cleary evident from PCA of the three LPAS groups of spectra.

The biology laboratory has focused the activities on the assessment of damage from the bug infesting palms (Rynchophorus ferrugineus) that has haunted the area around Rome. Several defense strategies and recovery have been studied and implemented on site in collaboration with UTAGRI-ECO.

Effects of week electromagnetic fields on cells

As part of a collaboration between ENEA and the Department of Physics, University of Rome Sapienza has been studied the influence of magnetic fields on weak solutions of amino acids contributing to the debate on the effects of electromagnetic fields (ELF) on living systems. This activity is carried on in the frame of the project InCamp (Interazione del Campo Magnetico a frequenza di ionorisonanza con enzimi e Proteine) as grant from INAIL (former Ispesl).

In particular, the FTIR vibrational spectroscopy technique has been applied on amino acid solutions in water in order to study the nature of changes induced by the ELF on biological structures and to measure its duration after removal of the perturbation. A significant change in the structure of Glutamic acid has been detected, which is reversible within about one hour after the exposure to the field. The most remarkable characteristic of this effect is the evidence of a long living state induced by the perturbation, i.e. the effect survives to the removal of the perturbation for long times compared to the characteristic relaxation times of the molecular excited states. The modification of the protonated vs deprotonated population of Glutamic acid in aqueous solution, induced by the field, lasts enough to be revealed by the IR spectroscopy in spite of the very feeble amount of the energy carried by the perturbation. This implies an high degree of correlation among a great number of molecules. The existence of a defined phase relationship among molecules can account for a coupling among molecules stronger than the coupling to the environment and explain how the energy can be transferred so efficiently. So that a new hypothesis may be suggested: the magnetic field effect is mediated by the water structure.

The effect is small even though out of the error bars, however we believe that it is useful to understand the origin of the effect of weak magnetic fields on the water solutions of amino acids and ions. The role of the magnetic field on water seems actually to be that of a “chaotrope” (disorder-maker) agent (Figure 6a and b).

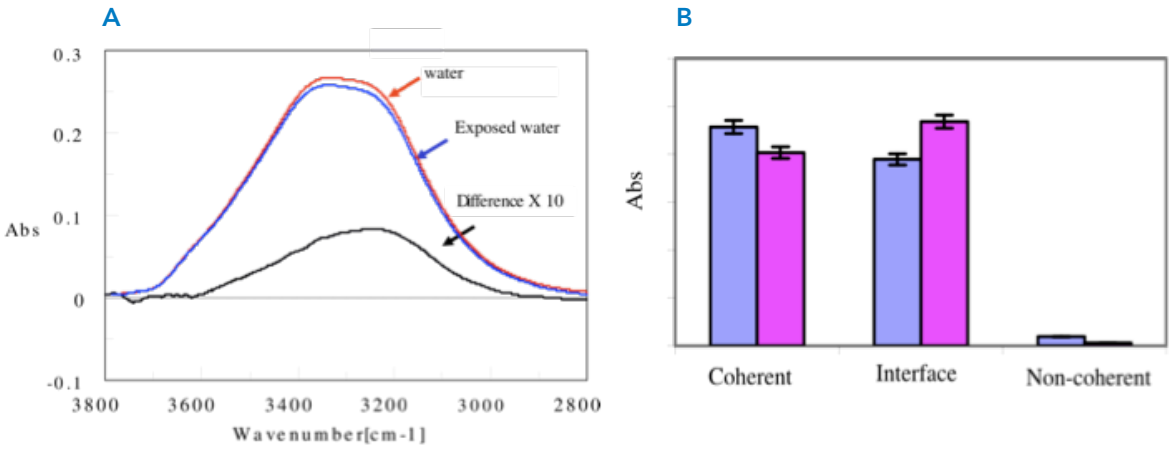

Figure 6 - IR spectra of liquid water: a) OH stretching band. Comparison between exposed and non-exposed sample. The difference is plotted with an amplification factor of 10 in order to be visible on the graph; b) comparison between different populations of water: coherent, intermediate and non-coherent. Blue bars refer to non exposed water; magenta bars to the exposed water.

Tissue engineering

Researches carried out in collaboration with other Italian and foreign institutes and universities, on the techniques for the muscle tissue reconstruction that may have important repercussions on the quality of life. An important contribution to this issue has been to understand the effect of weak magnetic fields on cell growth of the skeleton of the muscles and in particular in the understanding of the mechanisms of orientation of growth.

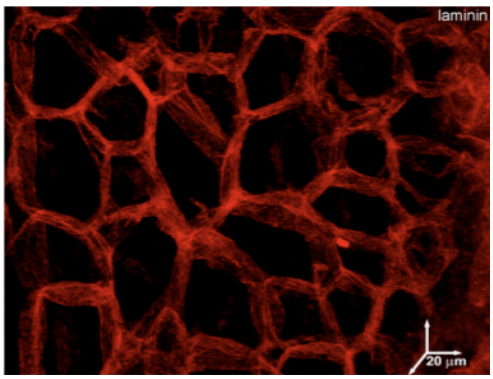

Figure 7 - Acellular skeletal muscle scaffolds maintain the 3D-architecture and can be stored. 3D image stack reconstruction of confocal microscopy images of a 20 µm thick cryosection of acellular skeletal muscle scaffold, following laminin immunodetection (red). The latter highlights the irregular, polyhedral tubular organization corresponding to that of the muscle fibers.

Regenerative medicine and engineering of musculoskeletal tissue need strategies to assist stem and precursor cell differentiation, survival and required orientation during growth. The research carried out this year has confirmed that low intensity static magnetic field (SMF) is able to affect directional growth of skeletal muscle cells. The shape acquired by the cells as result of changes in the cytoskeletal organization can influence their function.

The scaffolds produced retain their 3D architecture (Figure 7). Our studies represent the first molecular characterization of the bioactivity of scaffolds derived from decellularized muscles. Scaffold muscle reconstruction and the transplantation of these in mouse models represent a significant innovation in regenerative medicine techniques.

1.4. Environmental diagnostics

Marine diagnostics related with Climate Changes

UTAPRAD-DIM Laboratory aims to contribute to the comprehension of the climate change issue providing its own instrumentation already developed in order to collect environmental data and successively integration thereof with satellite images for a larger scenario vision.

The research activity during 2011 focused on two different but well related activities: field experiments and satellite oceanography.

Field experiment activity included the analysis of the data acquired during the TYR01 cruise in October-November 2010 and the preparation of the March 2012 experiment (WMED-BIOOPT).

The ocean remote sensing activity was mainly concentrated on study of the diurnal Sea Surface Temperature (SST) cycle in the Mediterranean including diurnal warming events and on the preparation of the algorithms for the satellite determination of the Phytoplankton Functional Types (PFT) in the Mediterranean Sea. Figure 8 shows an example of reconstruction of the SST field during a summer day with particularly intense diurnal warming at 14:00 UTC.

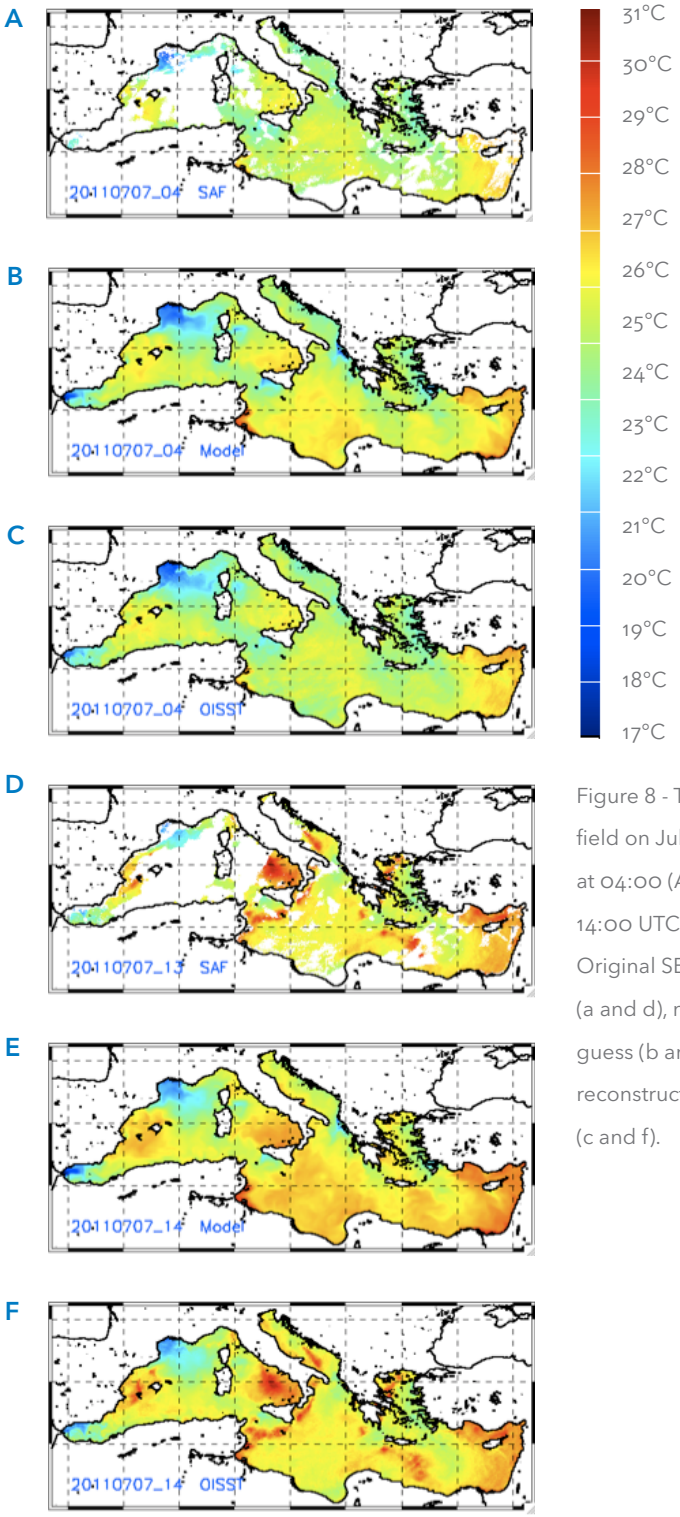

Figure 8 - The SST field on July 7TH 2011 at 04:00 (A, B, C) and 14:00 UTC (D, E, F). Original SEVIRI SST (a and d), model first-guess (b and e) and reconstructed SST field (c and f).

Ocean color activities have been conducted in preparation of PERSEUS (Policy-oriented marine Environmental Research for the Southern European Seas) project. This project started the 1ST January 2012 and will continue until the end of 2015. UTAPRAD-DIM is involved in WP 4 of PERSEUS that has the objective of evaluate the Southern European Seas environmental status with existing and upgraded remotely operated monitoring and modeling capabilities. In particular UTAPRAD-DIM will contribute to two tasks devoted to the estimate of the spatial and temporal variability of primary productivity and phytoplankton size classes.

The SST studies are conducted in the framework of the ERNESST (European Research Network for Estimation from Space of Surface Temperature) network.

The Lidar and Ocean Color research activities will also be part of the next RITMARE Project, the Italian national program for the scientific and technological research in the sea, that will very likely start in 2012. The Lidar activity for the ocean observation will also be included in the RIMA (Rete Integrata Mediterranea e Accesso a dati e prodotti) Project that has been proposed in the framework of the "Sviluppo di servizi di Accesso a Dati e Prodotti in supporto alla Gestione dell'Ambiente Marino e Costiero mediante l'utilizzo di un Sistema Previsionale".

During 2011 we also completed the work on the study of the multidecadal variability of the SST in the North Atlantic Ocean and in the Mediterranean Sea.

The activities of the two chemical and biological laboratories have been focused on data analysis of previous TR01 marine campaign, held in October-November 2010 and to the planning of WMED-BIOOPT. There was also an attempt to use the system in flow cytometry scanning CLASS, which has highlighted the difficulty of using marine samples, despite the effort placed in developing statistical algorithms for data analysis.

The phytoplankton biomass and productivity was determined by means of chlorophylls a and carotenoids concentration acquired by HPLC and absorption measurements.

The results obtained have given information about coastal dynamical processes (Figure 9) and they have been compared with High Performance Liquid Chromatographic (HPLC) analysis carried out in the Environmental Analytical Chemistry laboratory (Figure 10)

The different classes of phytoplankton were also identified by the other chlorophylls testing (chlorophyll b and chlorophyll c).

SeaTech Chorophyll estimates obtained after SPEX and HPLC calibrations where used to translate Lidar measurements

at 680 nm in terms of chlorophyll a. Due to problems in the optics of the lidar daytime measurements were perturbed by sun light reflected by the sea surface into the field of view of the instrument, then the calibration was limited to night measurements (Figure 11a).

The results of this calibration are very encouraging, establishing the existence of a linear response (in log-log terms) of the instrument to the variation of the chlorophyll (and other components) concentration. The concrete opportunity to translate Lidar acquisition into environmental variables will permit to quantify the interesting mapping capability of the Lidar system (Figure 11b).

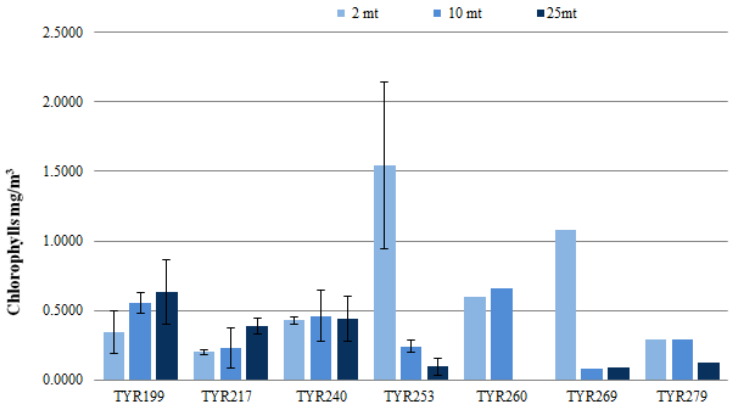

Figure 9 Chlorophyll a concentration at different station and at different depth

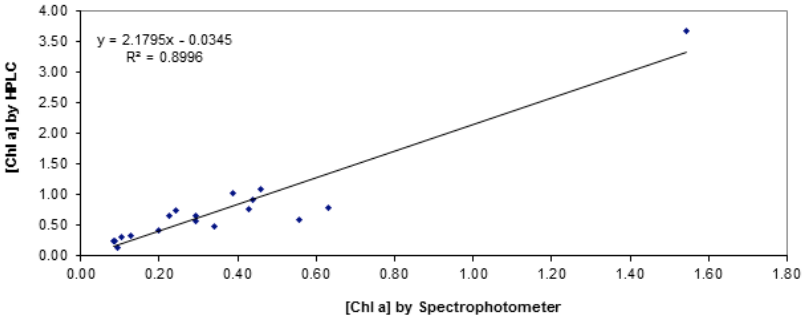

Figure 10 – Comparison of paired [Chl a] in extract from water samples analyzed by HPLC and Spectrophotometric methods

Italy-Canada bilateral cooperation on validation of bio-optical satellite data

The accurate monitoring of natural waters (aquifers, rivers, lakes, seas and oceans) is a key action for environment protection, ecosystem safeguard and life sustain.

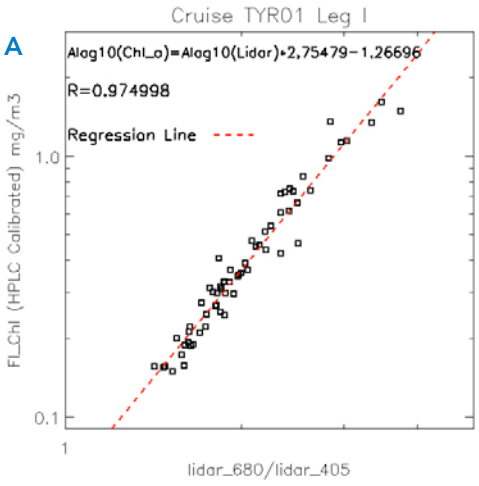

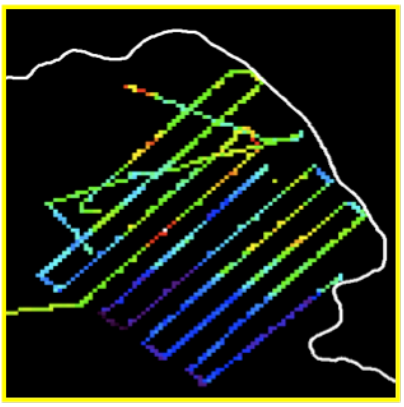

Figure 11 – Lidar data collected during the campaign: a) calibration of Lidar measurements at 680 nm in terms of chlorophyll a; b) surface map of chlorophyll concentration obtained during a night of lidar measurements in the gulf of Salerno.

Laser sensing can be very effective in significant measurements of the bio-optical parameters in natural waters. CASPER (Compact and Advanced laser SPEctrometer for Riade) has been realized for the project RIADE (Integrated research for applying new technologies and processes for combating desertification) and has been patented. It is based on double filtration (30 μm and 0.22 μm) and double excitation (frequency quadrupled Nd:YAG laser emitting at 266 nm and diode laser emitting at 405 nm) in order to detect both dissolved and particulate components of waters coming from aquifers, rivers and lakes.

In 2011, CASPER has been deployed in the St. Lawrence Estuary (SLE), near Rimouski (Quebec, Canada), in the frame of the project CLIMAT "Utilisation complémentaire du lidar afin de valider les données bio-optiques obtenues par mesures satellitaires dans l'estuaire du Saint-Laurent", in collaboration with ISMER-UQAR "Institut des Sciences de la Mer de Rimouski, Université du Québec à Rimouski" (Figure 12).

Figure 12 – Mr. Rodolfo Borelli (UTAPRAD-DIM ENEA) operates CASPER in a laboratory of ISMER-UQAR for fulvic acids and humic acids calibration.

1.5. Diagnostics for cultural heritage preservation and fruition

The UTAPRAD-DIM Laboratory has devoted resources to the development and application of new technologies to diagnostics in the Restoration of Cultural Heritage also transferring sensors on site for specific campaigns. International cooperation such as the bilateral agreement between Italy and Egypt's Minister of Foreign Affairs, between Italy and Spain and Italy and Romania are active in this area with the aim of carrying out non-destructive spectrochemical characterization of samples relevant to the cultural and monumental heritage. Main technologies are the Lased 3D and Laser Induced Florescence scanner and Laser Induced Breakdown Spectroscopy.

High resolution metrology and 3D rendering

Non-invasive active remote sensing systems based on low-power laser sources have lately found application as high-resolution scanning devices for reconstructing accurate images and for mapping the actual preservation status of investigated real scenes (e.g. Cultural Heritage surfaces). Within the IT@CHA project, started on July 1st 2011, the RGB-ITR (Figure 13) has been employed in some remarkable measurement campaigns in the Sistina Chapel in Rome and in historical buildings such as the Amore and Psyche Lodge by Villa Farnesina.

Examples of data acquired by the RGB-ITR during recent field campaigns concerning the frescos of the Amore and Psyche Lodge are reported in the following (Figure 14, Figure 15 and Figure 16). These frescoes were designed by Raphael Sanzio and realized by his school in 1518.

During the field campaign in Villa Farnesina, the RGB-ITR has operated for a couple of weeks in June 2011 for scanning the entire vault of the lodge and reconstructing its high-resolution, high-accuracy 3D color model. The entire vault of the 20m-long x 7.5m-large x 10m-high lodge has been scanned in 4 sections for a total scanning time of 100 hours. The digital 3D color model so obtained is shown in Figure 14, while some details are reported in Figure 15 and Figure 16. It is worth to notice that the high resolution (some hundreds of micron at a ten of meters) of the recorded images permits to appreciate details undetectable to the naked eye and to emphasize differences in the painting mode from one scholar to

Figure 13 - Photo of the non-invasive RGB-ITR system used for high-resolution, high-accuracy 3D color imaging. The black box is the optical head hosting the launching and receiving optics along with the motors for the horizontal and vertical scanning. The yellow casing, instead, contains the electronic modules (lock-in amplifiers, motor controller, etc.) and the three AM laser sources whose light travels by optical fibers. A laptop is used for the remote operating of the RGB-TR and for the analysis of the acquired data.

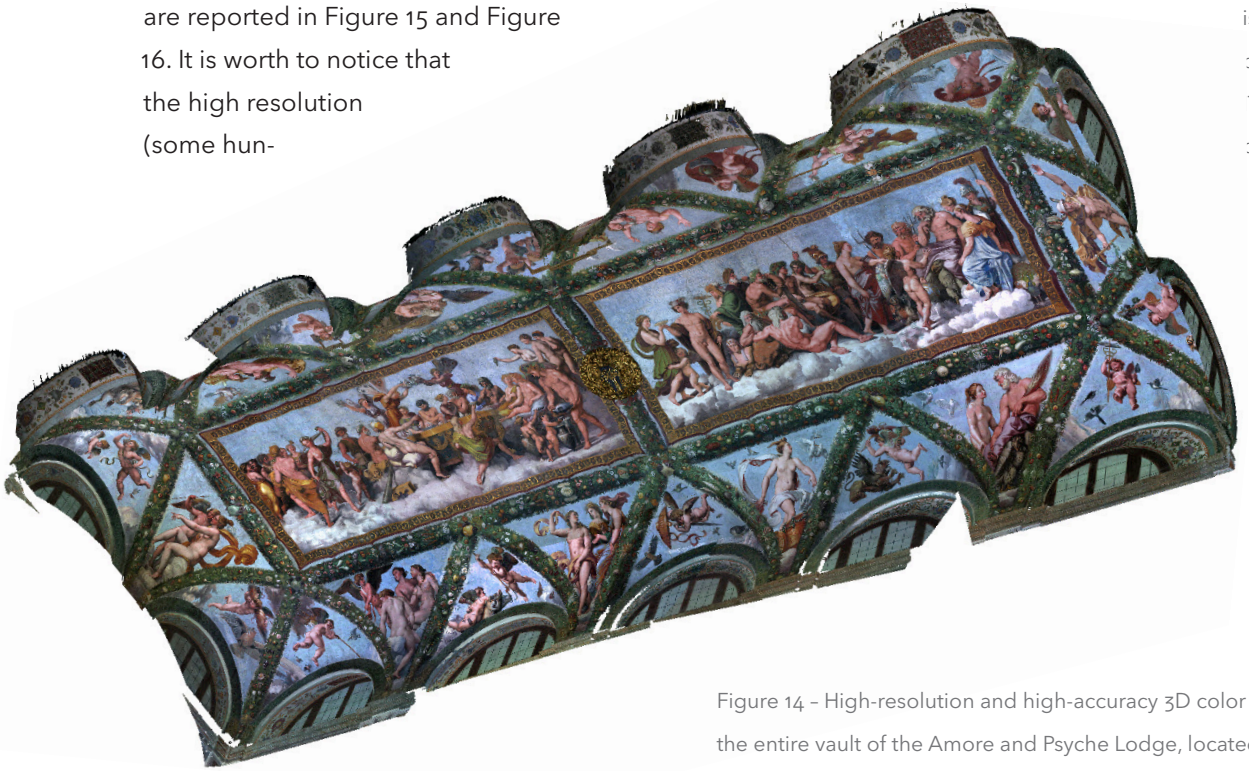

Figure 14 – High-resolution and high-accuracy 3D color model reconstructing the entire vault of the Amore and Psyche Lodge, located at Villa Farnesina (Rome) and frescoed by the Raphael Sazio school in 1518 (20m-long x 7.5m-large x 10m high). This model, obtained by RGB-ITR, is showed in the exhibition "Il Rinascimento a Roma - nel segno di Michelangelo e Raffaello" organized by "Fondazione Roma Museo" (Sciarra Palace, Rome, from 25 October 2011 to March 2012).

Figure 15 - Details of a portion of the frescoes of the Amore and Psyche Lodge acquired by RGB-ITR: Amore and Psyche wedding (central part of the vault on the right) (Area 8 x 3.5 m2).

the other, realizing different sections of the entire vault. A quantitative analysis of the preservation state of the lodge frescos is also possible from the recorded model by using ITR_Analyzer program for helping the restorers to schedule future restoration work.

The high-quality 3D color model of the vault of the Amore and Psyche Lodge and that of the entire vault of the 40.2 m-long x 13.4m-large x 20.7m-high Sistina Chapel are exposed at Sciarra Palace in Rome during the exhibition "Il Rinascimento a Roma - nel segno di Michelangelo e Raffaello" organized by "Fondazione Roma Museo" from 25 October 2011 to March 2012. The showed results have produced significant reactions of the field experts.

The metrology group has also recently completed the realization of RE-VUE facility (REmote Viewing in Underwater Environment), within the BLUARCHEOSY project ended on June 30th 2011, a 3D imaging system based on a continuous-wave (CW), amplitude-modulated (AM) laser source (405nm, 20mW). The device (Figure 17 left) is the result of several years of experimental and theoretical investigations aimed at realizing an effective and accurate underwater imaging laser system.

Figure 16 - Details of another portion of the frescoes on the Amore and Psyche Lodge acquired by RGB-ITR (Area 2.5 x 2.5 m2). On the left: Mercury (top of one pillar). On the right: small cupid with lion and marine horse (one lunette).

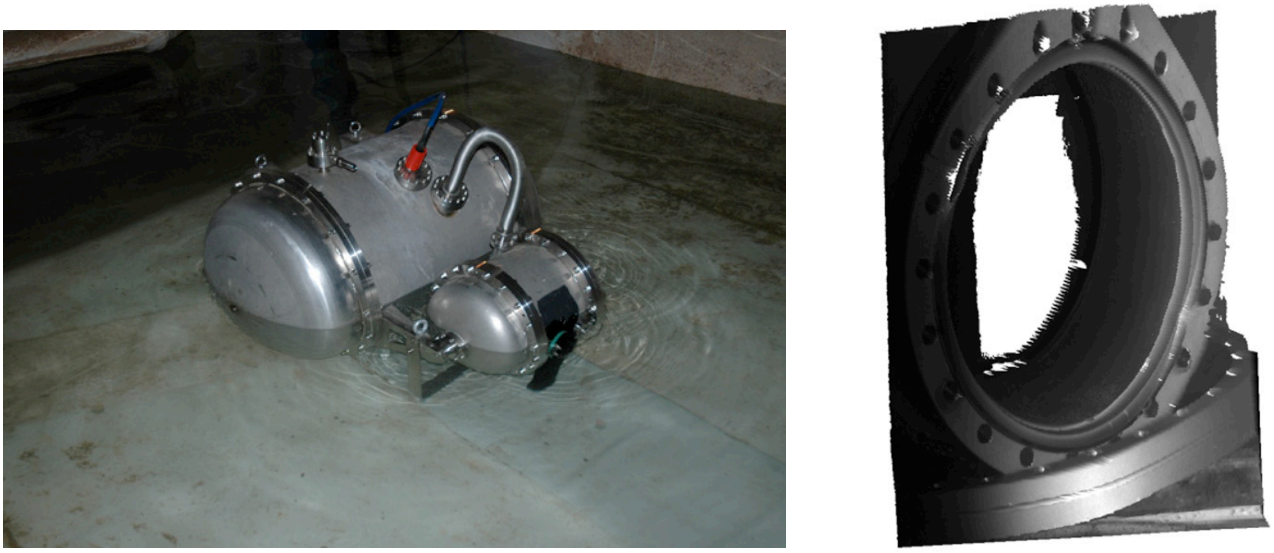

Figure 17 - RE-VUE facility: left) Photo of semi-immersed in the pool. The small cylinder contains the laser source, the scanning system and the receiving stage while the largest hosts electronic modules; right): high-resolution, high-quality 3D model of a gray-painted stainless steel disc with a large hole in the center and several small holes equally spaced along the perimeter (diameter about 1cm) immersed in relatively clean water at a distance of 5m from the sensor.

RE-VUE device can investigate scenes with a horizontal angle of view of 40° and a vertical one of several tenths of degrees. It is fully remotely operated by a laptop where a home-built software is properly installed and it is qualified to operate at a depth of 400m. During 2011 RE-VUE system has been immersed in relatively clean water and its actual performances of underwater imager have been opportunely evaluated. Examples of 3D models obtained by RE-VUE is shown in Figure 17 right.

In parallel with the experimental activities aimed at the realization and testing of the RE-VUE system, some progress has been made also on the theoretical side, by refining and further clarifying the recently developed semi-analytical model that describes the behavior of a modulated laser beam propagating in a scattering medium. In particular, some interesting theoretical results have been obtained that enable a clearer definition of the model itself in terms of the so-called adjoint radiative transfer formalism.

LIF and LIBS diagnostics within Italy – Egypt bilateral cooperation

In the frame of bilateral cooperation between Italy and Egypt (Prot. MAE01301362011-05-06), a series of spectroscopic measurements were performed by means of ENEA prototypes on samples coming from the archaeological area of Giza (Egypt): the measurements were aimed to the evaluation of the diagnostic potentiality of the LIBS and LIF sensors for a direct in situ application. Several textiles, wood fragments and biological samples have been

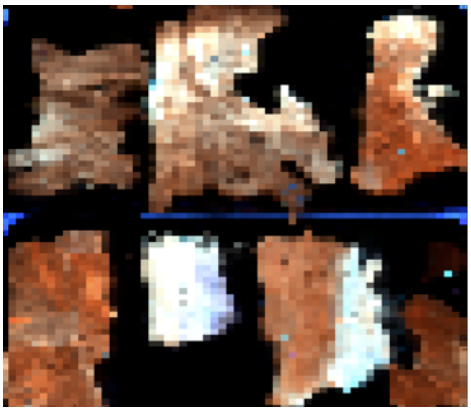

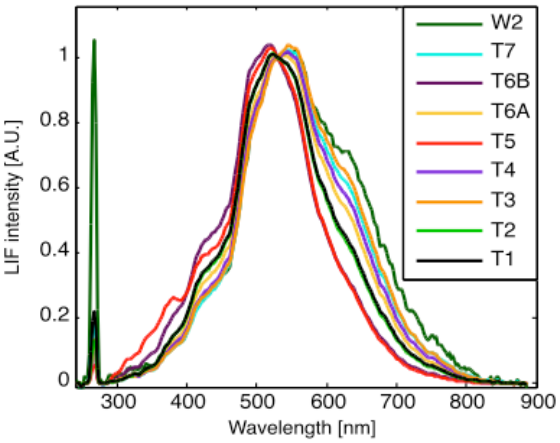

Figure 18 – LIF image of textiles represented as false colour RGB reconstruction with bands at 650nm, 520nm and 390nm (left image); LIF spectra of some of the textiles samples (T1-T7 from left to right) and of a wood fragment (W2 upper right side of second row); left and the right portion of T6 sample have separate spectra (T6A and T6B).

experimentally investigated. As the LIF is concerned, the adopted experimental technique allowed for the identification of deterioration processes caused by micro-organisms, and to differentiate bio-contamination from dust. Left side of Figure 18 shows the false colour image obtained by combination of the emission's intensities of the LIF emission at 650, 520, and 390 nm respectively for the red, green and blue channels with a bandwidth of 10nm. The spectra normalized at their maximum are shown in the right inset of the Figure 18; it is worth notice the significant spectral differences and an intensity ratio of 1:9 in the total emitted fluorescence (not shown).

A general trend concerns the complementarities of bands in 350-400nm band and at 630-680nm: for example the sample T5 has the highest relative intensity at 370nm, with low emission in the red, on the other hand the sample T3 shows an opposite trend. The observed spectral features are related with different contamination levels: samples with intense UV emission are likely contaminated with substances of biological origin as for example bio-deteriogens agents or biological traces not visible by the naked eye; on the other side samples with high relative intensity in red spectral region show evident dust and earth residues contamination.

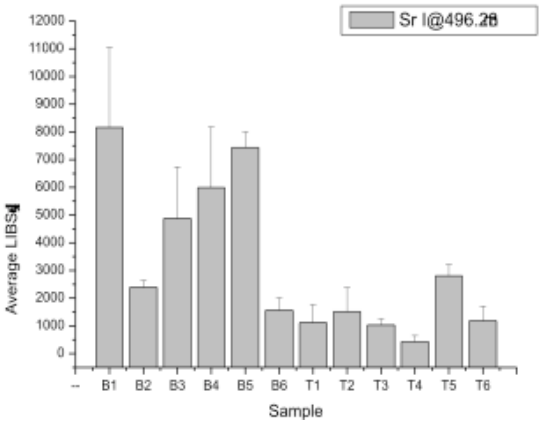

Figure 19 – Average line emission intensity of 496.23nm Sr I line from LIBS measurements on the analyzed samples.

LIBS technique has allowed the identification of heavy metals in biological tissues coming from excavation in Giza; while quantitative analysis is possible after proper calibration on reference data, the present experiments were aimed to determine the feasibility of qualitative determination of zinc and strontium content in bones and teeth. An interesting

findings is that the relative content of Ca and Sr (Figure 19) can be used to discriminate between bones and teeth. The discriminating capability could help the excavations for in situ and real time classification of the archaeological findings.

LIF imaging within ENEA – UPO cooperation

In the frame of cooperation between Italy (ENEA UTAPRAD)) and Spain (UPO Seville) the LIF scanning prototype has been applied to the diagnosis of historical artworks. Experimental measurements made on laboratory reference samples formed the basis to demonstrate the identification for some of the pigments found in the Glorification of Mary fresco the "Vergin of Buon Aire" chapel inside S. Telmo Palace in Seville scanned in February 2010. The result of a mapping procedure based on SAM algorithm is shown in Figure 20; several similarity maps have been computed by considering the reference spectra of laboratory samples prepared with historical pigments according to the ancient original recipes.

The LIF spectrum of the blackish regions (Figure 20B) reveals spectral features similar to those of carbon black pigment (not shown); it is worth noticing that the painter has probably used the black color to reinforce the outline of the mantle and other details to have a more contrasted picture.

The second similarity map (Figure 20C) details the use of blue pigment found in the mantle.

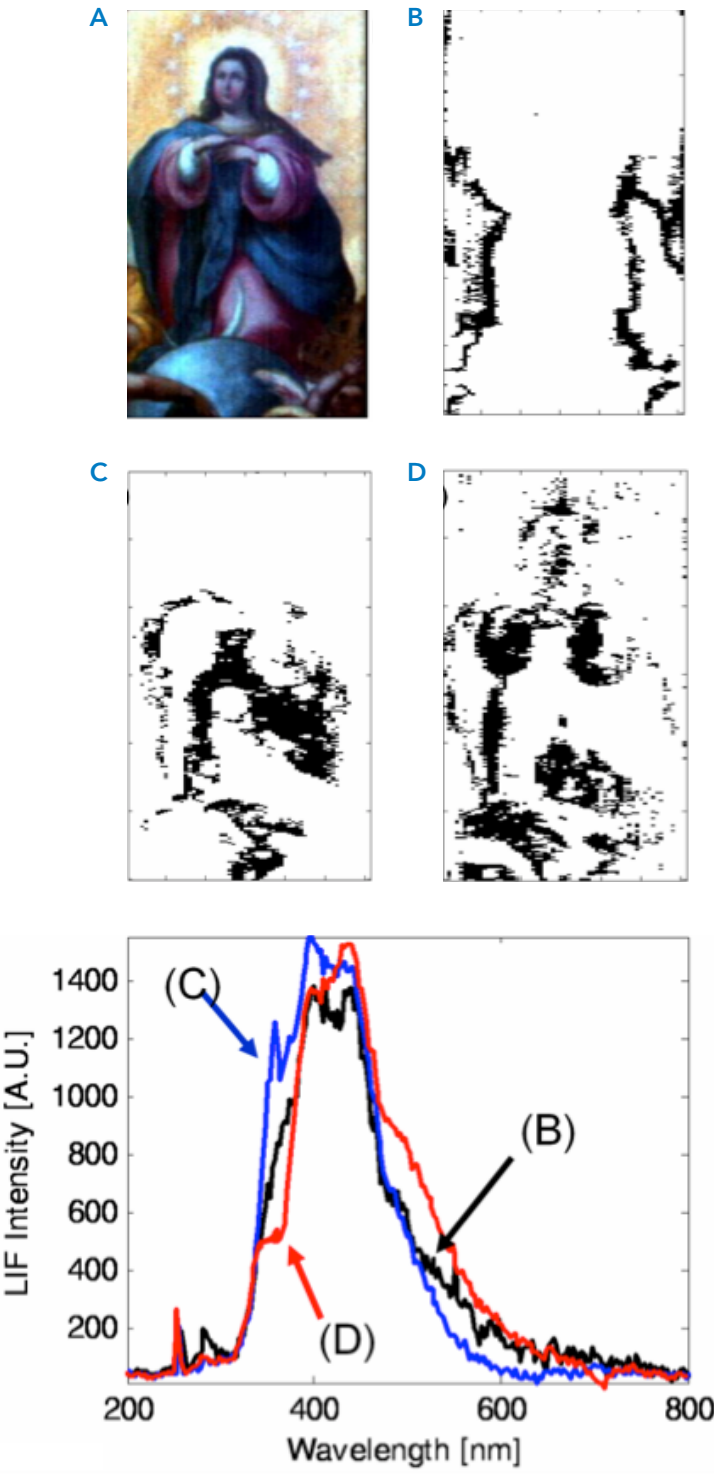

Figure 20 – Results from the application of the SAM analysis on the *La Glorificacion de la Virgen* fluorescence image; A) reconstructed color image, B), C) and D) similarity maps generated by considering the reference spectra shown in the right side

LIF is extremely attractive for its simplicity and speed of analysis, however some drawbacks should be not forgiven. Indeed some pigments efficiently characterized by non radiative de-excitation pathways do have a low fluorescence yield and from a practical point of view are difficult to detect and to identify (terras and okras). In those cases the presence of plaster worsens the possibility of detecting such pigments, because its fluorescence makes their contribution negligible. In the frame of the Cooperation further experimental activities are ongoing to find complementary techniques to resolve the ambiguity in pigment identification.

LIBS characterization of different CH surfaces (ceramics, pigments)

The LIBS technique has been applied for the determination of composition of ancient ceramics, including detection of minor elements, in order to establish origins and period of the artifacts. To this aim, and following a request from Italian Institute for Africa and Orient (IsIAO), we analyzed seventeen ceramic samples collected from different areas of a collapsed palace built in XII century by Sultan Ghaznavide Mas'ud III in Ghazni, Afghanistan. LIBS measurements were performed both on bare and glazed ceramic surfaces, by registering single shot spectra during the laser drilling. In this way, it was possible to study depth distribution of the elements, to identify surface contamination, then pigments used for decoration and for protective coverage, as well as to study mixing between different sample layers. Some elements detected by LIBS, such as copper, vanadium, barium and strontium, were not observed in comparative measurements performed by SEM-EDX. This work is a part of an undergraduate student's thesis from University Sapienza (Rome) together with pieces of stones original from two ancient Ethiopian churches.

LIBS spectra of complex surfaces are very rich of lines and the compounds identification can be very hard, just because of the big amount of information. In this context multivariate analysis can be a very useful tool thanks to its ability to reduce data set dimensions and to pull out effective information on the basis of variance analysis. In this frame the efficiency of the Principal Component Analysis (PCA) has been tested in the study of materials of interest in the field of Cultural Heritage as a technique for the resolution of problems related to characterization and recognition of artwork constituents. In particular different kinds of materials commonly used in fresco technique, as pigments, protective layers and consolidants, have been considered and analyzed on real substrates. LIBS spectra were collected and processed by statistic methods, before the PCA a normalization was carried out by the background signal. For LIBS spectra analysis only elements characterizing pigments and plaster substrate (both as principal components and as traces) have been taken into account.

For these a database of atomic and ionic lines free from superposition has been created from NIST database. Customized Matlab® routines have been built up for the database realization and for data analysis, starting from the acquired raw data. At first an automatic recognition of the lines of the database was performed and the presence of every element was checked. In this way a vector of 0 and 1 was created: 0 element absent, 1 element present in the analyzed sample. On such qualitative information a first run of PCA was carried out for an initial grouping of data. In a second stage of the data processing a semi-quantitative analysis the integrals of pre-selected atomic and ionic lines were computed. Absolute intensity values retrieved were normalized to the integrated intensity of the line of Mg at 5183.604 Å, which was always present in the examined samples.

Moreover, although the variables can all be measured in the same units, a standardization of data obtained was carried out to take into account the large differences in variance among different channels, due to their relative very different intensity values. On the data so obtained a second run of PCA was carried out in subsets of samples grouped by the first principal component analysis application.

As shown in Figure 21a, principal components analysis on qualitative data points out grouping for pigments characterized by analogous origin (earths, artificial chemicals, that in the present case correspond to lead based pigments,

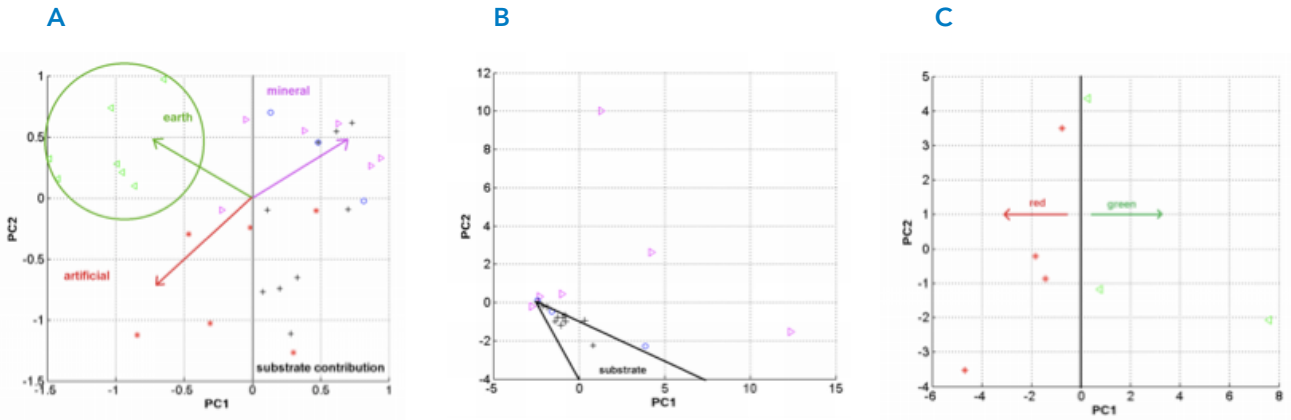

Figure 21 – Principal Component Analysis: a) PCA on qualitative data. Symbol colors correspond to pigment type: magenta for natural minerals, red for artificial chemicals, green for earths, blue for vegetable and black corresponds to samples without pigment; b) PCA on semi-quantitative data on the first subset containing organic pigments, consolidants, protectives and mineral pigments. PC1 vs PC2. Symbol colors correspond to pigment type: magenta from minerals, blue from vegetable, black no pigment; c) PC1 vs PC2 from principal components analysis on semi-quantitative data on the subset containing earths. Symbol colors correspond to pigment colors.

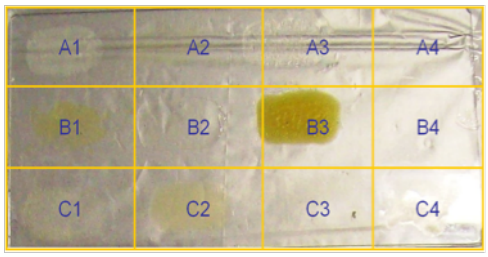

Figure 22 – Binders prepared according to the original historical recipes A1,A3= Casein, B1=Line seed oil, C1=Egg white, A2,C2=Rabbit glue, B2=Damar varnish, B3=Egg yolk, C3=background, A4, B4, C4 = vinyl polyacetate.

and a mixed group containing organic pigments, consolidants, protectives and mineral pigments).

The semi-quantitative analysis was performed separately on the two main subsets grouped thanks to the PCA application on qualitative data (first subset includes pigments with positive PC1, except lead containing outliers, the second contains the earths, characterized by negative PC1 and positive PC2). In the first subset (#1), as shown in Figure 21b, a clear separation among minerals and organic pigments (grouped together with consolidants) was obtained. Conversely in the second subset (#2) we finally obtained a sharp separation between pigments with different colour: PC1 is negative for red earths and positive for green earths (Figure 21c). In conclusion, principal component analysis applied on LIBS measurements on fresco materials allowed to manage a big amount of information, leading to an useful data mining and a grouping of the analyzed samples of interest of the conservators. These samples are typically hardly classified by methods of direct clustering because of the surface complexity and of the quantity of variables involved. In particular the consecutively application of the PCA on qualitative(presence or absence of preselected elements) and semi-quantitative (integrated intensities) data permitted to cluster analyzed materials in three main groups (earth pigments, artificial pigments and a mixed group containing mineral and organic pigments, protectives and consolidants) and to obtain, inside such single sets, further separations connected to intrinsic sample features as nature and original color.

Figure 23 - LIF spectra of a binders upon laser excitation 266 (left side) and 355nm (right side).

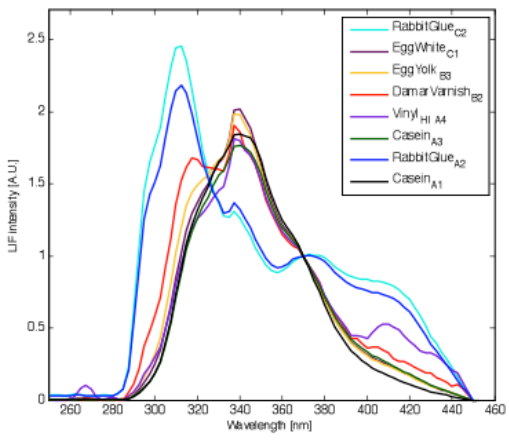

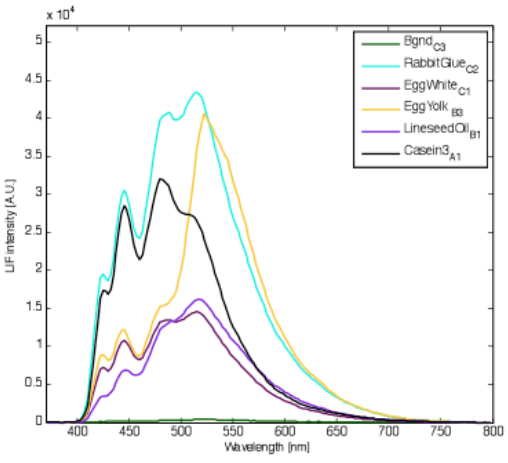

LIF characterization of CH materials (binders, marbles)

Within the frame of a collaboration between the ENEA UTAPRAD-DIM Department and the Chemistry Department of the Roma University Sapienza, the use of LIF as fast, in situ and real time technique for the detection and identification of materials used in the realization of artworks has been studied. Main purpose of this research is the design of enhanced user-friendly optical sensor. The formerly developed experimental apparatus - Hyperspectral Scanning LIF Sensor - was adapted to acquire high resolution spectra in the range from UV to VIS, giving details of the presence of consolidants and or binders on the sample under study.

Seven different reference compounds shown in Figure 22, were interrogated by LIF at two different excitation wavelengths.

Data were collected at 2 m distance upon laser excitation respectively at 266 nm and 355 nm, as shown in Figure 23. The spectra obtained upon excitation at 266 appear very similar with a maximum around 340 nm and a tail along the visible, with the exception of the rabbit glue since the latter is peaked at 310 nm, while spectra obtained upon excitation at 355nm have richer spectral features. Preliminary conclusions are that, once information on binders are searched for, it is worthwhile to combine the shorter and longer UV excitation to get spectral features enough to allow for the unique identification of the chemical compounds

Figure 24 - Picture of marble samples

The possibility to discriminate by Laser Induced Fluorescence (LIF) technique ancient marbles has been investigated. The rapid identification at naked eye of the different marble typology, in fact, is difficult for exposed marbles in real outdoor condition, due to their degradation. LIF has already been applied to stone materials in the field of cultural heritage to detect, for example, biodeteriogens not visible with the naked eye or to characterize different materials by means of their fluorescence spectral signatures.

In this work, LIF emission spectra have been studied with the aim to discriminate the different types of marbles and to contribute to build a database of ancient exposed white marbles. Four different kinds of marble from quarry have been investigated: 5 white Carrara samples and 13 grey Carrara (size 5x5x2 cm), 4 Paros and 5 Pentelic (size 1x1x3 cm) (Figure 24).

In order to simulate thermal effects, ageing tests have been performed in climatic chamber. All samples were submitted to three artificial thermal processes (Figure 25).

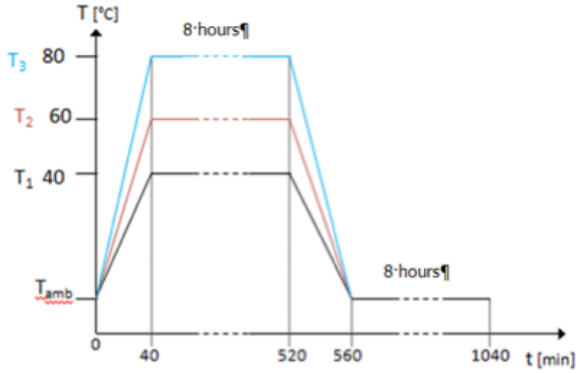

Figure 25 - Scheme of applied thermal processes

LIF emission bands were well detected on all samples. The main fluorescence emission bands observed on the analyzed samples are centered at: 435 nm and 490 nm for λ_{exc} = 355 nm; 345- 365 nm, 435 nm and 490 nm for λ_{exc} = 266 nm, confirming data reported in literature for this material. The different kinds of marble seem not to be discriminated by LIF emissions at λ_{exc} = 355 nm, showing very similar spectral shapes, while at λ_{exc} = 266 nm Carrara marbles are well distinct from Paros and Pentelic, due to the presence of different bands.

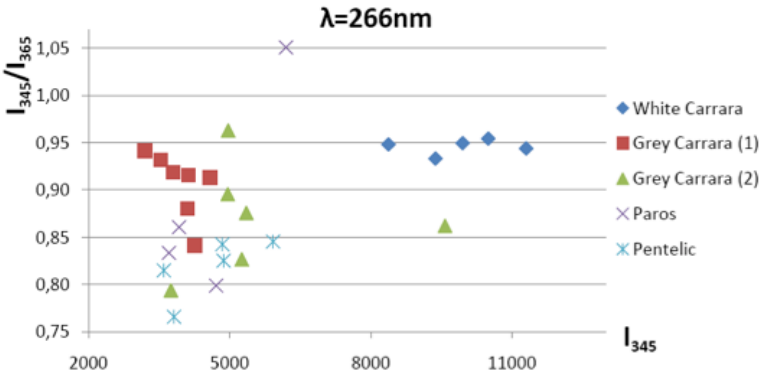

Figure 26 - LIF intensities ratio at 345 and 365 nm as a function of 345nm LIF intensity at the excitation wavelength of 266 nm.

LIF did not detect any effect of heat treatment. However, by analyzing in more detail the intensity ratios of the relevant peaks, it can be observed that at λ_{exc} = 355 nm grey Carrara marbles can be distinguished from the other ones by mean of I435/I490 , while at λ_{exc} = 266 nm white Carrara marbles are differentiated by mean of I345/I365 (Figure 26).

The LIF results show that the method is capable of discriminating between different saccharoid white marbles, once the optimal experimental parameters have been determined. For our study the choice of the excitation wavelength was crucial. The obtained results suggest this technique can be successfully employed to recognize exposed white marbles offering the advantage to be used without any sampling, remotely and speedily respect to the conventional diagnostic techniques.

LIBS application to submersed archaeological materials

The project AQUALAS, in which ENEA participates together with University of Malaga (UMA), has the aim to develop a LIBS system for in-situ characterization of the archaeological materials on sunken ancient ships close to Andalucia coast. During the last year of the project, the experiments were executed at ENEA by double pulse laser excitation directly under water in order to study the laser coupling with a submerged solid mate-

rial. The measurements performed on a metallic sample inside water, involve different detection techniques: laser scattering, laser beam transmission and reflection, shadowgraphy, fast photography and LIBS signal detection after the second laser pulse. The laser produced craters were measured by a high resolution profilometer and by an optical microscope.

The optimum LIBS signal was obtained for a relatively short interpulse delays, and this was explained by here demonstrated defocusing effect of the cooled gas bubble formed after the first laser pulse. Furthermore, the expanded and cooled vapour condensates inhomogeneously, thus causing a not uniform scattering and deflection of the second laser pulse. Here described findings have a great importance in underwater material processing in presence of liquids, also for medical applications.

Figure 27: Left: a) particle and gas ejection; b),d) plasma after the second pulse for two interpulse delays; c) inhomogeneities inside the expanded bubble (by shadowgraphy). Right: crater produced by the first (inner circle) and of the second laser pulse (outer circle)

1.6. Diagnostics for industry

In situ diagnostics in reactors for nuclear fusion

In the framework of the EFDA task WP11-ETS-DTM-zero1-zero5 "dust and tritium management" LIBS experiments have been performed in order to complete the studies leading to the qualification of laser techniques for deposited layer removal in fusion machines and for the development of a LIBS apparatus to be installed on the future ITER experimental set up in order to perform H and D inventory surface measurements. To this aim DLC and a-C mixed with W and Al on W substrate samples have been prepared ad hoc to prove the ability of LIBS to reveal the presence of H and D and to remove and measure step by step the coating layer. In Figure 28 the LIBS spectrum of a DLC sample, centered in the same spectral region, is shown. In this case, also, the D intensity peak is weak respect to the H peak, but the two peaks are well distinguishable.

LIBS measurements have been performed in order to characterize laser

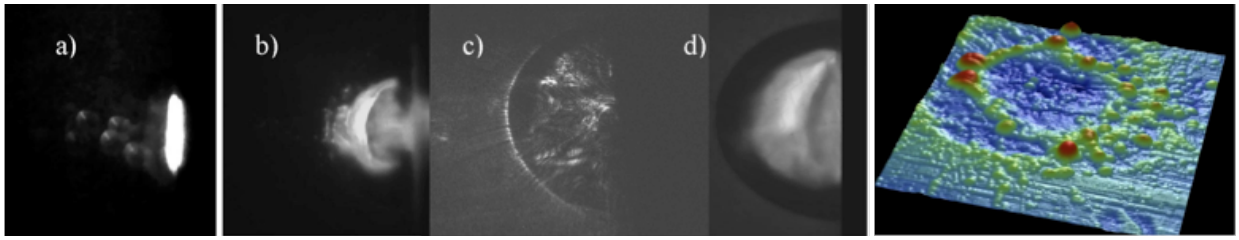

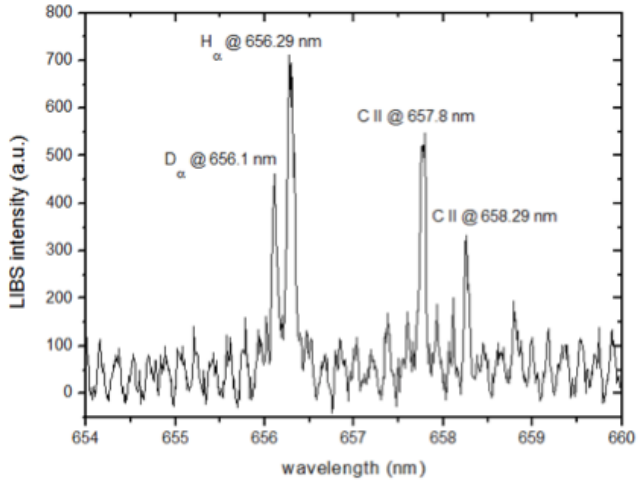

Figure 28 - LIBS signal from the DLC superficial layer in the spectral region around 656 nm.

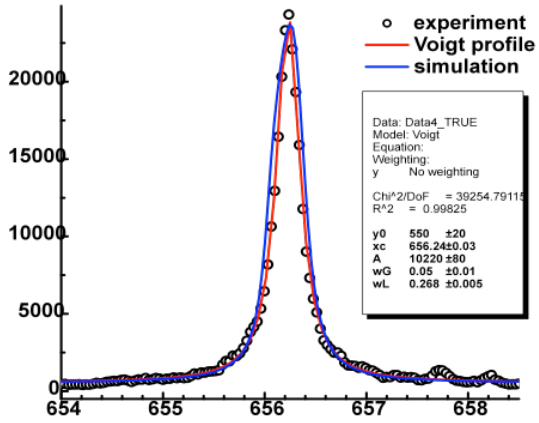

Figure 29 - Profiles of H+D lines at 656.24 nm from experiments (open black circles), its Voigt fitting (red curve) and simulation at 5.5×10^{16} cm^{-3} and ratio of D:H at 3:7.

plasma produced by palladium samples pure and added by H and D at low pressure ($5x10^{-3}$ mbar). LIBS spectra were investigated around 340 nm (Pd strong lines) and 656 nm (Hα line). Several values of isotopes ratio and electron density were used to calculate line profiles and to do a comparison with the real measured spectra. In Figure 29 an example is reported. The experimental result, with its Voigt fitting, was compared to the simulation and it was obtained, in this case, that for electron density of $5.5x10^{16}$ cm^{-3} and isotope ratio of 3:7 (30 at.% of deuterium) the simulated profile is close to the experimental points.

The experimental results demonstrate the LIBS feasibility for wall plasma interaction diagnostic. The achieved sensitivity allows for quantitative determination of trace detection of light elements and paves the way for remote Tritium inventory.

2 PHOTONICS MICRO- AND NANO-STRUCTURES LABORATORY

2.1. Mission and infrastructures

Photonics has been recognized by the European Commission as one of the key-enabling technologies for the future. "*Photonics* is the science of the harnessing of light. Photonics encompasses the generation of light, the detection of light, the management of light through guidance, manipulation, and amplification, and most importantly, its utilisation for the benefit of mankind" (Pierre Aigrain, 1967, http://cordis.europa.eu/fp7/ict/photonics/).
The major challenges in the modern world, solution for energy, life science and health, information and communication, imaging, lighting, displays, safety and security, are driven in their development by the production and manipulation of photons, the basic unit of light. In the last decades, important advances in the field of nanotechnologies enabled major breakthroughs in various scientific domains, due to the possibility of controlling and tuning the physical properties of materials at the nanoscale.
Today one of the main objectives of photonics is the R&D of technologies for miniaturization of optical and optoelectronic devices and sensors, including functionalisation with nanomaterials, control of interfaces at nanoscale and engineering of semiconducting-dielectric media of sub-micrometric dimensions for exploitation of light-matter interactions and confinement effects.
The first Italian policy position paper on the future Common Strategic Framework for Research and Innovation to contribute and on line with the European Horizon 2020 programme priorities identifies the "Nanotechnologies" and "Photonic sensors and sources" Technology Platforms as essential ones to be sustained for supporting the competitiveness and excellence of European and national research and industry.
At ENEA C.R. Frascati, in the Technical Unit for the Development of Applications of Radiations, the Photonics Micro- and Nano-structures Laboratory (UTAPRAD-MNF) carried out scientific activities on synthesis and functionalisation of nanomaterials and on R&D of novel light-emitting micro-devices and radiation detectors; they are combined with consolidated expertise in applications of optical fibre sensors for structural monitoring and activities in seismological field. They found applications in scientific (high-energy physics, biomedical imaging diagnostics, aerospace, cultural heritage) and industrial (photonics, ICT, transport, infrastructures, seismic prevention) fields, as well as for innovative energy production systems, including nuclear.
Available infrastructures consist well equipped laboratories and advanced instrumentation for photonics material

synthesis, micro-devices developments and their characterization:

- evaporators for the growth of dielectric, metallic and organic thin films;
- plants for laser assisted synthesis of nanopowders (LUCIFERO), nanowires and carbon nanotubes;
- electron spectroscopy laboratory;
- optical spectroscopies and confocal laser microscopy laboratories;
- interferometry and fibre optical sensor laboratories.

On the basis of high-level competencies, the MNF staff carried out technical and professional training of researchers and students, in collaboration with national and international universities and research institutions.
Technical contacts are frequent and fruitful with several small and medium companies operating in the field of optical components, spectroscopy, microscopy, lasers, and vacuum evaporation systems.

Funding and projects

In 2011 UTAPRAD–MNF Laboratory major funds came both from national projects of industrial research supported by Ministero Istruzione, Università e Ricerca (MIUR), such as TECnologie per la Visualizzazione di IMmagini (TECVIM) and MAteriali, dispositivi e sistemi MAgnetici e Superconduttivi (MAMAS), and from European projects (Framework Programme in the NMP area) such as Enhanced Nanofluids Heat–Exchange (HENIX).

2.2. Organic and nano-structures thin films for OLED and PV innovative cathodes

In last decades there has been a considerable interest in the use of organic materials for light-emitting devices based on thin film hetero-structures, due to their promising application in the fabrication of flat and flexible panel displays and for low-consumption solid state illumination.

Nowadays, their degradation is one of the challenging issues of basic and applied research in the field, and chemical and physical mechanisms of these complex phenomena are under study (ENEA patents) in the framework of the promotion activities of TECVIM (TEcnologie per la VIsualizzazione di IMmagini) project (MIUR FAR) led by CRF (Centro Ricerche FIAT) together with ENEA Frascati and ENEA Portici with UTAPRAD coordination, whose final evaluation was successfully completed in 2011.

Many efforts have been devoted to increase the lifetime of the encapsulated devices above the standard value of 10.000 h at initial display brightness (luminance) of 100 cd/m^2 by studying the effects of several degradation processes, primarily associated with degradation mechanisms of the electrode materials and electrode/organic interfaces.

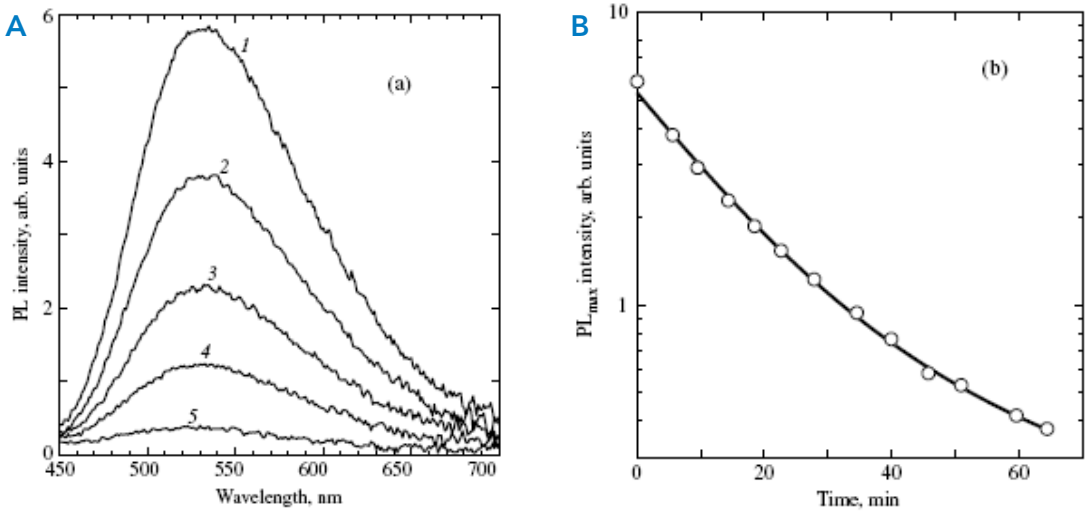

Figure 1. a) PL spectra of an Alq_3 film (50 nm thick) thermally evaporated on a silica substrate, measured at different irradiation times under UV LED illumination: 1 - 0 min, 2 - 5 min, 3 - 15 min, 4 - 30 min, 5 - 60 min. b) PL peak intensity at different irradiation times under UV LED illumination. The best fit (solid line) of the experimental points with a double exponential decay curve is reported.

Photo-degradation of Alq_3 thin films for organic photonics

The most studied low-molecular weight molecule is a metal-chelate, tris (8-hydroxy-quinoline) aluminum (Alq_3), commonly vacuum deposited as the active layer in green OLEDs, based on thin film technology. The exposure of transporting molecular layers to ambient factors, like moisture, oxygen and light also induces degradation phenomena and the quenching of the green photoluminescence (PL).

The photo-bleaching effects of selective ultraviolet and blue light illumination on the photoluminescence spectra of thermally evaporated Alq_3 thin films exposed in air were investigated by fluorescence spectroscopy and advanced optical imaging techniques. Alq_3 thin films of different thicknesses, from 50 to 80 nm, were thermally evaporated onto amorphous glass and fused silica substrates. They were kept in the evaporation chamber under low vacuum pressure (10^{-3} mbar) in the dark for a few days and, after the first exposure in air and the measurement of their initial optical characteristics, the time evolution of their PL spectra was regularly monitored under selective illumination with UV and blue LEDs. UV light illumination at 385 nm induced a strong and fast decrease of the Alq_3 films PL intensity. In Fig. 1a several PL spectra measured at different irradiation times under UV LED illumination were reported. In Fig. 1b, the experimental values of the peak intensity of the PL spectra, measured every 5 min, were reported in a logarithmic scale as a function of the irradiation time.

The observed behaviour can be described as the sum of two exponential decays, whose time constants are 17 and 80 min, respectively, as derived from the best fit. We obtained also that the significant reduction in the PL intensity is accompanied by a slight modification of

the spectral characteristics of the Alq_3 film broad emission (blue shift).

In order to explore the role of the energy of the impinging light, similar experiments were performed under illumination with the blue diode, whose emission is peaked at 455 nm, in the spectral range where the optical absorption and emission spectra of Alq_3 films are superposed. Again a decrease in the Alq_3 films PL intensity was observed. The observed behaviour can be described by a single exponential with a decay time of 90 min, five time longer than the case of UV illumination. As the excitation power density was similar to the UV one, the less effectiveness of the photo-bleaching processes should be attributed to the fact that the blue light it is outside of the main absorption band of Alq_3 films. Indeed, at the longer wavelengths of the blue LED with respect to the UV LED, which is centred on the peak of the Alq_3 main absorption feature, the excitation probability is reduced. The observed behaviour show that Alq_3 molecules in their exciting state are involved in these complex phenomena. A joint research project to study the stability of organic broad-band light-emitting Alq_3 thin films was proposed within the executive programme of scientific and technological cooperation between Italy and Romania for the years 2012-2013. The photo-bleaching processes were also exploited for direct laser patterning of the investigated Alq_3 thin films in a confocal laser scanning microscope (CLSM).

Nano-structured LiF thin films for OLED cathodes

A typical OLED consists of one or more organic layers sandwiched between a high work function and transparent anode, and a low work function metallic cathode. A smallest injection barrier height at the organic/metal electrode interface is favored to increase their efficiency. Al is preferred due to its better environmental stability and its straightforward use as contact material in Si-based integrated circuits. Insertion of an ultra-thin LiF layer between organic films and Al cathode was found to significantly reduce the threshold voltage in Alq_3-based OLED. The morphology of LiF films of different nominal thickness from

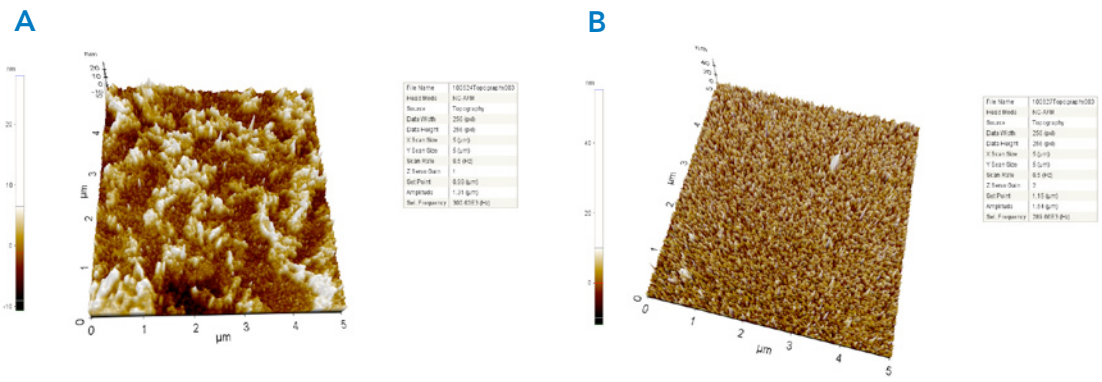

Figure 2. 3D AFM images of a LiF film grown on glass substrate, final INFICON frequency = 5 nm, a) and of a LiF film grown on Si(100) substrate, final INFICON frequency = 15 nm, b) (courtesy of Dr. A. Rufoloni, UTFUS-COND).

few nanometers up to 100 nm, grown by thermal evaporation on insulating and conducting substrates kept at RT were analysed by means of a PARK System AFM, model XE-150 operating in air in non-contact mode (Fig. 2), in collaboration with ENEA UTFUS-COND.

Electron spectroscopy for investigation of the band alignment at the In_2S_3/ITO interface in hybrid polymer-semiconductor solar cells

As a result of more than three decades of research on semiconductor devices, the understanding of the interface properties and the control of the interface formation is crucial for device tailoring. Being layered devices, thin-film solar cells performance is strongly affected by the interface properties as well, and the basic parameters characterizing the interface are the band discontinuities at the heterojunctions between the layers constituting the cell stack.

Photoemission Spectroscopy (PES) has been found to be an effective tool in interface analysis. In the past decades a great amount of work has been devoted to the study of semiconductor interfaces by this method. More recently, many papers have reported the use of this technique for determining the band offsets at various interfaces in thin film solar cells and photonic devices, including OLED.

At the UTAPRAD-MNF nanoscience and electron spectroscopy laboratory we have investigated the band discontinuities at the interface between ITO (Indium Tin Oxide) and a In_2S_3 layer deposited by chemical spray pyrolysis by means of X-Ray Photoelectron Spectroscopy (XPS). The interface ITO/In_2S_3 is an important building block in the hybrid organic/inorganic solar cell architectures.

Research on organic polymer-based photovoltaics has been attracting an increasing interest because cells can be manufactured at low temperatures on flexible substrates by simple fabrication processes like coating, spraying and printing techniques. In_2S_3 thin films were deposited on ITO coated glass substrates by Chemical Spray Pyrolysis (CSP) at the Physics Department of Cochin University (India). X-Ray – Photo-electron Spectroscopy (XPS) data were acquired in a UHV system operating at $4x10^{-10}$ mbar base pressure and equipped with a VG Al Kα monochromatised X-Ray source and a CLAM2 hemispherical analyzer working at constant pass energy mode.

Figure 3 shows selected XPS survey sequences taken on a sample with In/S=1.2/8 on two binding energy ranges of interest. The XPS data are plotted for different cumulative sputtering times starting at t=0 from the "as inserted" sample, which shows a C and O contaminated In_2S_3 surface. The survey spectra show the expected In4d, In4p, In4s, S2p and S2s photoemission peaks with the

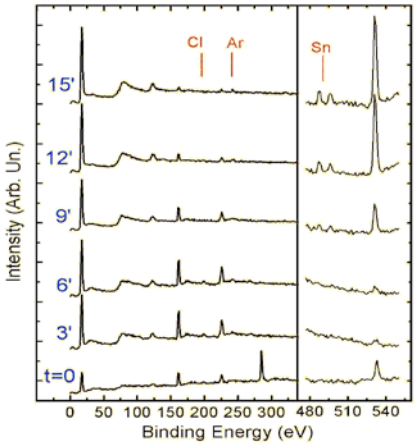

Figure 3. Selected XPS survey spectra as a function of sputtering time

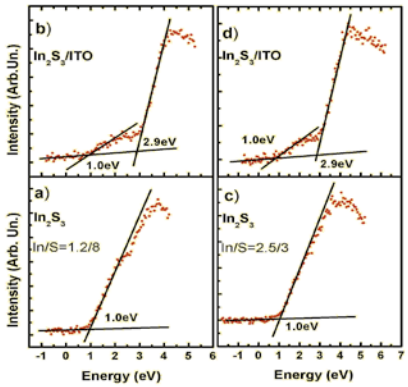

Figure 4. a) and c): VB edge on In2S3. B) and d): VB edges at the In2S3 interface.

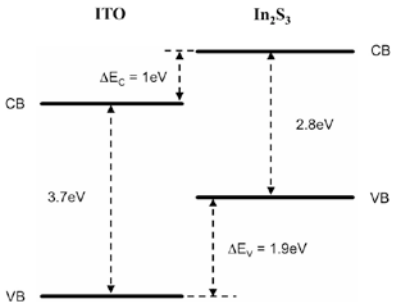

Fig.5. Sketch of the estimated band diagram.

additional presence of Sn3d and O1s (see right panel) and a small amount of Cl2p. Cl was found only in the In_2S_3 layer and is due to the InCl3 precursor used in spray pyrolysis and shows an intensity estimated to be less than 3 at.%. Oxygen is a contamination probably due to the synthesis method as it is found to have a constant amount of 8±1 at.% within the In_2S_3 layer. After 9' sputtering, S2p core level intensity is observed to decrease, while at the same time an increase of the O1s intensity is registered and the Sn3d spectral intensity at about 487eV BE becomes detectable. This indicates that the interface region has been reached and the simultaneous contributions from In_2S_3 and the underlying ITO layer are detected by XPS.

Figure 4 shows the valence band (VB) XPS spectra measured on two different samples. In Figs. 4a and 4c are shown XPS VB spectra taken on the In_2S_3 layers and Figs. 4b and 4d show the XPS VB data measured on the In_2S_3 /ITO interface regions. The top of the valence band was measured by linear extrapolation of the XPS valence band leading edge. Data show that on the In_2S_3 layer (Figs. 4a and 4c) the VB onset occurs at 1.9eV above the ITO VB onset (Figs. 4b and 4d). VB data at the interface show the simultaneous presence of both In_2S_3 and ITO-induced valence bands. By taking into account the uncertainties on the VB onset determination (±0.1eV) the In_2S_3/ ITO VB offset can be estimated to be 1.9eV±0.2eV.

By knowing the VB offset, the conduction band offset between the conduction bands can be estimated if the gap energies are known. By assuming a energy gap of 2.8±0.1eV for In_2S_3 and 3.7eV±0.1 for ITO, the conduction band offset results 1.0eV±0.4eV. In Fig. 5 is shown a sketch of the estimated band diagram.

2.3. Laser synthesis of nano-particles

Nanoparticles (NPs) are the building blocks of many approaches for realizing nanostructured materials and devices, hence their synthesis is a critical part of the rocketing research effort in nanoscale science. To date, the production of large amounts of pure, non-agglomerated NPs, with desired size and narrow size distribution, results to be an extremely difficult task. To this respect, the technique of laser pyrolysis of gas-phase reactants appears as a very flexible tool for the synthesis of a variety of NPs in developmental quantities.

A technology has been developed for the CO_2 laser pyrolysis of gas-phase and vapour-phase reactants, a scalable synthesis route for preparing NPs with controllable morphologies and in quantities sufficient to be tested for structural and functional applications. In particular the synthesis of NPs was performed with the set-up LUCIFERO, that is fit for large scale production (up to 100 g/h) of NPs with different chemical characteristics and dimensions tuned from 5 to 80 nm.

NPs of silicon carbide (SiC), titania (TiO_2) and silica (SiO_2) by using gaseous and liquid precursors were synthesized. Characterization of nanopowders was performed also with the collaboration of other ENEA Technical Units and Laboratories (UTTMAT-SUP, UTFUS-COND, UTRINN-IFC, UTTMAT-CHI).

Current efforts include: (i) the production of developmental quantities of SiC for nanofluid preparation (ii) the production of nanoparticles for new, challenging applications such as doped and pure TiO_2 NPs for photovoltaics and photocatalysis and NPs containing zero-valent iron for contaminated soil and ground-water remediation and (iii) the realization of nanocomposite coatings containing SiO_2 and TiO_2 NPs for cultural heritage preservation. Increasing attention has been paid to initiatives having as objective the assessment of the risk to human or ecological health in the widespread use of NPs.

Production of SiC nanopowder

The influence of synthesis parameters on SiC NPs production using a mixture of silane (SiH_4) and acetylene(C_2H_2) has been investigated. The precursor flow rates were changed to optimize the final chemical composition of the nanopowders. The collected NPs are spherical, nearly mono-dispersed in size, almost pure, and with very good productivity. X-ray diffraction (XRD) and infrared spectroscopy (IR) confirm the very good quality of our nanopowders. In fact the IR spectra (see Fig. 6a) show no bands or very weak bands for CH, SiH and SiO, and the XRD spectrum shows only the presence of SiC peak, while peaks typical of free nanocrystalline Si are absent. SEM (Scanning Electron Microscopy) measurements of nanopowders show that the NPs dimensions are of about 25 nm. Research

is in progress to increase the dimensions of NPs up to 80 nm to investigate the influence of NPs size on the heat transfer coefficient for the NanoHex (Enhanced Nanofluids Heat-Exchange) Project.

Synthesis of SiO_2 and pure and doped TiO_2 nanoparticles

Silica NPs were prepared by use of laser pyrolysis of tetraethoxysilane (TEOS), a liquid precursor, with ethylene as sensitizer. The obtained powder generally appeared dark and contained free-carbon coming from TEOS and ethylene decomposition. In order to remove these contaminants it was necessary to perform a thermal treatment at 600°C for 6 hours, but DLS (Dynamic Light Scattering) measurements revealed increased powder agglomeration after thermal treatment, that is undesirable for most applications. Tuning of process parameters such as laser power and ethylene flux was performed and carbon contamination less than 4% w/w was observed (as shown by thermal gravimetric analysis). Moreover, the color of as prepared powder resulted to be almost white. Further control on NPs dimensions was achieved and nanopowders diameter from 10 to 40 nm were produced, as shown by SEM photos in Fig 6b.

Pure and N-doped titania NPs were synthesized by laser pyrolysis of titanium tetraisopropoxide (TTIP) by using as sensitizer ethylene and ammonia, respectively. The obtained nanopowders show well-defined morphology and structural properties that can be finely tuned by accurate control of the main experimental parameters (flow of precursors, laser power density, pressure). In particular powders with different percentage of N-doping, crystalline phase and dimension were synthesized and the influence of different features on the optical properties of NPs are under investigation.

Nanomaterials for energy efficiency: nanofluids from nanopowders

Nanofluids are a new class of high performance nanotechnology-based coolants engineered by dispersing and

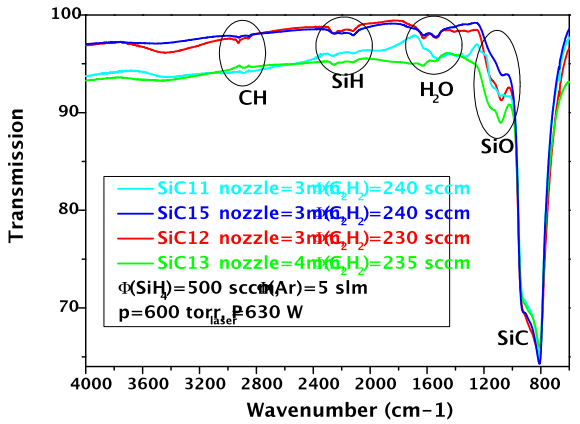

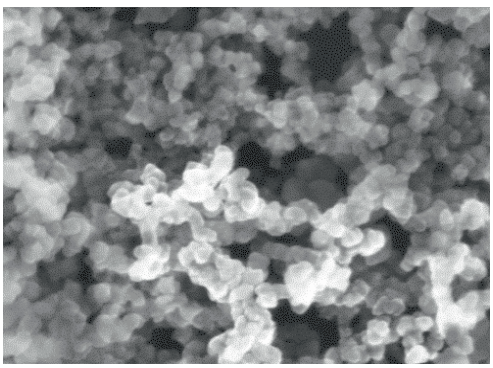

Figure 6. a) IR spectra of SiC nanopowders. b) SEM image of SiO2 NPs.

stably suspending in base fluids a limited amount of nanoparticles (metallic or non-metallic) with typical size on the order of 10-250 nm. A firm assessment of the enhancement in nanofluid heat transfer with respect to conventional coolants and a deep comprehension of the mechanisms behind it would pave the way to industrial development of nanofluids for a variety of applications ranging from cooling of electronic components, transformer oil and heat-exchange devices to improving heat transfer efficiency of chillers, domestic refrigerators-freezers and more. To this respect, nanopowders for the preparation of selected nanofluids are produced by CO_2 laser pyrolysis in the framework of the EC FP7 Project NanoHex, having as objective the development of high performance nanofluid coolants for Data Centres and Power Electronic Components. An enhancement in the thermal conductivity (with respect to distilled water) was observed in all the nanofluids based on ENEA pyrolytic NPs (TiO_2, SiO_2 and SiC) in water. Thermal conductivity of the nanofluids was determined either with conventional methodologies (at the University of Birmingham-UK and the Royal Institute of Technology-SW) or with an optical, laser-induced grating set-up which provides the possibility for in situ monitoring of coolant performances (in cooperation with ENEA UTTMAT-SUP). Measurements of the heat transfer coefficient of water based nanofluids containing pyrolitic NPs are currently in progress (in cooperation with ENEA UTTEI-TERM) to evaluate perspectives for exploitation of nanofluids based on pyrolytic NPs.

Nanomaterials for Cultural Heritage preservation

In the last few years, nanomaterials have been frequently applied for restoration and conservation of artworks. In fact, it has been demonstrated that inorganic oxides nanoparticles, such as silica and titania, improve the performance of materials used in conservation field.Properties of consolidant and protective materials modified with SiO2 and TiO_2 NPs produced by CO_2 laser pyrolysis with dimensions about 15

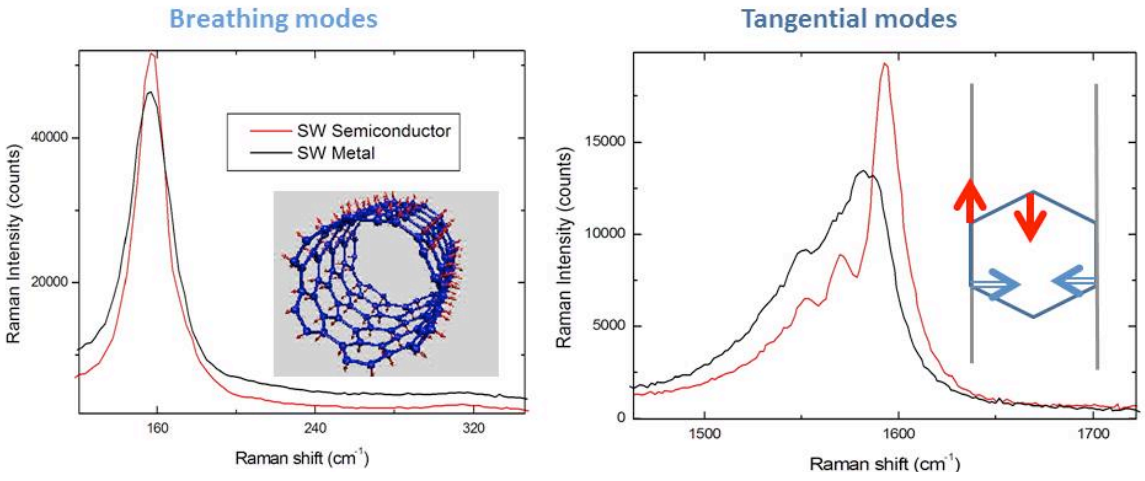

Figure 7. Raman spectra of single walled metallic (black line) and semiconductor (red line) CNTs.

nm and low polydispersity, were studied after application on marble (in cooperation with ENEA UTTMAT-DIAG and UTAPRAD-DIM). To this purpose solutions of acrylic polymer and silicon-based resins with silica and titania NPs were prepared in different percentage and spread on marble surfaces by brushing. Different Carrara marble samples were used: a few from cave, some aged in climatic chamber or at open air and others very old from the deposit of an ancient roman art museum. Treated marbles samples were submitted to aging processes in a climatic chamber, taking into account temperature and relative humidity, and in a solar box, for considering solar light irradiation, in view of simulating a natural open air exposition. Colorimetric measurements were carried out to verify the color modification of the protective film due to the solar exposition; ultrasonic velocity were measured to estimate the structural modification; laser induced fluorescence were performed to investigate the molecular changes due to the atmospheric parameters.
The results have demonstrated that the addition of nanoparticles enhances the efficiency of the consolidant and protective materials.

Figure 8. PCA chart of vegetable oils

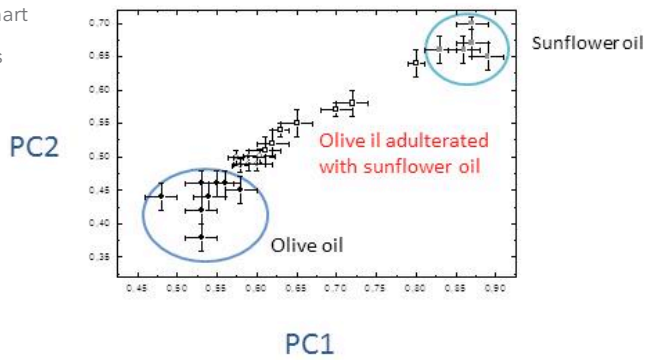

2.4. Optical technologies for nanomaterials and photonics

Raman spectroscopy for material investigation and development

Recently the R&D activities were mainly dedicated to the application of Raman spectroscopy (RS) in different fields. Raman spectroscopy is a powerful technique for “point and shoot” identification of materials because it has the inherent ability to distinguish between molecules with great similarity. Raman spectra consist of sharp bands that are characteristics of the specific molecule in the sample because each line of the spectrum corresponds to a specific vibrational mode of the chemical bonds in the molecule. In the last years there is an increasing demand for the development of analytical methods non destructive and accurate to be applicable also “on the field”.

An integrated Raman system (i-Raman Bwtek) with wavelength range 789-1048 nm, corresponding to Raman shifts of 75-3200 cm-1 (resolution 3 cm^{-1}) was used. The excitation source was a solid state laser operating at 785 nm and a power scalable in the range 30 - 300 mW. The near-IR excitation eliminates most of sample fluorescence. The Raman system is equipped with a micro-positioning system for fine xyz adjustments and a video camera for sampling viewing. Depending on the mounted microscope objectives, the laser spot has a diameter of 80 μm or 50 μm

on the sample, allowing Raman measurements with a good spatial resolution.

Raman spectroscopy on metallic and semiconductor single walled nanotubes

All the carbon nanotube (CNT) synthesis methods produce both semiconductor and metallic nanotubes mixed together and up to now it was not possible to address a synthesis process to a preferential formation of only one kind of CNTs. However, post synthesis processes evolved rapidly and the possibility to select semiconductor from metallic nanotubes was explored. The RS is a valuable technique to discriminate between semiconductor and metallic nanotubes and can be considered as suitable support for CNTs separation processes. In Fig. 7 the Raman spectra of single walled nanotubes semiconductor and metallic (Nanointegris. Inc, USA) are reported.

The radial breathing modes depend only from nanotube diameter and for a given diameter the chirality of the CNTs can be different. Only the tangential stretching modes of C-C bond give information on nanotube chirality: semiconductor nanotubes have sharp vibration modes at 1550, 1570 and 1590 cm^{-1}, whereas metallic ones have modes at 1550 and 1580 cm^{-1}. The semiconductor nanotubes have a higher number of transitions resonant with laser energy, and their vibration can be amplified better.

Raman spectroscopy for investigation of olive oil adulteration

The RS is of great value for the analysis of vegetable oils because non polar groups as C=C give intense Raman scattered bands. Olive oil mainly consists of monounsaturated oleic acid (i.e. with only one C=C double bond), whereas the other vegetable oils show a high content of linoleic acid, which has the same chain length of oleic acid, but contains one more C=C double bond. Consequently, the Raman intensity of the vibration at 1265 cm^{-1} and 1655 cm^{-1}, which are correlated with the double carbon bonds, increases as the degree of unsaturation (i.e. the number of C=C bonds) increases.

This finding was used to discriminate between olive and the other edible oils. Principal components analysis (PCA) was applied to Raman spectra of olive oils, sunflower oils and olive oil adulterated with different known percentages of sunflower oil. Figure 8 shows a distribution chart resulting from PCA, in which each Raman measurement is represented by a dot with a unique x, y coordinate.

Apparently, the olive oil can be easily distinguished from sunflower oil by the different distribution region in this chart. The olive oil sample mixed with sunflower oil are represented by dots with horizontal and vertical coordinates which increase with the content of unsaturated fatty acid in the mixture, moving toward

the top of the right side of the chart. Samples with sunflower content smaller than 4% are represented by dots near the edge of olive oil region, anyhow they can be distinguished from olive oil dots, also considering the error bars.

RS was also applied in homeland security projects coordinated by DIM laboratory: in RADEX for standoff detection of energetic materials and BONAS for trace level detection of explosives. In this last case, the RS was combined to the surface enhancement effect (SERS) to reach the desired limit of detection.

Optical spectroscopy of organic TPB films for photo-detectors

Tetraphenil-butadiene (TPB) is the preferred organic material for the detection of UV radiation in modern particle detectors based on liquid Argon, especially for the Dark Matter search. TPB exhibits an intense broad emission band peaked at about 440 nm under light excitation at smaller wavelengths so it works as a wavelength-shifter (128 nm - 440 nm). TPB films grown by different methods on several substrates were optically characterised. This activity was started under a Research Contract with Istituto Nazionale di Fisica Nucleare-Laboratori Nazionali del Gran Sasso (INFN-LNGS) and it is going on in collaboration with the Physics Department of Rome Tor Vergata University.

Optical spectroscopy to study the effects of heavy metals doping in LiF crystals

LiF is a well-known dosimeter material in pure and doped form. LiF crystals can be doped with special impurities to enhance their radiation sensitivity. Their presence modifies the structural properties of doped LiF crystals and influences the formation and stabilization processes of electronic defects, such as F_2 and F_3+ colour centres.
The evidence of the incorporation of Pb^{2+} ions in the LiF matrix and their stability during annealing procedures was investigated by optical spectroscopy (absorption and photoluminescence) and by X-ray Absorption Spectroscopy (XAS) measurements (Fig. 10), performed at the European Synchrotron Radiation Facility,

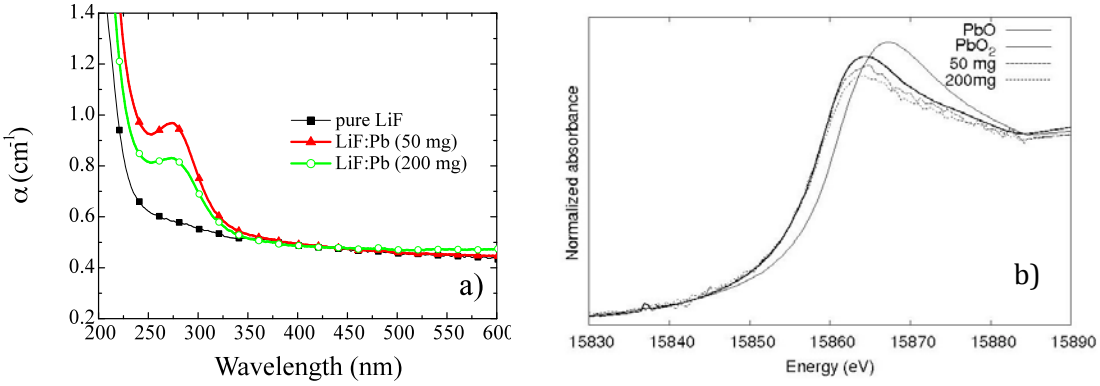

Figure 9. Absorption coefficient of an undoped and of two LiF:Pb crystals (50 mg and 200 mg in 60 g of LiF), a). XANES spectra at the Pb – LI edge. The results for LiF:Pb (50mg and 200mg) are compared with model compounds for Pb^{2+} (PbO) and Pb^{4+}(PbO_2), b).

ESRF, Grenoble (France).
This activity was performed in cooperation with the Dep. of Physics of University of Rome Tre, in collaboration with partners at National Institute of Material Physics, Bucharest, in Romania. Optical measurements performed on LiF:Pb crystals were able to reveal the incorporation of Pb^{2+} ions in the LiF matrix, even in very low concentrations. These results are confirmed by means of Extended X-ray Absorption Fine Structure (EXAFS) measurements, which provide further insights on their characteristics. The XAS data reveal that the PbF_2 precursor has undergone a complete dissolution and a new phase is really formed in the investigated crystals. There is a non trivial atomic ordering also beyond the first shell, which suggest the incorporation of Pb^{2+} in the crystalline environment. The structural parameters found by XAS measurements suggest the presence of Pb^{2+} in a Li-substitutional site and bound to a lithium charged-compensating vacancy. Further experiments are in progress on coloured crystals, also in collaboration with the Institute of Physics, National Academy of Sciences of Belarus, Minsk (Belarus).

Confocal laser microscopy of photo-induced Bragg gratings and colour-centre waveguides in LiF crystals

Point defects in LiF present very interesting spectroscopic properties, which are extensively investigated, particularly because find application in the realization of broad-band emitting lasers and amplifiers operating at room temperature in the optical domain. The use of a grating to reduce the laser threshold and to narrow the line-width has also been demonstrated. More recently, LiF gained increased attention due to the development of colour centre lasers using gratings induced by high energy femtosecond laser pulses.

Photo-induced Bragg gratings and waveguides in LiF were produced by laser CW illumination and by femtosecond laser direct writing (collaboration with Federal University of Technology–Paraná, Curitiba, Brazil).

Gratings were realized in previously coloured LiF samples using low power continuous wave ultraviolet lasers. The used LiF crystals were previously coloured by soft X-ray irradiation. The use of soft X-rays to produce colour centres has the advantage of resulting in a thin coloured layer because of the reduced penetration depth. As a result, the background emission from the crystal during fluorescence measurements is largely reduced. Bragg gratings were recorded in coloured LiF using standard illumination of the sample in a Talbot interferometer, using 244 nm light from a frequency doubled Ar ion laser. The zero-th order beam was blocked by a beam trap after the diffracting element (phase mask).
The optical structures were characterized by optical microscopy, laser confocal imaging, optical absorption and emission

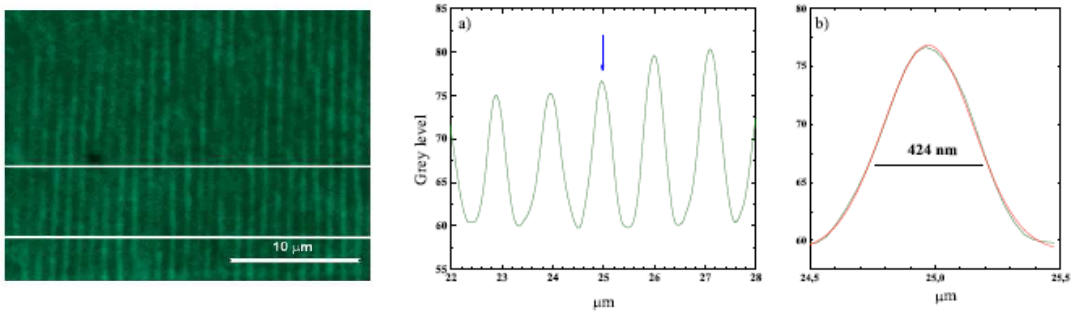

Figure 10 a) Confocal laser fluorescence microscopy image of a Bragg grating recorded in a surface coloured LiF crystal by CW ultraviolet illumination in a phase-mask interferometer. b) intensity profile between the two white lines of figure a).

linear spectroscopy. Figure 10a shows the CLSM image obtained from a Bragg grating recorded by CW ultraviolet light in a surface colored LiF, obtained under Argon laser excitation at 458 nm. The periodic pattern was analyzed by using imaging processing techniques and a best fit in the region between the two longitudinal white lines in the figure resulted in a grating pitch of about 425 nm (figure 10b)).

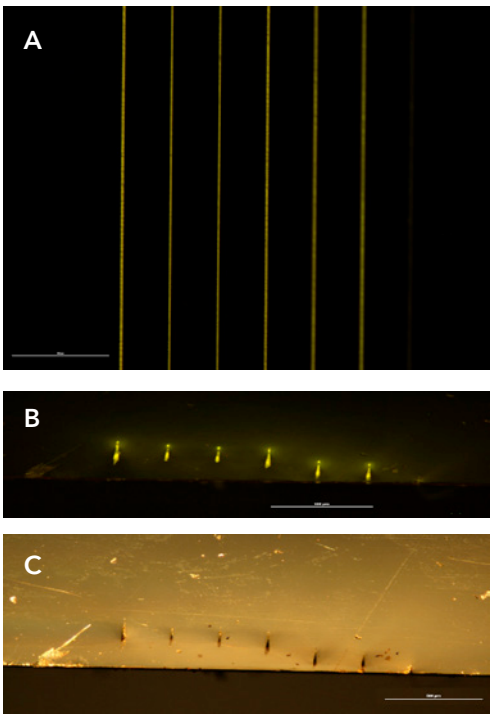

Figure 11 Optical images of the channel waveguides in a blank LiF crystal direct written with a fs laser: a) top view in fluorescence mode, b) one of the crystal side facets in fluorescence mode under blue light illumination and c) the same facet under white light illumination in transmission mode. (scale bar = 500 μm)

Colour centre channel waveguides have been recorded in LiF crystals using a femtosecond laser. The obtained waveguides are characterized using several techniques. Near field measurements are carried out to determine the mode dimension of the propagated light. Optical scattering and insertion loss measurements are done to estimate the wave-guide losses. Conventional and confocal optical microscopy were used to obtain the morphology of the recorded structures and their imaging in fluorescence mode.

Figure 11 shows optical microscopy images of the waveguides obtained in a LiF blank crystal. On Fig. 11a the channels are shown in top view in fluorescence mode, whereas Figures 11b and 11c shows the entry facet of the waveguides on the crystal lateral side in fluorescence mode and under white illumination, respectively.

The damage caused by laser ablation on the crystal surface can be clearly observed; the waveguides are several millimetres long and are regularly spaced by about 200 μm. The yellow brightness of the waveguides is due to the visible photoluminescence of F_2 and F_3+ colour centres.

2.5. Imaging radiation detectors based on Lithium Fluoride Crystals and films

Electronic point defects can be produced in LiF crystals and films by different kinds of ionising radiation. Some of these electronic defects, known as colour centres, are optically active, with broad absorption and emission bands in the visible spectral range. Novel X-ray imaging detectors based on photoluminescence from aggregated colour centres in LiF have been proposed and are currently under development, successfully extending their operation in the soft and hard X-ray region. Among the main peculiarities of LiF-based detectors, there are intrinsic high spatial resolution, in principle limited only by the point defect size, large field of view and wide dynamic range. They also present a great versatility, as they can be grown in the form of thin films on different substrates by well-assessed physical deposition techniques. The peculiar features of LiF-based imaging detectors make them very promising and attractive as imaging plates for X-ray microscopy, for material science, in the characterization of X-ray sources and biological investigation, even for in vivo specimens.

Further study are in progress to extend their use to high energy particle beams, like electrons and protons, and to increase their versatility by investigation of LiF film compatibility with different substrates.

High-resolution X-ray imaging by polycapillary optics and lithium fluoride detectors combination

High-resolution X-ray imaging by a table-top laboratory system based on LiF imaging radiation detectors and a X-ray tube combined with X-ray polycapillary optics was successfully obtained (collaboration with XLab, Istituto Nazionale di Fisica Nucleare-Laboratori Nazionali di Frascati, INFN-LNF). Imaging experiments of thick geological samples showed the potentialities of this approach for the development of compact laboratory X-ray microscopy apparatus. The characteristics of LiF imaging detectors allow us to use very simple contact imaging techniques. Figure 12a shows the image

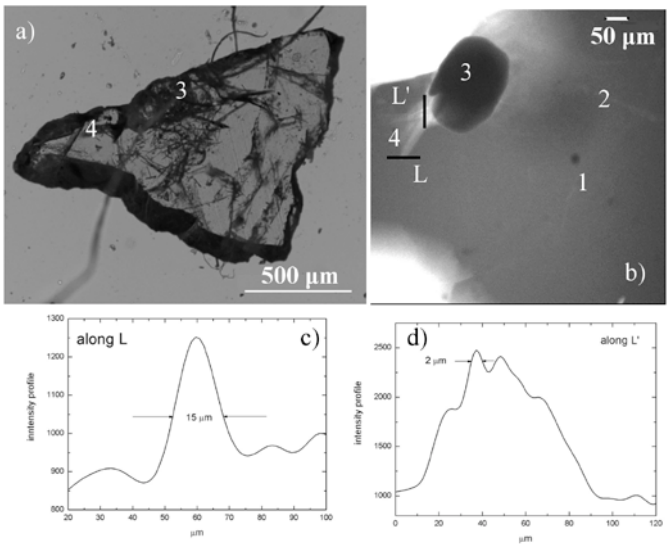

Figure 12. a) Optical image under white light illumination in transmission mode of a doubly-polished (010) section of cordierite. b) X-ray microradiography of sample 1 stored in a LiF crystal and read by a CLSM in fluorescence mode; c) and d) show the intensity profiles, with the corresponding FWHM, of brighter inclusions along lines L and L' of b).

of a doubly -polished (010) section (thickness 140 μm) of cordierite (a silicate with ideal composition $(Mg,Fe)_2Al_4Si_5O_{18}x(H_2O, CO_2)$) directly obtained by the optical microscope under white light illumination in transmission mode. Figs. 12b shows the X-ray radiography of the same sample stored in a LiF crystal detector and read by a CLSM in fluorescence mode. Several features and internal structures can be identified (1, 2, 3, 4). Fig.12c and d show the intensity profiles, with the corresponding FWHM, of the brighter inclusions (4) along horizontal L and vertical L' black lines of Fig.12b. Inspection of these profiles suggests that the high spatial resolution and the dynamic range of LiF detectors allow to distinguish details few microns wide.

White beam X-ray imaging experiments with lithium fluoride detectors at the TOPO-TOMO beamline of the ANKA synchrotron

White beam X-ray imaging experiments have been performed at the ANKA/ TOPO-TOMO beamline, Research Center Karlsruhe (Germany) by using imaging detectors based on photoluminescent colour centres in LiF crystals and films. For the first time these detectors were tested with broad band X-ray beam in the 6-40 keV interval to study their response at different irradiation doses and to obtain high resolved images of commercial test patterns. Absorption and photoluminescence spectra of LiF crystals irradiated at different irradiation time were analysed to study the optical response of the LiF-based detectors. R&D activities are going on to improve the performances of these promising radiation imaging detectors and to study the best approaches and conditions for imaging experiments at TOPO-TOMO beamline, including phase contrast techniques. Figure 13a shows the X-ray microradiography of a XRADIA test pattern (gold mask on a 500x500 μm^2 Si_3N_4 window) stored in a LiF film, about 1 μm thick on a glass substrate, and read by a CLSM in fluorescence mode. All the mask details were recorded. Figure 13b shows the optical absorption spectra of LiF crystals irradiated with different exposure times. The formation of stable primary F centres and aggregated defects was derived by the presence of the main F and M absorption bands.

LiF radiation detectors for imaging of high energy particle beams

LiF thin films deposited by thermal evaporation on several substrates and in different growth conditions have been proposed as LiF-based detectors for high energy particle beams characterization. They are based on the optical reading of PL radiated by F_2 and F_3+ colour centres. To test their sensitivity and get preliminary information about the characteristics of the LINAC high-energy electron beam (UTAPRAD-SOR), in particular to measure its intensity spatial profile and angular divergence, LiF-film radiation-imaging detectors were irradiated in air at a distance

A

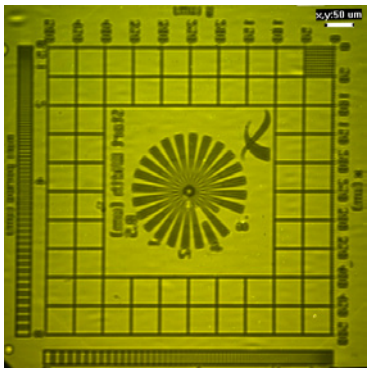

B

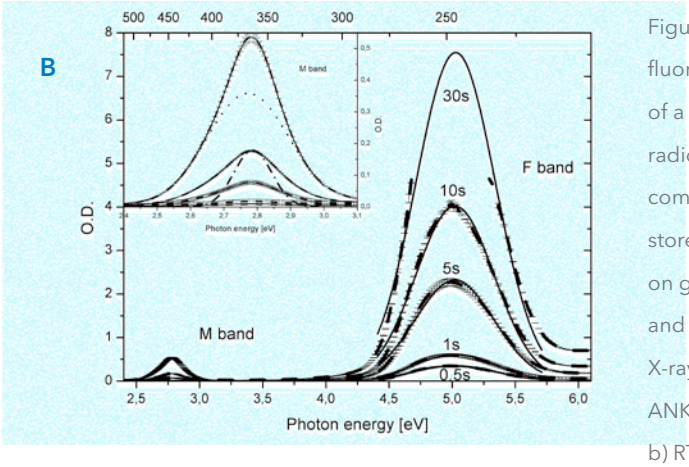

Figure 13 a) Confocal fluorescence image of a X-ray micro-radiography of a commercial test pattern stored in a LiF film on glass substrate and irradiated by the X-ray white beam at ANKA synchrotron. b) RT absorption spectra of LiF crystals irradiated by the X-ray white beam at ANKA synchrotron for exposure times from 0.5 to 30s (dashed curves). The best fitting by Gaussian bands are also reported (solid curves). In the inset a magnification of the M absorption band is reported together with the interpolation obtained with two superimposed Gaussian bands, whose contributions are shown for an exposure time of 30s with dash dotted (F_2) and dotted (F_3+) lines.

of 30 cm from the titanium exit window of the high-energy electron LINAC source. Similar preliminary tests are also under way for a 7 MeV proton linear accelerator (UTAPRAD-SOR).

LiF thin films grown on plastic substrates for EUV imaging

LiF films of thickness between 500 nm and 1.5 μm were deposited by thermal evaporation on plastic, flexible and adhesive substrates kept at RT during the growth. Under exposure to ionizing radiations of these LiF thin films at the EGERIA soft-X ray source (UTAPRAD-SOR), it was possible to store predetermined invisible markings, based on the stable formation of visible-emitting F_2 and F_3+ colour centres. The irradiated LiF films on different plastic substrates, even flexible and adhesive, can be used as tags for the identification and the traceability of goods. Work is in progress to study and improve their quality.

^{6}LiF thin films for functionalized thermal neutron sensors

Measurements of thermal neutron fluxes are needed in several experimental and technological environments, such as in the field of nuclear applications (decommissioning and storage of radioactive waste, mapping the flux in the out-of-core regions of fission reactors). In collaboration with Istituto Nazionale di Fisica Nucleare-Laboratori Nazionali del Sud (INFN-LNS), a compact and cheap prototype of thermal neutron detector was investigated. It is well known that 6Li isotope can be employed as neutron to charged particle converter by mean the following nuclear reaction

$$^6Li + n = {}^3H + {}^4He + 4.78\ MeV$$

The capture cross-section is of around 960 b for thermal neutrons and scales down as the inverse of neutron velocity with increase in kinetic energy. LiF films, few μm thick, were grown by thermal evaporation on glass substrates starting from LiF powder enriched to 95.6 % in

^{6}Li. A LiF film was assembled in a suitable mechanical structure in contact with the middle point of a bundle of nine plastic scintillating fibres coupled to a pair of tiny silicon photomultipliers (Fig. 14). The results of the tests proved that the technique is indeed feasible and promising. The direct growth of ^{6}LiF thin films on the surface of the plastic scintillating fibers may improve the performances of these radiation sensors.

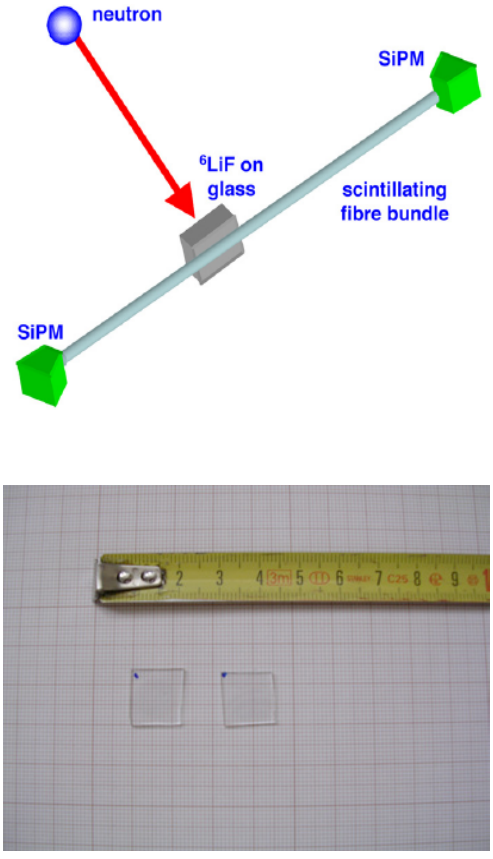

Figure 14. Schematic view of the detector setup, a). Photograph of two 6LiF films, thickness = 1.4 μm, grown on glass substrate, b).

2.6. Optical fibre FBG (Fibre Bragg Grating) sensors

FBG sensors are optical fibre sensors that allow the development of monitoring systems of various parameters, such as temperature, deformation, pressure, humidity. FBG sensors are well suited for applications in many fields, from Structural Health Monitoring of large civil engineering structures to measurement of biomedical parameters and physiological variables for diagnostic and surgery. In the MNF laboratories monitoring systems based on FBG technology are currently been developed and applied for both R&D activity and industrial applications.

Structural monitoring of large civil engineering works

FBG sensors allow the development of structural monitoring systems well suited for permanent and long term applications on civil engineering works. Monitoring systems based on FBG sensors have been developed and installed by MNF laboratories on both modern civil engineering works and historical architectural complex. Various monitoring systems installed in previous years have been managed and periodical measurement campaign have been done.

Scheduled measurement campaigns have been performed using the monitoring system previously installed on retaining walls made in San Giuliano di

Puglia within the earthquake reconstruction works of the town. Acquired data are analysed in cooperation with the ENEA UTPRA-PREV laboratory. Figure 15 (left) shows on-site measurements made by use a mobile laboratory installed on rover vehicle; the inset shows the patch-panel with optical connectors to access the FBG sensors deep embedded in the concrete reinforced pillars.

The monitoring system developed for the sporting complex 'Città dello Sport', already exploited to verify the correct curing of massive concrete pouring, has been used for scheduled structural control and will be used to measure the static settlement of beams and pillars during the future construction works of the huge dome metallic frame. The application is run in cooperation with the Department of Civil Engineering of Rome University 'Tor Vergata'.

Structural monitoring for Cultural Heritage

The monitoring system previously installed on the archaeological complex of the Aurelian Walls of Rome has been used for scheduled measurement campaigns of the opening of cracks in masonry elements. The activity has took place in cooperation with the Department for Cultural Heritage of the Municipality of Rome. Figure 15 (right) shows an aerial view of the monitored section of the roman ruins of the Mura Aureliane; the inset shows the ending of the optical fiber backbone used to collect the signal from FBG sensors installed along the guard pathway and the guard towers.

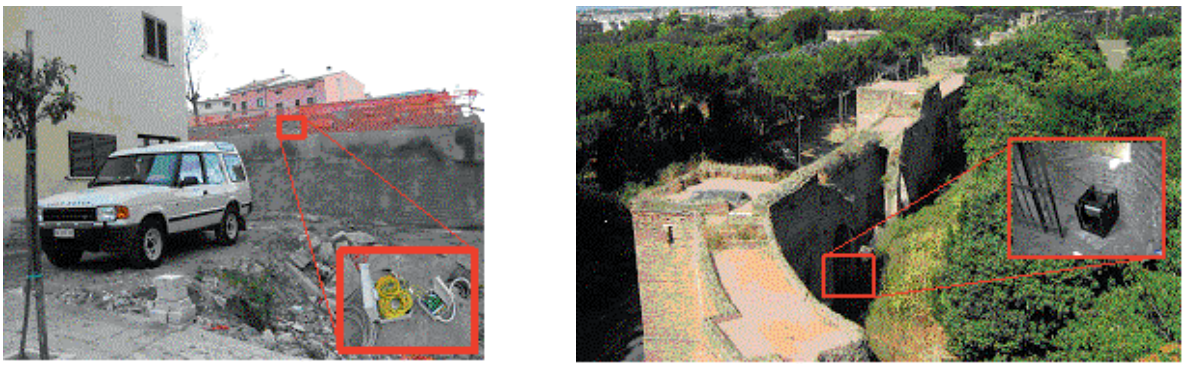

Figure 15. Structural monitoring of civil engineering works. Left: on-site monitoring of retaining walls by mobile laboratory; the inset shows the patch-panel with optical connectors to access the FBG sensors embedded in the concrete pouring. Right: aerial view of the monitored section of the roman ruins of the Mura Aureliane; the inset shows the ending of the optical fiber backbone used to collect the signal from the installed FBG sensors.

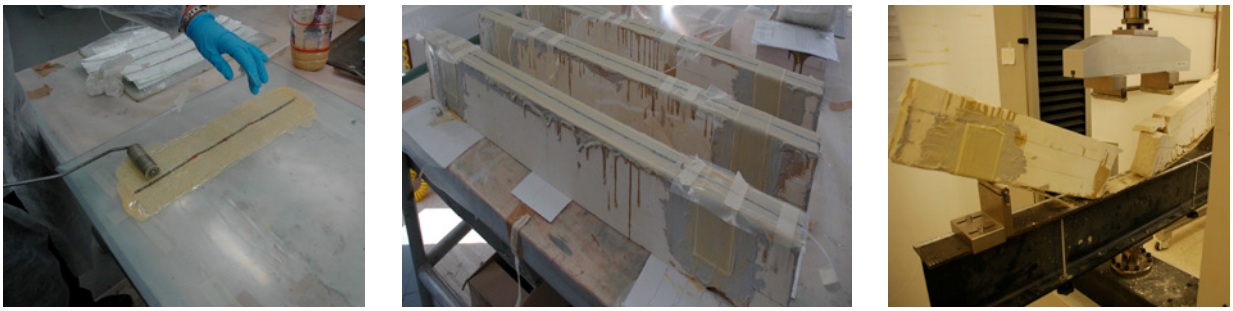

Fig.16 Left: production of a smart FRP patch. Middle: beams prepared with smart patch on upper surface, to be tested by four-point bending test. Right: four-point bending test till beam cracking.

Development of Smart Composite Materials

In the last years, within R&D activity for public funded projects, large experience has been achieved in the MNF laboratories about use of FBG sensors in the development of 'smart' composite materials, i.e. composite materials with embedded sensors that allow monitoring the experienced thermal and structural stresses.

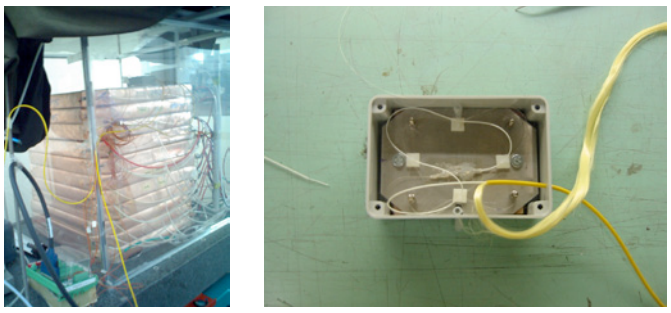

Figure 17. Monitoring temperature of gas mixture fluxed in closed-loop pipe of high energy physics detectors. Left: the RPC detector used for the development of the gas temperature sensor; Right: FBG temperature gas sensor prototype being installed in sealed tubing box.

In the framework of the Research Project 'MAMAS', closed in August 2011, the MNF laboratories have worked as consultant of Consorzio CETMA for the development of effective solutions for 'in-the-yard' production of smart composites for civil engineering retrofitting works. In particular, work was done in order to assist the development and validation of two types of smart FRP (Fiber Reinforced Plastic) devices with embedded FBG (Fiber Bragg Grating) optical sensors, conceived for both structural reinforcing and health monitoring. In the former device the developed FRP packaging gives to the optical fiber the necessary protection against accidental damaging during handling and installation, allowing also structural reinforcing. In the latter device the FRP packaging consists of a FRP rebar, conceived for internal or NSM (Near Surface Mounted) applications. Figure 16 shows the production of a smart FRP patch, test beams with smart FRP patch applied on the upper surface ready for four-point bending test, and test performed till beam cracking.

Development of functionalised FBG sensors for environment monitoring

The scientific community is currently hardly working to apply the FBG technology to make sensors suitable for monitoring environment parameters, such as temperature, humidity and chemical species concentration of mixture.

The MNF laboratories are working on such task in cooperation with INFN-LNF and the Dept. ICMA of Sapienza University of Rome in the framework of the GASP project of the 2010-2012 PRIN (Programmi di Ricerca di Interesse Nazionale). Work is in progress to develop a novel optical fiber sensor for the monitoring of gas temperature. Results so far obtained assess the feasibility of both various reference industrial applications and a challenging research application aimed to perform real time monitoring of temperature and environmental variables for the gas system of the RPC (Resistive Plate Counters) of the CMS (Compact Muon Solenoid) experiment currently run at CERN (European Centre for Nuclear Research). Figure 17 shows the sensor gas prototype being mounted and the experimental RPC detector in the ASTRA experimental Hall of the INFN-LNF used to perform calibration tests of the sensor prototype.

2.7. Seismological activities

The activities in seismological field, performed in strict cooperation with the ENEA UTPRA-PREV laboratory, concern the evaluation of seismic hazard at regional and local scale by the acquisition, interpretation and analysis of geological, geotechnical, geophysical and historical data. A significant effort has been devoted to the analysis of data and information related to seismological and engineering studies, also by the realization of original computer algorithms, relational databanks and GIS / Web-GIS applications. The main results obtained in seismological field are here reported.

Seismic microzonation of some Latium Region Municipalities

Following the research projects funded by Latium Regional Administration in 2010, a new Research Agreement was signed in 2011 for the application of the seismic microzoning techniques reported in Regional Guide-Lines in some Latium Municipalities, namely Borgo Velino, Petrella Salto, Fiamignano (Province of Rieti); Isola del Liri, Gallinaro (Province of Frosinone). In detail the activities were focused on the realization of Level 1 seismic microzoning, consisting in the identification of areas characterized by a homogeneous seismic response. The collection and interpretation of geological, geotechnical and geophysical data from archives and bibliography allowed the re-

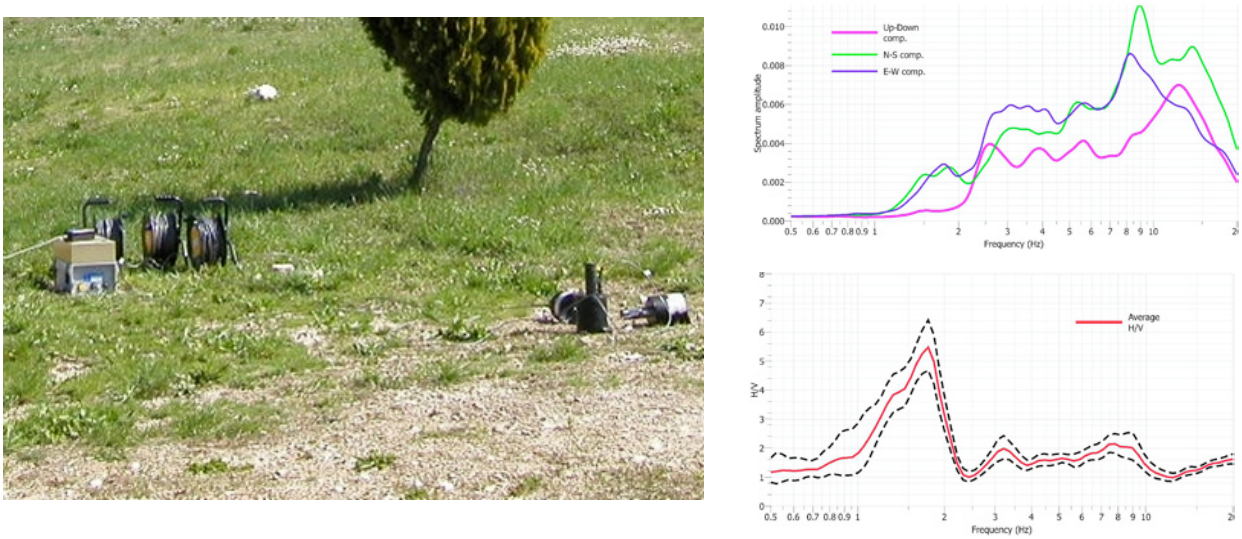

Figure 18. Site recording of ambient noise obtained by a Kinemetrics data acquisition system consisting of one K2 Digital Recorder connected to three SS1 velocity transducers, one for each component (N-S, W-E, Up) of the ground motion (left). Example of elaboration by the Nakamura's technique: plot of the Fourier spectra of the 3 components of ambient noise North-South, West-East and Up-Down (right-up); average spectral ratio of the Horizontal vs. Vertical components showing in this case a resonance frequency of the site at 1.8 Hz (right-down).

construction of a preliminary geological model of the studied areas. On this base, geophysical surveys were planned and executed in order to analyze the dynamic characteristics of the local deposits by the Nakamura ambient noise H/V spectral ratio technique (Fig.18). Parallel field geological surveys provided information for the final geological models. By a cross analysis of the acquired geological, geotechnical and geophysical data, a zonation of areas homogeneously susceptible of local seismic amplification was obtained for each Municipality (Fig. 19).

The ENEA Strong-Motion Database

As result of an activity executed in the last years by ENEA laboratories, the collection and processing of ground motion time-histories recorded by an accelerometric network specifically settled in Umbria Region (Central Italy) was performed. Subsequently, a Strong-Motion Database was implemented in form of a relational database stored on a CD available for distribution. (Fig. 20).

The Database includes up to 117 recordings mainly acquired during the 1997 Umbria-Marche seismic series in Norcia, Cerreto di Spoleto, Foligno and Preci. The CD contains also seismological and

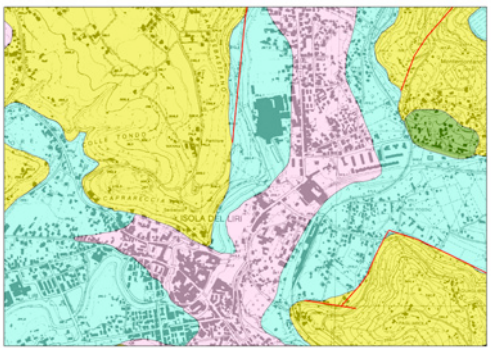

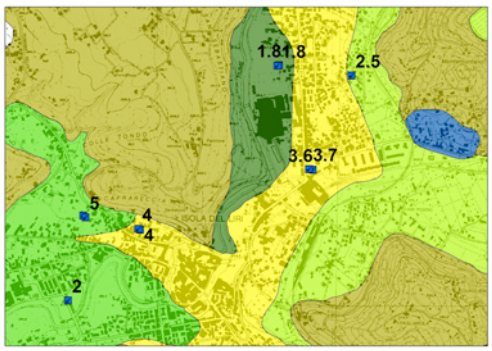

Figure 19. Geological model of Isola del Liri downtown surroundings: in the plain area alluvial deposits of the Liri river (light blue) and travertine (pink) are located; on the hilly area (yellow) conglomerate deposits outcrop (left). Sketch of areas with different susceptibility to seismic amplification obtained crossing the geotechnical and geophysical characteristics of the local deposits and the results of ambient noise surveys in terms of resonance frequencies (right).

macroseismic data of the recorded earthquakes, together with the raw time-histories and the output of ENEA processing in form of corrected time-histories (acceleration, velocity and displacement of the ground-motion), elastic response spectra and peak values. The data can be viewed in graphic form and exported as numerical data in ASCII format. The CD has been produced in 1000 copies and distributed to several National and International Scientific Institutions.

Historical sources on 1898 Rieti earthquake

One of the tasks of the Research Agreement signed by Latium Regional Administration and ENEA concerned the analysis of an historical earthquake representative for the local hazard. The earthquake of 1898 was considered one of the most important earthquakes for the Rieti Province. The archive researches in the National Archives of Rieti (ASR) conducted to an agreement signed by ENEA and ASR in order to digitalize all the archive documents regarding this earthquake. The images have been collected, processed and stored in a DVD with other historical sources (newspapers, pictures and

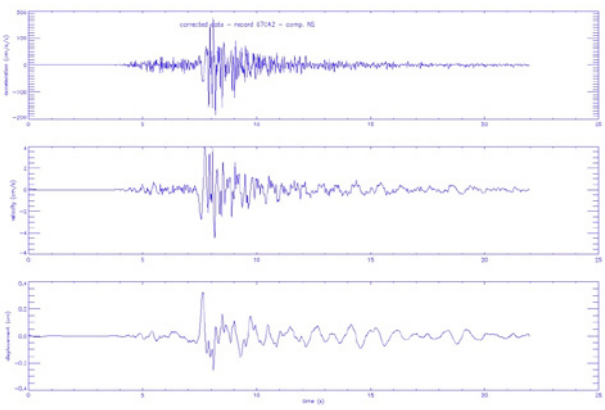

Figure 20. Front page of the ENEA Strong-Motion Database available as an interactive CD (left). Example of acceleration, velocity and displacement time-histories contained in the relational database (right).

Figure 21. Home page of the DVD archive containing the historical sources on 1898 Rieti earthquake (left). Example of navigation in the DVD archive in order to search and read the archive documents (right).

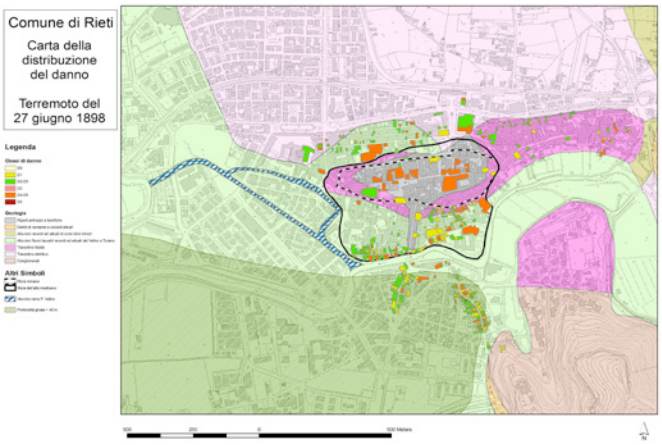

Fig.22. Distribution of the damages caused by the 1898 earthquake in the downtown of Rieti. The colour scale from yellow to green to dark red represents the increase of the damage level on buildings. The pastel colours indicate the geology of the area: brown represents conglomerates; dark and light pink, more or less lithoid travertine; dark and light green, alluvial deposits with different thickness; grey, debris or filling material due to human activity. The distribution of damages is in good agreement with the different geotechnical characteristics of the outcropping deposits.

scientific - technical articles) regarding the same earthquake (Fig. 21). This work is important for the study of Italian history in late nineteenth century especially during an exceptional event like an earthquake. All documents are now available on line at the URL: http://www.asrieti.it/PUBBLICAZIONI/terremoto/index.htm). One of the possible use of historical documents in studies focused on seismic risk reduction concerns the analysis of damage distribution compared to the geological characteristic of the area (Fig. 22).

Classification of national seismic hazard by means of statistical parameters

Main objective of this work was to obtain a seismic hazard map of Italy, based on an analysis of the probability distribution of the ground acceleration parameter. The input data consisted in the intercept values of the uniform hazard response spectra corresponding to a probability of exceedance up to 10% in 50 years (T = 475 years, see INGV, http://esse1.mi.ingv.it). The methodology was designed to fulfill a classification of the national territory, particularly taking into account the coherence of shape and the similarity of spectral curves, by the use of a cluster analysis procedure (Fig. 23). In second instance, a comparison was performed between the results obtained by applying the same methodology to data from two different sources: probabilistic hazard data provided by INGV on the one hand and data obtained in compliance with Italian Technical Code for Construction (Decree of the Ministry of Infrastructure of January 14, 2008) on the other hand. The final result was a map highlighting the differences between the requirements of the Italian Technical Code and the probabilistic hazard data provided by INGV (Fig. 24).

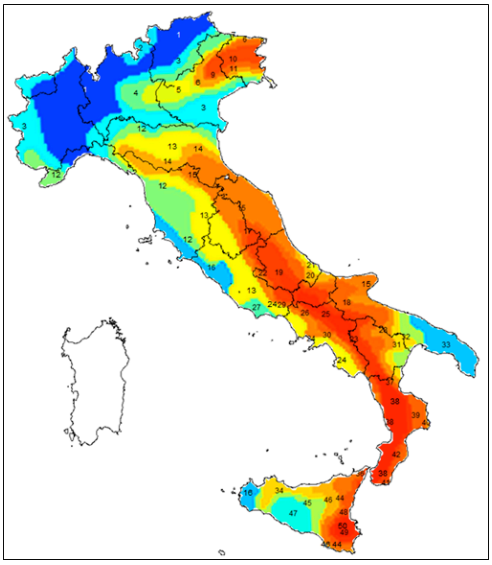

Figure 23. Cluster analysis on INGV data: numbers represent the highlighted clusters; colours from cold to warm represent the increase of a synthetic hazard index. This index is expressed by median value of acceleration spectra integral, from a minimum of 0.045g to a maximum of 0.667g.

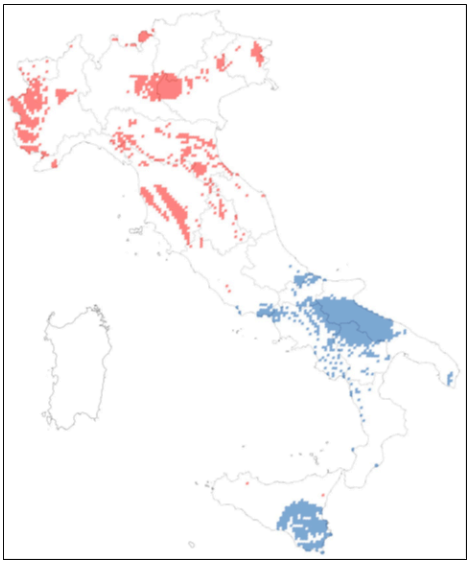

Fig.24. Map of the statistical significant differences between the results obtained from the two considered seismic hazard data sets: in red areas with $p \geq 0.01$ of a positive difference; in blue areas with $p \leq 0.01$ of a negative difference.

3 RADIATION SOURCES LABORATORY

3.1. Mission and infrastructures

The Radiation Source Laboratory (UTAPRAD-SOR) performs R&D work in the fields of generation of coherent radiation and in the acceleration of charged particles. Research activities include emerging technologies in photonics and microlithography, development of laser systems and accelerators for scientific, industrial and medical applications.

Current activities are focussed on:

- Design and constructions of high energy-per-pulse excimer lasers, plasma driven X-ray sources and their applications;
- Design and constructions of Free Electron Laser (FEL) sources for the generation of electromagnetic radiation in the Far InfraRed and in the Terahertz region;
- Development of low-energy electron accelerators for material processing, medical applications and as a driver for FELs;
- Development of medium-energy proton accelerators for cancer therapy
- Development of cybernetic models, artificial vsion and automation systems.

These activities are undergoing a rapid development worldwide with an increasing number of applications such as microlithography in the extreme ultraviolet, X-ray microscopy of biological systems, effects of electromagnetic radiation, imaging systems applied to material characterization, biology, biomedicine and, more recently, art conservation studies.

The facilities formerly developed by UTAPRAD-SOR and utilized for current activities include:

- Excimer laser laboratory
- Soft X-ray plasma sources laboratory
- Compact FEL (90 – 150 GHz)
- FEL-CATS (400 – 700 GHz)
- TOP-LINAC
- 5 MeV Electron LINAC

Funding and projects

2011 has seen a considerable effort of the Laboratory in updating the existing infrastructures to host the new accelerator for proton therapy IMPLART, a project carried out in collaboration with the National Institute of Health and IFO (Institute Physiotherapy Hospital, Rome) and funded by the Regional Government of Lazio. This effort has also required the design and implementation of new safety systems for all electron and proton accelerators operated by UTAPRAD-SOR .

As to new project proposals, in response to a call of the Ministry of Education, University and Scientific Research (MIUR), the Laboratory UTAPRAD-SOR has submitted a proposal for creation of the Center for Interdisciplinary Studies CARMINE " Center for Advanced Research Methods and Instrumentation for the Environment ", dedicated to the development of research projects, training and dissemination of innovation in the agro-environmental field in the Plain of Sybaris in Calabria. Partners of the initiative are: ENEA, Italy Telecom, University of Calabria, Mediterranean University of Reggio Calabria, Enetel Srl, the District Agricultural and Food Quality of Sybaris. The interdisciplinary character of the Centre, and in particular its research and training activities, will also contribute in other areas, such as, cultural heritage, renewable energies,tourism and ICT.

Within the program "Security" of FP7, the SOR Laboratory has also propposed a " Capability Project" coordinated by ENEA in response to the invitation-SEC 5 ¾/2012 entitled ACTIVA " Terahertz imaging and millimeter waves active in aviation Infrastructures".

The Radiation Source Laboratory is also actively involved in the realization of the SPARC/X FEL, a joint project between ENEA, CNR, INFN and the University of Rome "Tor Vergata", aimed at the development of a Free Electron Laser in the VUV and X-ray regions.

In the following a brief review of the above activities is reported together with the most recent results and perspectives.

3.2. Short-wavelength Sources and Applications

In the extreme ultraviolet (EUV) spectral region (20 eV - 280 eV) laser-plasma and discharge-plasma sources can produce energies per pulse and repetition rates sufficient to be considered a valuable alternative to synchrotrons and short-wavelength free-electron lasers (X-FELs) in many irradiation experiments, namely when the peak power and the brightness are more important than the average power and when a narrow spectral band is not required.

In past years the SOR Laboratory has developed a Micro-Exposure-Tool (MET) for micro- and nano-lithography. The MET is a complex apparatus comprising a laser-driven plasma source called EGERIA, a debris mitigation system, an optical collector and an accurate optical projection system able to print a pattern with a spatial resolution better than 100 nm. Detailed information can be found on the website: **www.frascati.enea.it/Impianti/SorgenteRi-X%20da%20laser-plasma/SorgenteR-Xdalaser-plasma.html**.

It is worth mentioning two experimental activities, concerning, respectively, the surface coloration of linen textiles for reproducing archaeological images and the proof of a novel anti-counterfeiting system based on an invisible writing method which uses lithographic techniques on luminescent materials. The experimental results have shown that this technology is suitable to fabricate robust anti-counterfeiting tags, which are almost impossible to counterfeit and can be applied to almost every kind of objects, independent of their shape and size. This technology is patent-pending.

Discharge-plasma source of EUV radiation

During 2011 the work on the Discharge Produced Plasma (DPP) source of Extreme Ultraviolet (EUV) radiation has been devoted to the characterization and optimization of the apparatus as well as to an application of the DPP in the framework of the anti-counterfeiting technique developed by ENEA.

As shown in Fig. 1, the DPP is supplied by a 50 nF glycol cylindrical capacitor (C1) which produces a high voltage (18 kV) and high current (10-11 kA) electric discharge in a low pressure xenon gas contained in a short (7 mm) alumina capillary tube. The high magnetic field (> 1 T) generated by the current, pinches the gas toward the capillary axis, thus increasing the temperature up to approximately 30 eV.

After a further optimization of the gas flow and of the discharge electrodes shape and, after an improvement of the charging circuit, the peak current has now been increased approximately by 10%, the EUV pulse duration has overcome 100 ns, and the temporal behav-

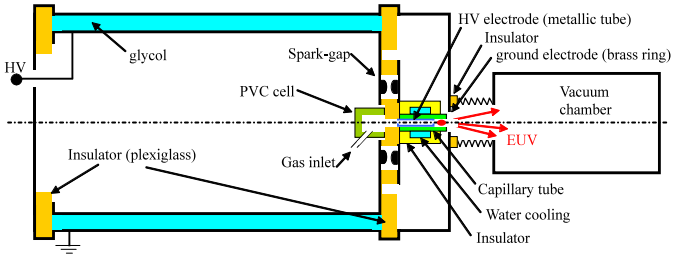

Figure 1: Schematic of the DPP source.

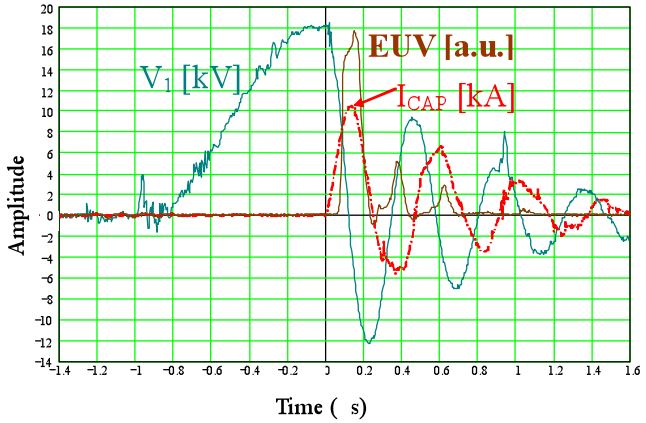

Figure 2: Temporal evolution of the voltage on the cylindrical capacitor (V1), of the discharge current in the capillary tube (ICAP) and of the EUV emission power in the 10-20 nm spectral region.

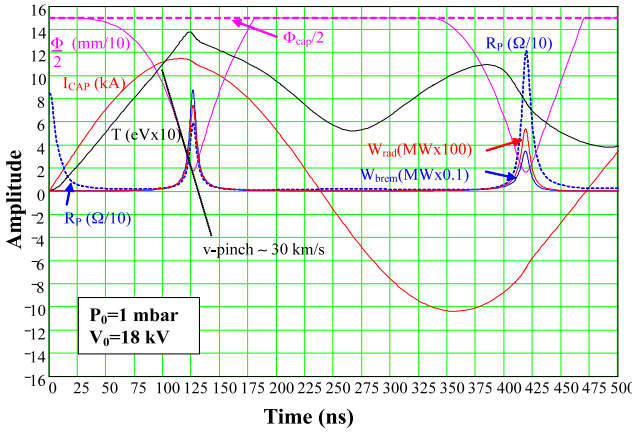

Figure 3: Temporal evolution of the discharge parameters simulated by the simplified numerical code for an initial gas pressure of 1 mbar and a C1 charging voltage of 18 kV. See text for symbols explanation.

iour of the EUV emission, detected by a Zr-filtered PIN diode, is characterized by multiple pulses corresponding to the discharge current oscillations, as shown in Fig. 2. In these conditions the total energy in the 10-20 nm wavelength band has reached approximately 20 mJ/shot.

The DPP source can now be operated for long time (hours) at 10-20 Hz repetition rate with a 3% r.m.s. pulse energy stability (improved by almost a factor two with respect to the previous configuration, see Progress Report 2010). Its efficiency is the same of high-quality commercial sources and its reliability is demonstrated by several successful applications, like the anti-counterfeiting dedicated exposures described below.

In order to better understand the DPP pinch behaviour, a simplified numerical code has been developed: as shown in Fig. 3, the plasma column diameter ø collapses at a speed as high as 30 km/s, reaching a minimum diameter approximately one order of magnitude smaller than the initial one. At the maximum of the plasma compression, the discharge resistance RP grows quickly thus generating a peak of the plasma emission (in the whole spectrum starting from IR up to X-rays) both by lines transitions (Wrad) and by Bremsstrahlung (Wbrem). This peak of emission probably corresponds to the tip at the end of the first pulse of the EUV radiation experimentally measured in the 10-20 nm range (see Fig. 2). Even the multiple emission by the current subse-

quent oscillations is well reproduced by the code (see Fig. 3).

The source size has been estimated by imaging the source on a suitable EUV sensitive film (Gafchromic HD-810 film) through a multi-pin-hole camera; in this way the source has been imaged simultaneously from different directions with respect to its axis. As an example, Fig. 4 shows the source image obtained for a viewing angle of ~20°. Based on the demagnification factor (1/4 in this experiment) and on the pin-hole diameter (70 μm) a source size of approximately 200-300 μm has been estimated.

The clean emission (almost debris-free) of this source makes it particularly suitable for applications to direct EUV treatment of different materials. As an example, a test exposure of a Lithium Fluoride (LiF) crystal has been performed. After few thousands shots (about 10 minutes exposure) at 10 cm from the source, very intense luminescent patterns, shown in Fig. 5, have been obtained without any visible damage to the LiF surface. The high resolution shadow of the supporting structure of a zirconium filter placed in contact with the crystal is well visible in the image and this confirms the absence of significant blurring, thanks to the small size of the source.

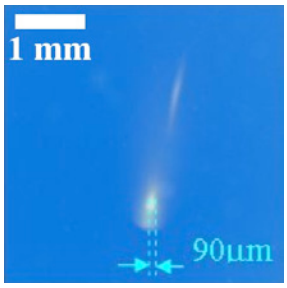

Figure 4: DPP source image on a Gafchromic HD-810 film obtained by a 70 mm in diameter pin-hole camera at a viewing angle of 20° off-axis. The size of the high intensity disk (90 μm) is just a bit larger than the pin-hole one, while the low intensity smudge belongs to a very low energy part of the spectrum (it disappears when limiting the spectrum to the 10-20 nm range by a zirconium filter).

The DPP is now a reliable EUV source and it can be considered complementary to the other EUV source of the Laboratory (the laser plasma source EGERIA). While EGERIA allows to write patterns at very high spatial resolution (~90 nm) through its EUV projection tool and to expose samples to radiation at higher than EUV spectral energies (XUV), the DPP allows a direct and debris-free EUV exposure over a wide cone of emission (~1 sr) at average power levels higher than the EGERIA ones.

A B C

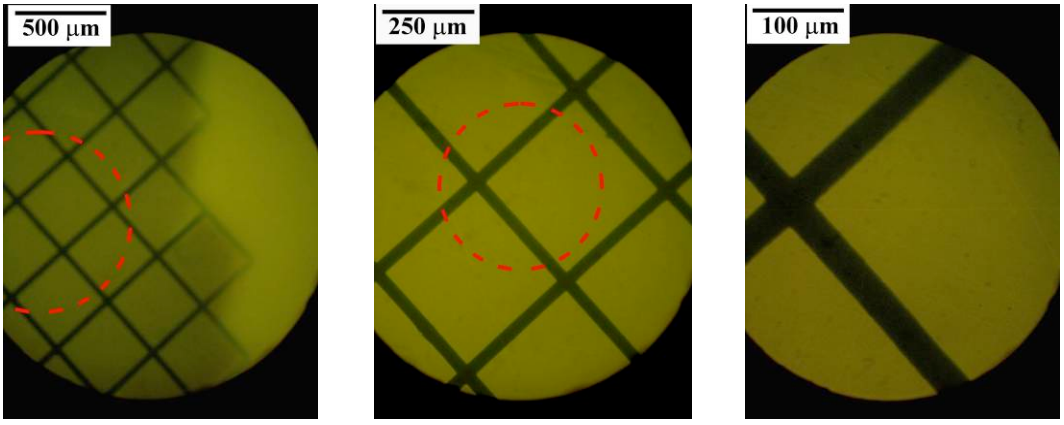

Figure 5: Images of a LiF crystal (partly covered by a Zr filter) exposed to 8000 DPP shots at a 10-cm distance from the source, observed by a fluorescence microscope at different magnification levels: 10x (a), 20x (b) or 50x (c) objective. In a) and b) a dashed circle highlights the region respectively enlarged in b) and c) .

Experiments with other gases aimed at the radiation emission in spectral energy ranges higher than the EUV are planned in the near future.

Anti-counterfeiting ENEA technology: new applications

In contrast with other anti-counterfeiting techniques, like for example those based on the use of fluorescent inks, the ENEA patented (patent number RM2008A000218 and EP2266115) anti-counterfeiting technique is based on writing invisible pattern by exposing LiF films to EUV radiation (through a mask) rather than by ink jet. Consequently the spatial resolution can be orders of magnitude better. After the successful demonstration of this anti-counterfeiting technology on an identification badge (see the Activity Report 2010), in 2011 other objects have been tested by using the DPP as EUV source.

For this purpose, LiF films were evaporated, at the UTAPRAD-MNF Laboratory, on thin plastic transparent tags, showing the ENEA logo and the schematic of the lithium atom (see Fig. 6a), which could be stuck on whatever item. Films were exposed to few thousand shots of the DPP at about 10 cm distance from the source. A 0.1 mm thick mask having the "E" letter was placed almost in contact with the film during the irradiation. Figs. 6b and6c show the appearance of the letter only when the tag is properly observed.

The list of most frequently counterfeited items includes also microelectronic components. To demonstrate the applicability of the ENEA technique also to this type of objects, LiF films were evaporated (at the UTAPRAD-MNF Laboratory) on the surface of several packaged integrated circuits and exposed to the EUV radiation from the DPP source as done for the tags, but with the ST Microelectronics logo in the mask. Both in the case of metallic and plastic packages the results were very good, notwithstanding a peak-to-valley roughness of the substrate surfaces up to 10 μm. As shown in Figs. 7a and 8a, the patterns are absolutely invisible at naked eye (even if observed under a microscope with white light illumination, see Fig. 7b), while they are easily readable by a microscope in fluorescence mode, as evident from Figs. 7c and 8b.

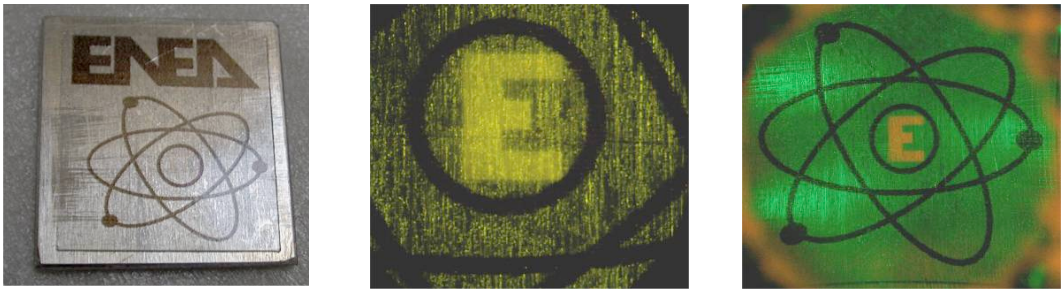

A B C

Figure 6: Plastic adhesive transparent tag stuck on a rough metal plate where, in the area corresponding to the central circle (4 mm in diameter), a LiF film has been deposited and then exposed through a metallic mask to the EUV radiation from the DPP. (a) the tag observed when illuminated with natural light. (b) Same tag observed by a microscope at low magnification (2.5x objective) in fluorescence mode or (c) by a simple lens equipped with proper filter and illumination.

A

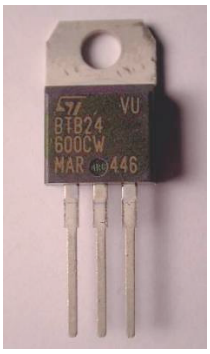

B

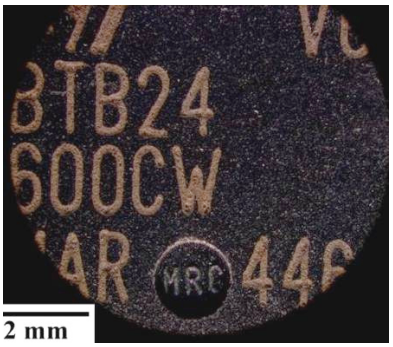

C

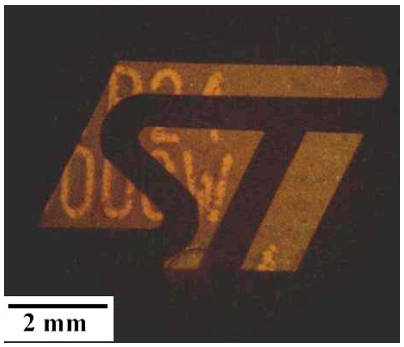

Figure 7: (a) Standard transistor with plastic packaging covered by a LiF film and exposed through a metallic mask to the EUV radiation from the DPP, as observed when illuminated with natural light. The treated area is observed by a microscope at low magnification (b) with white light illumination and (c) in fluorescence mode.

The exposed samples are a validation of the real feasibility of a writing tool for anti-counterfeiting tags/labels production based on the ENEA technique.

Figure 8: Standard transistor with metallic packaging covered by a LiF film and exposed through a metallic mask to the EUV radiation from the DPP, as observed (a) when illuminated with natural light and (b) by a simple lens equipped with proper filter and illumination.

Irradiation of linen fabrics

In the frame of experiments of Shroud-like coloration by UV and VUV lasers (see Progress Report 2010) one wonders about the differences between the linen fabric that is used in the Lab and the linen of the Shroud of Turin, besides the age. To this end, we measured some additional optical characteristics of our linen to be compared with the linen of the Shroud. For this purpose, we used a spectrophotometer Perkin-Elmer Lambda 950TM, equipped with a 15-cm-diameter integrating sphere. The interior of the sphere is covered with a plastic material known as Spectralon, whose characteristics of reflection are almost 100% Lambertian and constant over the whole spectrum UV-visible-near infrared. Additionally, this instrument has an internal calibration of the Spectralon, which allows to directly obtain absolute reflectance spectra.

In collaboration with UTTMAT-OTT we measured the hemispherical absolute spectral reflectance R(λ) (i.e. the percentage of light reflected by our linen with

A

B

Figure 9. The solid lines show the absolute reflectance of the linen of the Shroud, in areas of no-image as a function of the wavelength. The dashed line shows the absolute hemispherical reflectance R(λ) of the linen used in our experiments.

respect to the incident light) and the results are shown in Fig. 9, together with the results of spectral reflectance measured on the Shroud.

Figure 9 shows that the reflectance spectrum of our linen is similar to that of the Shroud. There is a small difference in the spectral region between 520 nm and 600 nm, showing our linen is less yellowish than the Shroud, possibly because of the different age. Most important, the absolute reflectance at the laser wavelengths we used, 193 nm and 308 nm, is almost the same. Thus, from the optical point of view, when irradiated in the UV and VUV our linen behaves like the linen of the Shroud.

Using the same spectrophotometer we also measured the hemispherical transmittance T(λ) of the linen (i.e. the percentage of light transmitted by our linen with respect to the incident light) as a function of wavelength. Then, knowing R(λ) and T(λ) we can deduce the spectral absorbance A(λ) as follows:

$$A(\lambda) = 1 - R(\lambda) - T(\lambda)$$

that is, A(λ) is the amount of light absorbed by linen as a function of wavelength, and the results are shown in Fig. 10.

In order to verify experimentally whether the UV and VUV light emitted by our excimer laser interacts with the linen by photochemical processes, without inducing a significant heating of the irradiated fabric, in collaboration with Padua University we used the infrared camera ThermoShot F30 equipped with micro-bolometers sensitive in the spectral range 8 μm - 13 μm. This camera is able to measure the surface temperature of objects with the uncertainty of 0.2 °C.

The camera was aligned in front of the linen during laser irradiation, monitoring in real time the temperature of the whole linen fabric, both in the irradiated and non-irradiated areas. Figures 4.2.11a and 4.2.11b show the results. During laser irradiation the room temperature was ranging between 20 and 21 °C, and the linen region irradiated by the XeCl laser (λ = 0.308 μm) was heated up to 33 °C, while the linen irradiated by the ArF aser (λ = 0.193 μm) was just heated up to 25 °C. It is known that thermal effects can color the linen only when the linen temperature approaches 200 °C, and we can conclude that excimer laser coloration is due to a photochemical process that does not involve significant thermal effects.

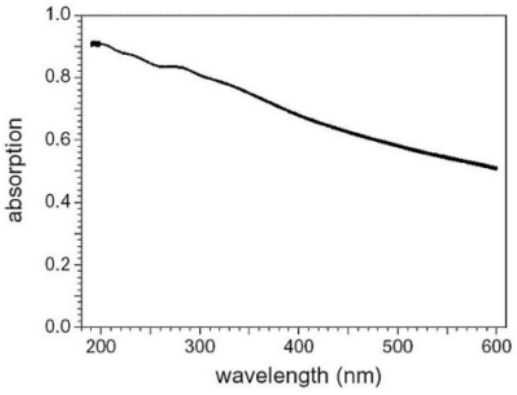

Figure 10. Plot of the absolute value of the absorbance of the linen vs. the wavelength

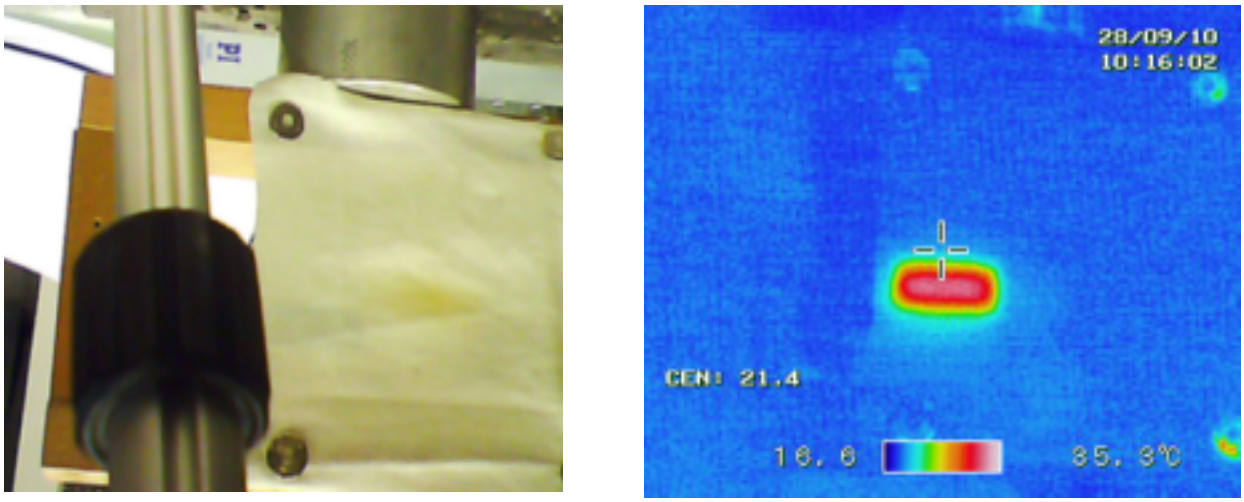

Figure 11a. Left: photo in visible light of the linen during XeCl laser irradiation. The area irradiated is visible as a yellowish spot. On the right, the same picture in infrared light, where the area irradiated by the XeCl laser is well visible. The color scale at the bottom allows to ascertain that the hottest region of the linen (in the middle of the laser spot) reaches 33 °C, while the non-irradiated area is at the temperature of 20 °C.

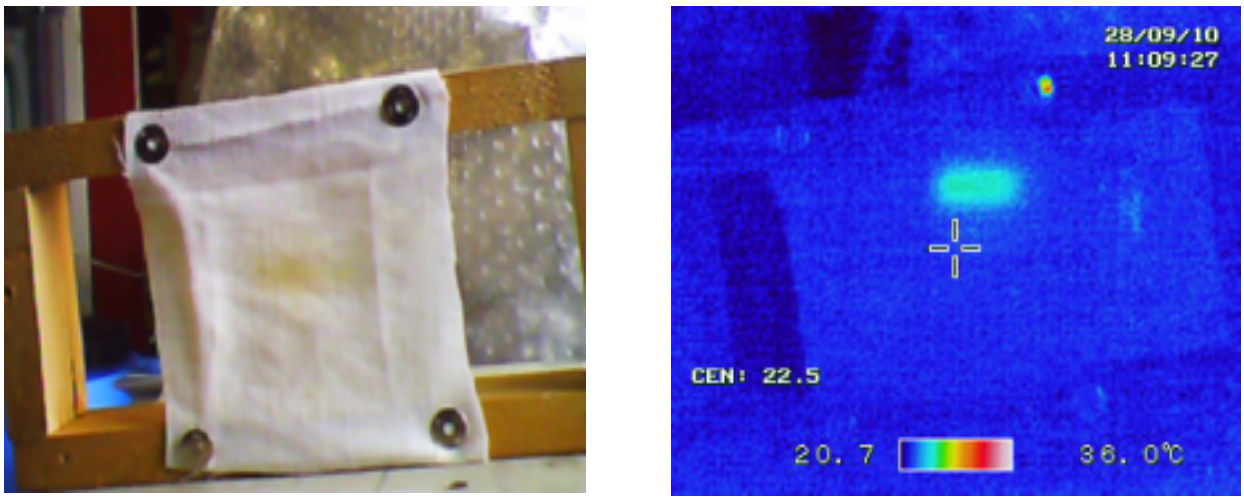

Figure 11b. Left: photo in visible light of the linen during ArF laser irradiation. The area irradiated is visible as a yellowed spot. On the right, the same frame seen in infrared light, where the area irradiated by the ArF laser is well visible. The color scale reveals that the hottest area of the linen (in the middle of the laser spot) reaches 25 °C, while the non-irradiated area is at the room temperature of 21 °C.

3.3. Terahertz Sources and Applications

Terahertz radiation covers the frequency range between 100 GHz and 10 THz (i.e. a wavelength between 3 mm and 30 μm), which spans the spectral interval between the microwave and the infrared regions of the electromagnetic spectrum. THz radiation has been raising a growing interest in recent years due to a variety of applications in the field of biology, biomedicine, environmental sciences and homeland security, in particular regarding the development of imaging techniques that allow the identification and investigation of structural and functional properties of a variety of materials. The development of coherent, tunable and powerful sources of THz radiation is therefore an important issue addressed by a number of research groups in the world.

Terahertz Free Electron Lasers

Two Free Electron based sources of the THz radiation are currently available at the ENEA laboratories in Frascati, covering altogether the spectral range from 90 GHz to 0.7 THz. These two sources are the first two FELs realized in Italy and, as far as the Compact FEL is concerned, it has been the second realized in Europe. Both sources have been described in detail in the 2010 UTAPRAD Report.

The ENEA Compact FEL, is based on a 5 MeV Microtron providing an electron beam with 4 A peak current in 13 ps bunches. The electron beam is injected into a 8-period permanent magnet undulator (λ_u=2.5 cm) and the emitted radiation is stored in a hybrid resonator, which utilizes a WR42 waveguide for transverse confinement of the mode and wire-grids electron transparent mirrors (ETM) for the longitudinal confinement. Peak power in excess of 3kW is obtained in the micropulse at 130 GHz. Micropulses occur with 330 ps spacing in a 4 μs long macropulse, which is repeated at 10 Hz. When the beam is focused to a spot size of about 0.5x1 cm^2 a peak electric field greater than 2 kV/cm is obtained in the micropulse.

The second source, named FEL-CATS, is based on a 2.5 MeV Linac powered by a 15 MW Klystron. The electrons accelerated by the Linac enter into a RF device that correlates their distribution in energy and phase. This correlation creates an intrinsic order within the electron bunch in such a way that coherent emission occurs with a single passage inside the undulator and without the use of any optical cavity. Power levels up to several kilowatt have been measured over a pulse length of about 5 μs. The absence of resonators, and the use of a short length undulator, result in a broad band emission from 400 μm up to 800 μm.

Measurements on art manufacts

Experiments conducted at the ENEA research center of Frascati in recent years, utilizing a Free Electron Laser (FEL) THz source, demonstrated the possibility of measuring the optical properties of materials using nondestructive techniques. In particular measurements were conducted on pigments used for paintings in ancient artworks. The FEL source is ideal for such measurements, because, due to the low duty cycle, it is possible to deliver high peak power to the sample (about 1 kW) while keeping the average power low enough (in the range of mW) to avoid damages or heating of the precious samples.

The reflective THz imaging system at ENEA-Frascati, makes use of the 150 GHz FEL source. The system is capable of measuring the radiation reflected back from a sample and to scan a surface as large as 5x5 cm^2. Since the system has been designed to provide phase information, it is possible to measure simultaneously the topologic characteristics of the sample, together with it's optical properties at the emission frequency of the FEL. Radiation is delivered to the sample by means of a light pipe followed by a waveguide system, which allows the constant comparison of the generated power and the reflected one by means of two directional couplers. This allows the normalization of the signal and the compensation of source fluctuations, keeping constant the performance of the system.

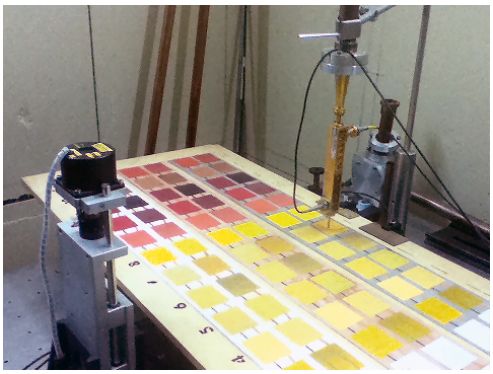

Figure 12.
THz Exposure system for pigments at ENEA-Frascati

Radiation is launched to the sample by means of a truncated WR6 waveguide. The reflection from the sample is injected back into the waveguide and, by changing the distance of the sample, utilizing a stepper motor, it is possible to obtain phase information. Fitting the obtained data with a simple diffraction model it is possible to calculate the optical parameters of the sample (real and imaginary part of the refraction index).

Due to the different optical response, the system is able to distinguish different pigments for imaging applications. Experiments are being carried out at the ENEA Center of Frascati on a complete series of samples provided by CISA3 (Fig. 12). Samples were prepared in 1983 at Editech, Florence. All samples reproduce typical material preparation for painting pigments, used for realizing works of art over the centuries. The combination of 26 different pigments, painted with 5 different thicknesses over 3 different substrates, using 2 different binders results in a total of 780 samples, covering most of the experimental situations.

Figure 13

On all panels visible light analysis, infrared reflectography, B/W and false color IR photography, UV fluorescence and radiographic measurements were performed in the past by M. Seracini at Editech and later by G. Gallio. These results will be compared with the THz data to evaluate how THz spectral reflectivity (TSR) can provide a complementary and/or additional contribution to multispectral analysis of a work of art.

Since THz radiation penetrates dielectrics we expected to be able to identify the response from pigments, binders and substrates: by comparing the optical behaviour of the same pigments with different substrates and binders we will be able to determine the contribution of each component. Four different "wire patterns" were deposited between the substrate and the painted samples using

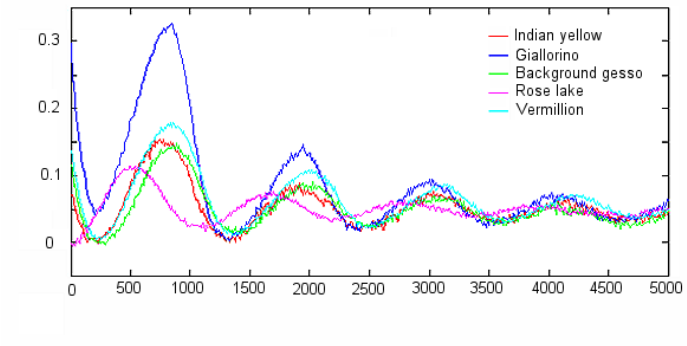

Figure 14: Comparison between different pigments response

the following materials: carbon, lead, silver and yellow ocre. It's important to verify if those materials can be detected under the painting because these are the main components used for the preparatory drawings, usually underlying the final painting.

First measurements were carried out at 135 GHz, but a further improvement could come from the use of the FEL-CATS source, operating in the range from 0.4 to 0.8 THz. The use of sources above 2 THz has to be considered to explore the spectral range where specific fingerprints are expected to appear.

Preliminary measurements were systematically performed on 13 samples with 2 different binders to verify the capability of the imaging device, to determine the optical properties of the samples at 0.135 THz and to verify the relationship between pigments and binders. Hardware and software modifications have been performed on the exposure apparatus in order to avoid unwanted vibrations, that would cause phase errors in the measurements. "On the fly" measurements have been therefore performed, avoiding vibrations arising by the "step by step" procedure and reducing the measurement time.

Experimental results confirmed the possibility of using the system to distinguish pigments in a painting. In the example depicted in Fig. 14 the reflection from different pigments, together with the gesso

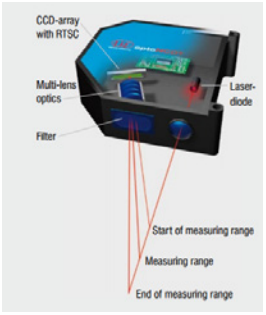

Figure 15: Laser triangulation system

background, are reported as a function of the distance between the probe and the sample. It is easy to see that imaging is best performed at specific distances, where the response difference between pigments is maximized (around 850 μm in the graph).

It is also possible determine the optical properties of pigments (real and imaginary part of the refraction index). The phase information from the reflected signal provides information about the topology of sample, together with optical properies of the sample. It is necessary to distinguish these two contributes to obtain a correct evaluation of the optical parameters. This can be accomplished by upgrading the system in order to measure precisely the distance between the sample and the painting. A new laser system has been then acquired in order to perform this task (Fig. 15). This laser can also be used to increase the precision for the imaging measurements and to perform measurement at a fixed distance from the sample, that is especially useful for non perfectly planar samples, like paintings.

Preliminary results showed typical behaviour of pigments with metallic com-

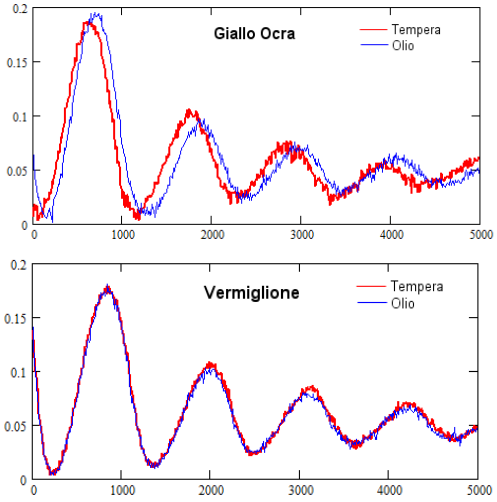

Figure 16: Effect of binders on different pigments

position and demonstrate that in many experimental situations it is not possible to treat separately the contribution of the pigments and that of the binders. Some of the pigments show the same response with different binders while other pigments show a clearly different behaviour. This is shown in Fig. 16, where a phase shift is clear in the Giallo Ocra sample, while the response of the Vermiglione looks identical for both binders. This demonstrates that some chemical reaction occurs in some samples, producing changes in the optical parameters in the THz region.

Electromagnetic Pulser for biological applications

Short duration electric pulses produce significant changes in cell membrane potential. One of the most important questions in bio-electromagnetics today is whether cellular systems can rectify rapidly oscillating electric fields at frequencies

Figure 17:
Pulser diagram

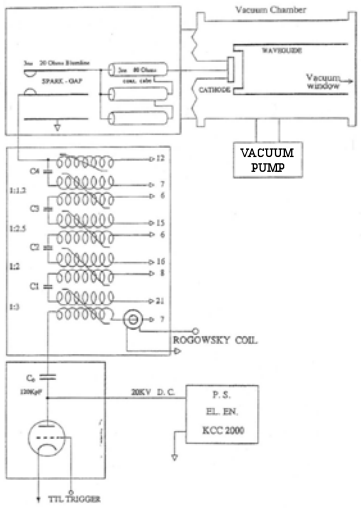

which have pulse time durations ranging from pico-to-microseconds. A positive answer to this question would provide a unified view of ultrafast electromagnetic interactions with cellular systems. This would imply that short electric pulses can produce effects similar to those obtained irradiating the membrane with millimeter and THz waves with a comparable time duration. The cell membrane is in fact a complex polymolecular structure, whose transmembrane voltage controls the transport of chemicals into and out of the cell. The interaction mechanisms can be investigated by using model membrane systems and electrically excitable cells (neurons) by applying electric pulses and RF carrier waves between 30 and 3000 GHz for possibly controlling cell function.

Figure 18:
FEL configuration

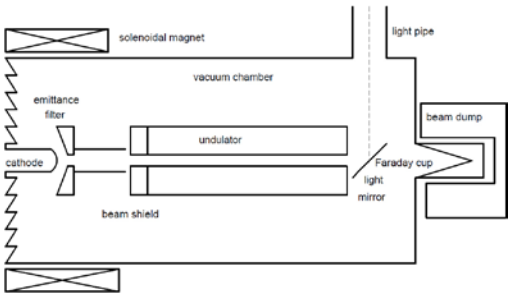

ENEA has a long term expertise in the design and operation of electron-based electromagnetic sources, with a special focus on Free Electron Lasers operating in the long wavelength spectral range. A novel Electro-Magnetic pulser was then designed, based on a short pulse electron gun, capable of providing both nanosecond THz electromagnetic (EM) radiation pulses as well as electrostatic (ES) pulses in the same device, with identical time duration. The pulser will allow, for the first time, direct comparison of EM and ES pulses on biological systems, a major goal of the project. The pulser will provide a core measurement capability as it will produce peak electric fields in the samples that are significantly higher than any reported to date, while keeping the average power low enough to avoid sample heating.

The pulser diagram is schematically reported in Fig. 17. The electron gun is composed by a 20 kV power supply charging a capacitor bank C0 that is the primary energy reservoir. A six-stage magnetic pulse compressor reduces the pulse from a discharge time of 1 μs down to about 30 ns and rises the voltage up to 350 kV. The final condenser of the compressor is connected to a transmission-line transformer, made by three coaxial cables charged in parallel and discharged in series on a mismatched diode load, raising the voltage up to 1.5 MV.

A Free Electron Laser based on this accelerator can be assembled in a compact configuration as shown in Fig. 18.

The electron beam, generated by the cathode is transported into the undulator by means of a solenoidal magnetic field to minimize the space-charge effects. The cathode and the magnetic undulator are contained inside a single vacuum chamber to simplify the e-beam transport system and the vacuum pumping system.

A peak current of about 5 kA allows the use of the pulser as a driver for an FEL. The expected e-beam quality parameters, emittance and energy spread ($\varepsilon_{x,y}$ = 30 mm mrad, σ_e = 1 %) are good enough for long wavelength operation.

The magnetic undulator considered in this study is a compact structure presently in use in the ENEA 2.5 MeV microtron based Compact-FEL (see Fig. 19). The undulator consists of 8 periods of 2.5 cm of length with a variable gap; it can reach a parameter K = 0.8 at a gap of b = 8 mm generating, in this condition, an on-axis field of about 3.5 kG. The described FEL source is capable of reaching saturation at megawatt level at a central frequency of 200 GHz as reported in Fig. 20.

3.4. Accelerators Development

The scientific experience acquired in many years of activity in the field of particle accelerators structures, devices and equipments, today constitutes an important national presidium for service and further development. It can satisfy the increasing demand of the scientific community, the industry, the medical community with its need of new therapy and diagnostics, and moreover it stimulates the training of new human resources.

The field of particle accelerators is cross-sectional to many activities: in particular the accelerator activities deal physical technologies employing ionising particles and X rays for special applications (treatment of the materials) and for medicine. In the applications of non-ionising radiation, in particular with free electrons laser (FEL), electron accelerators are used as a powerful driver.

In the following we briefly describe the main results of the activities in the field of

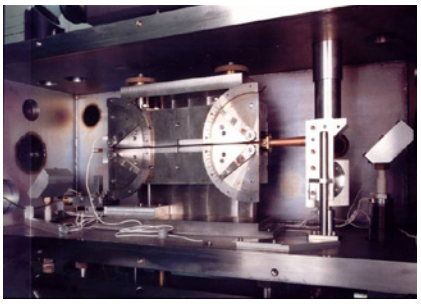

Figure 19: ENEA compact undulator

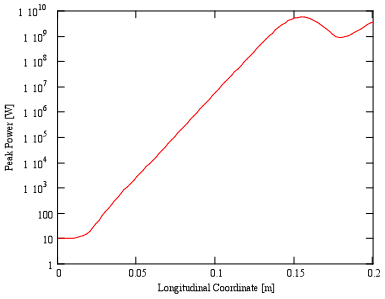

Figure 20: FEL saturation

the development of protons and electrons accelerators at the ENEA Frascati Centre, for different applications: industrial and medical applications and FEL radiation source generation.

Electron accelerators at ENEA-Frascati

During 2011 a considerable effort has been devoted to the update and completion of fire and security measures for the safe operation of electron and proton accelerators operating at ENEA-Frascati. In particular, new sensors were installed with a new central fire control.

Exploiting this stand-by in the operation, extraordinary maintenance work has been carried out to improve the performance of the following accelerators:

- Pulsed (4 μs) S band (3 GHz) standing wave linear accelerator with electron energy in the range 3 to 5 MeV and 0.2 A macropulse current, used for irradiation test and studies on the effects of the interaction of electrons with matter for scientific, medical and industrial applications (Figures 21, 22). A new modulator has been tested and installed.
  The 5 Mev Linac can be usefully employed in irradiation experiments on cross linking of polymers, degradation of pesticides, degradation of phenols in waste waters, degradation of polychlorobiphenyls (PCB), cracking of oil products, sterilization of water infected by pathogenic agents, functionality of blood cells, production of colour centres in alkali halides for solid state lasers, generation of x-rays by Bremsstrahlung.

Figure 21: 5-MeV Linac

Figure 22: Output window of the 5-MeV Linac

- Circular accelerator (microtron) in S-band (3 GHz) with a maximum energy of 5 MeV, 0.3A, 4 μs used as pilot of a compact FEL for the generation of electromagnetic radiation in the millimetre-wave region (90 - 150 GHz). A new method to hold the LaB6 cathode in its heating enclosure has been designed, constructed and successfully tested, resulting in a better stability, duration and efficiency.

- Pulsed (4 μs) S-band (3 GHz) standing wave linear accelerator with a maximum energy of 3 MeV, equipped with a particular device for the manipulation of the e-beam, used as pilot for the generation of electromagnetic radiation in the sub-millimeter (0.4 – 0.8 THz) by means of a magnetic undulator (FEL-CAT). In spite of the limited financial resources, during 2011 an effort has been devoted to refurbishing the RF system.

Proton accelerator facility (ISPAN and TOP-IMPLART Projects)

During 2011 the activity on proton accelerators has been mainly focused on the development of the ISPAN Project, funded with 570K€ by Regione Lazio-Filas and aimed to setup a radiobiology facility with two beam outputs: a 17.5 MeV horizontal beam for small animals irradiation and a variable energy up to 7 MeV vertical beam for cells irradiation. The Project is leaded by two Italian companies NRT (already operative in the field of medical accelerators by producing electron machines for IORT) and CECOM, whilst ENEA and ISS have the role of scientific co-leaders. The facility is based on the use of a linear proton accelerator (a PL7 ACCSYS-HITACHI model, bought within the ISS-ENEA convention) operating at 425 MHz composed by two linear accelerators (RFQ up to an energy of 3 MeV + DTL up to an energy of 7 MeV) to be used as injector of a 3 GHz SCDTL (Side Coupled Drift tube Linac) booster, consisting in a sequence of linear modules. The injector is followed by a four magnetic quadrupoles transport line used for matching the 7 MeV beam in the transverse planes to the following accelerating structure with an adequate space between the two couples of quadrupoles to place a 90° magnet for the vertical bending of the beam. The ISPAN accelerator is also the prototype of the first part of a 230 MeV linear accelerator for oncological therapy with protons (fig. 4.4.4) in the framework of the TOP-IMPLART Project

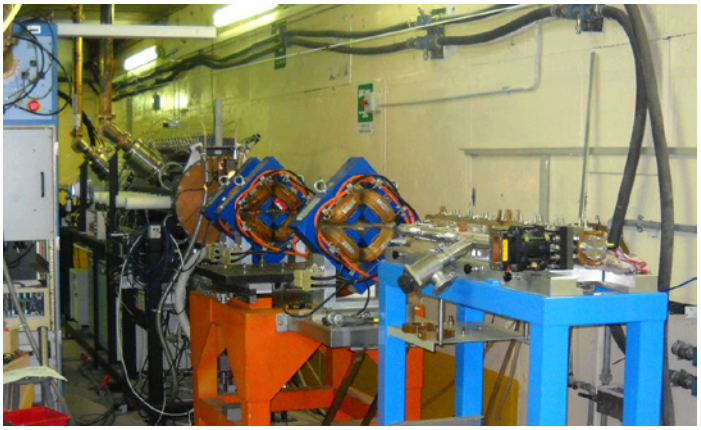

Figure 23: Photo of PL7 injector in the proton accelerator bunker

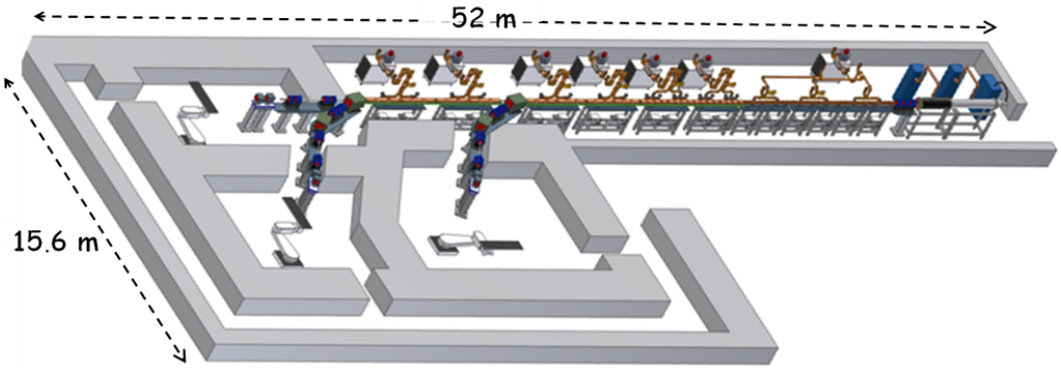

Figure 24: TOP-IMPLART layout showing the proton linear accelerator with two treatments rooms at different energies

launched by ENEA in collaboration with ISS (Italian National Institute for Health) and Regina Elena National Cancer Institute-IFO-Rome for the construction of the 230 MeV facility at IFO Hospital. The Project has been approved in 2010 by the Regional Government of Lazio.

In 2011 two main activities have been conducted:

1. Optimization of the experimental setup for cells irradiation by a 3 MeV horizontal beam;
2. Realization of the first SCDTL module (7 – 11.6 MeV).

The 3 MeV beam (RFQ off, DTL on) has been characterized transversally (transverse emittance) and longitudinally (energy, range). The setting of the injectors parameters (extraction voltage from source, focusing einzel lens voltage, RFQ cavity field) has been optimized in order to minimize the transverse emittance at the accelerator exit. The emittance has been measured by the "quadrupole scan" method by varying the beam size on a fluorescent target by changing the gradient in one of the quadrupoles following the injector (Fig. 25).

The energy of the beam effectively impinging on the biological sample has been retrieved by measuring the particle "range" as the distance for which the beam transmission is halved after the beam passage in an array of PVC layers and the measurements results have been compared with the numerical predictions of SRIM2011 Montecarlo code: the energy

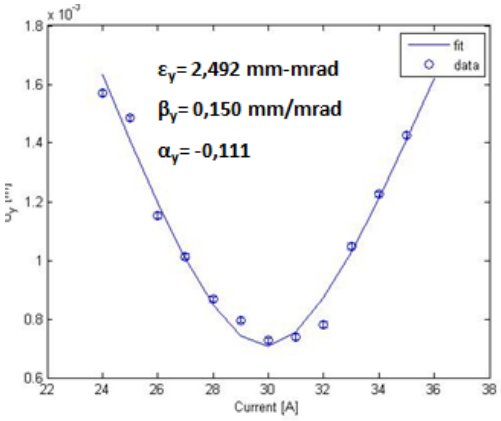

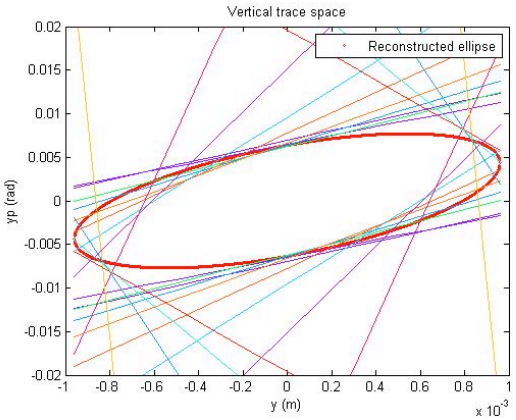

Figure 25: Transverse emittance measurement: (left) experimental data and fit for beam spot vs current (right) Transverse phase space reconstruction by measurements

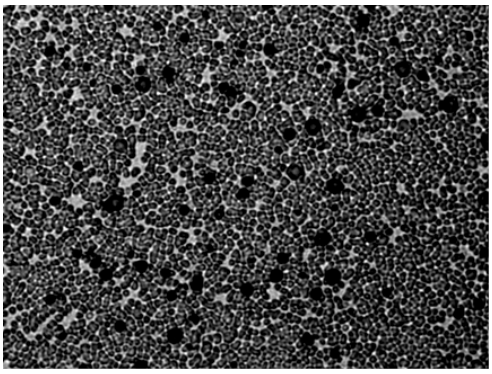

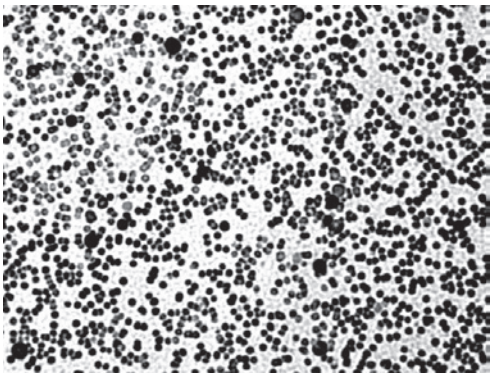

Fig. 26: CR39 dosimeter irradiated by the ISPAN horizontal proton beam (0.2 pC/pulse,energy=2.15 MeV); (left) 50 pulses, (right) 20 pulses

drops from 3 to 2.15 MeV due to the crossing of a 50 μm thick window.

Preliminary dose measurements have been done on some dosimeters (CR39 type) of ISS able to measure the low dose levels (0.1-6 Gy) required by the radiobiology experiments with the low energy beam. The dose can be varied by the accelerator (that operates in pulsed mode) changing the number of beam pulses. Figure 26 shows two of such dosimeters irradiated by the proton beam after the standard surface treatment ("etching") read by the optical microscope: each black point corresponds to the passage of one proton, that allows to retrieve the fluence of protons, that combined with the LET, gives the absorbed dose.

The second activity concerns the machining and tuning of the SCDTL tanks designed buy ENEA on realization at CECOM. ENEA follows all the phases of construction, provides to the tuning of the cavities and to the RF parameters measurements on RF bench. Figure 27 shows the assembly of four of the nine accelerating tanks composing the first SCDTL module (SCDTL-1) and the measured amplitude of the different oscillation modes in the resonant structure.

SPARC Project

During 2011 the accelerator group has also participated in the SPARC project in collaboration with INFN-Frascati and

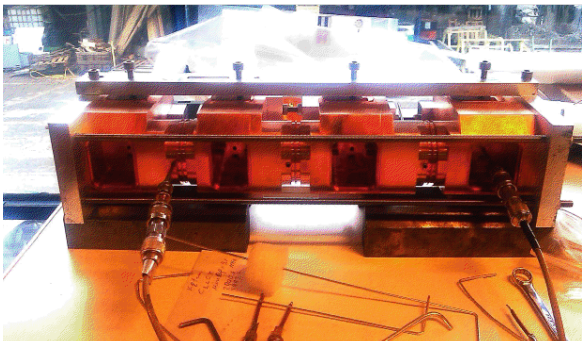

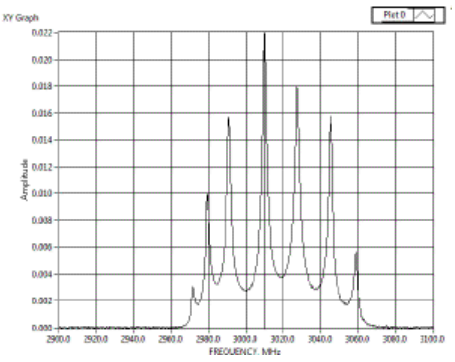

Fig. 27: SCDTL-1 (tanks 1,2,8,9) and measured distribution of resonant modes

in particular to the so called "COMB" experiment aimed to the generation of trains of high brightness electron bunches in the picoseconds regime through a novel technique (linac in "velocity bunching" overcompression regime), to drive tunable and narrow band THz sources, FELs and plasma wake field accelerators. Two and four pulses trains have been transported on a straight line to SPARC undulators and on a bypass line to a THz station. The ENEA contribution dealt with the optimization of experimental parameters and the analysis of results with e-beam dynamic calculations.

New developments in RT

In the framework of a collaboration with ADAM – Geneve, a CERN spin-off society for accelerators development, ENEA participated to the tests of one of the two compact C-band (5712 MHz) electron linacs for medical applications (respectively for IntraOperative Radiation therapy (IORT) and X-rays production) realized on ENEA design. The measurements were done at NRT at Aprilia. Figure 4.4.8 shows the C-band IORT linac in the test stand and the measurement of the relative dose versus penetration depth in a water phantom (PDD curve) for a beam energy of 10 MeV.

A proposal for a low-cost single-room facility has been submitted to the ERC Synergy Grant 2012. The acronym of the proposal, COMPLIANT, stays for "COMPact LInear Accelerator for ProtoN Therapy" and indicates a full-linac single room PT system based on a 200 MeV proton linear accelerator, equipped with a local shielding structure, two fixed (not rotating) beams, and pure digital 3D scanning and capable of intensity modulated therapy (IMPT) and respiratory gating. The entire facility, that should cost around 25 M€ all included, is intended to comply with a high quality RT department in a medium size specialized hospitals. The low investment cost, joint to the low installation impact on the hospital site, changes also the perspective of the use of the therapy with protons in the general framework of a RT: the combined use of X-rays and protons would allow an enhancement of the quality of the treatment, increases the use of hypofractioned treatments for all tumor types, reducing the treatment times.

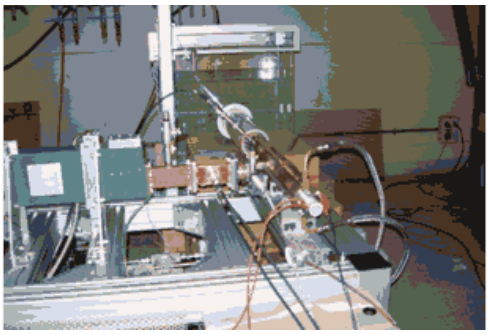

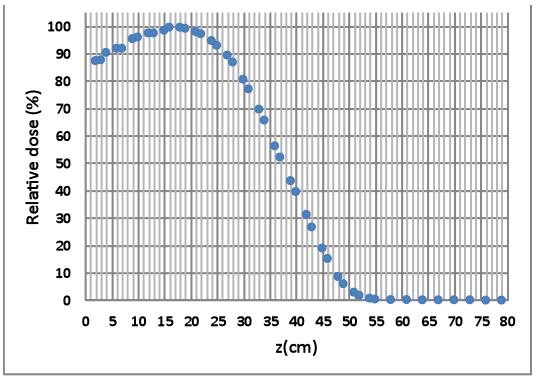

Fig. 28 - (left) C-band IORT linac under measurement (right) C-band linac: measured PDD curve in a water phantom

3.5. "Olocontrollo Emulativo" Technology

This activity is devoted to the development of the cybernetic model of synthetic intelligence named GIASONE, and its technological application named "Olocontrollo emulativo". During 2011 the activities were primarily focused on the relationship between intentional and emotional processes and their interaction, with regards to the implementation process of the action, considering the emotional phase as a basis for action.

In particular we have considered the process of forming the resentment, as a perturbative process, motor for action. We have observed the elementary components of resentment and have identified, in the space-time frame of the body system, the possible intervention point before and during the implementation phase.

Within the activities on the vision system (VISIO) we explored the aspect of vision as a mental process, analysing the visual input path as a light front, and neurological message in the phases of acquisition, recording, projection of the mental image towards the source, searching the coincidence. A possible model of neural network was conceived, for the transmission of signals to and from the environment.

Scenario of activities and results

Starting from the results of studies on "Adaptive Prosthetics" carried out in 2010, which anticipated the creation of an intelligent module for a trans-femoral prosthesis able to dynamically adapting the reservoir to the stump of the patient, a new project "Articulated Prosthesis" was started in 2011. This project is aimed at designing a prosthesis that functions like a biological leg that is in harmony with the rest of the body, and that is able to satisfy the amputated patient desiderata.

To realize a prosthesis that autonomously meets the intent of the individual means:

- inserting an artificial component in a physiological system, which constitutes a new harmonic system without discontinuity;
- obtaining, in the implementation process, a new continuity of interaction between the new system and the environment.

The final effect will be the recovery of the state of harmony before the amputation.

In the leg prosthesis, this means to integrate the prosthesis into the cognitive process of movement of the amputated patient, being able to solicit and respond coherently to the context of environmental and volitional stimuli.

Figure 29: "Articulated prothesis" design phases

All this is achieved by restoring the possibility of implementation of previous dexterities, that are still present in the memory of the individual and may even re-emerge from it, but are not able to trigger the movement process, because the new limb presents a solution of continuity with the rest of the body. In particular we have made functional laboratory prototypes, to investigate the kinematics of the knee joint, ankle, hip and investigate the process of the movement (see Fig. 29)

In the framework of this project, a thesis entitled "Dalla cibernetica alla protesi adattiva" (From the cybernetic toward the adaptive prosthesis) has been assigned in collaboration with the University "La Sapienza" of Rome, Faculty of Engineering, Degree in Biomedical Engineering. The aim of the thesis is the use of the GIASONE cybernetic model in the study and design of a trans-femoral prosthesis for an amputee of thigh that is consistent with the intentionality of the patient

4 MATHEMATICAL MODELING LABORATORY

4.1. Mission and Infrastructures

Advanced Mathematical Methods for the study of the classical and quantum optics, and for modeling the transport of charged particle beams, to study and modeling of complex systems, including biological systems.

Competences available in the Laboratory are originated from expertise in different scientific disciplines as charged beam dynamics and transport, accelerators, RF structures, lasers, free electron lasers, optics and resonators, mathematical modeling.

UTAPRAD-MAT is currently involved in the development of the SPARC free electron laser test facility at LNF-INFN.

In 2011 the personnel participating the Laboratory activities has been substantially increased through the 4 Co.Co.Co. contracts assigned to young researches within the SPARX project, and some internal re-assignment.

Funding and projects

The research activities of the UTAPRAD-MAT Laboratory are mainly funded in the frame of National research programs (MIUR) as partner of collaborations (SPARX)

4.2. The SPARC and SPARX free electron lasers: the development of innovative laser sources

In this section we will discuss the scientific activity carried on within the framework of the SPARC and SPARX collaborations, during the year 2011.

The acronym SPARC stands for Sorgente Pulsata Amplificata Radiazione Coerente and is a free electron laser (FEL) test facility funded by MIUR in 2004. The FEL was developed by a collaboration coordinated by ENEA, where the other partners are CNR, INFN and Sincrotrone Trieste. The SPARC FEL test facility, is located at Laboratori Nazionali di Frascati (INFN), and is in full operation since 2009. Under the acronym SPARX on the other side, goes the design and development of FEL components and subsystems devoted to X-Ray free electron lasers, an experimental programme originally funded by MUR and currently on-going.

These projects include the development of exotic magnetic undulators (mostly on charge to ENEA), the study and experimentation of specific FEL configurations, and the operation of a single pass FEL in seeded mode. We will review different aspects of the research relevant to SPARC/SPARX, including experiments, technical

and theoretical work and the general design effort. In the next section we report on experiments on SPARC in SASE mode, where by shaping the electron beam phase space, we generated quasi Fourier transform limited pulses. This work, done in collaboration between SPARC and the beam physics laboratory at UCLA (University of California), included the design and construction of a fast resolved optical gating (FROG) diagnostics operating at variable wavelength (in the visible-UV spectral range) which has been successfully implemented to measure the FEL pulses of few tens of femtoseconds, generated in this FEL configuration. In section 2 we report on the generation of high order harmonics in superradiance which extended the SPARC operation range down to the VUV spectral range (36nm). The experiments were done in 2010 and repeated in 2011, with the data analysis and calibration of the diagnostics completed the last year. In Section 3, we report we report on the design of undulators characterized by ultrashort period. The design of a prototype for SPARX was completed in 2011 and the device is planned to be installed at SPARC for the first tests during 2012.

Direct measurement of ultrashort pulses from a Free Electron Laser operating in Self Amplified Spontaneous Emission Mode (SASE) with a chirped beam and tapered undulator.

Ultrashort pulses are of great interest for their prospective applications in ultra-high time resolution studies. Single pass SASE free electron lasers are capable of generating X-rays pulses ranging from hundreds to tens femtoseconds, allowing the direct observation of nuclei dynamics, such as localized and collective motions in solids, molecular vibration, etc. However, to resolve faster processes, as for instance electronic rearrangements, probes in the attosecond region are required.

The SASE FEL radiation is the result of the amplification of the e-beam shot noise and the output pulse structure is characterized by mutually incoherent spikes extending over the e-beam pulse length. Methods of shaping of the longitudinal or transverse electron beam phase space permits to increase the gain in a small longitudinal portion of the beam. Single cooperation length (or single spike) regime can be achieved by using electron bunches shorter than the

Fig. 1: Perspective view of the SPARC Undulator installed at LNF-INFN

average distance between two adjacent SASE spikes, as demonstrated at LCLS. These pulse shortening methods rely on the degradation of the FEL gain when the radiation slips outside the effective gain region and lead to an increase of the gain length and a drop in the FEL performances. A solution where the gain shaping has a correlation in the longitudinal phase space combining an energy chirp in the electron beam longitudinal phase space with a taper in the undulator field (smooth variation of peak magnetic field along the longitudinal axis) enables the preservation of FEL performances. The energy chirp detunes the resonant frequency in a local position along the bunch while the undulator taper compensates this detuning for a spike initiated in the rear part of the bunch and drifting with the appropriate velocity. We refer to this scheme as a chirp/tapered configuration. This first experiment was performed at SPARC (see 2010 activity report and references therein). The possibility of generating isolated spike radiation pulses in a single pass FEL operating in SASE mode, by combining a chirped electron beam with an undulator taper was demonstrated. This result was obtained without any increase of the gain length or loss of efficiency, but observing an increase in the energy per pulse and a simultaneous narrowing of the spectral width. While this first results were encouraging, a direct measurement of the pulse profile in time domain was still missing. At this purpose it was necessary to develop an ad hoc diagnostic.

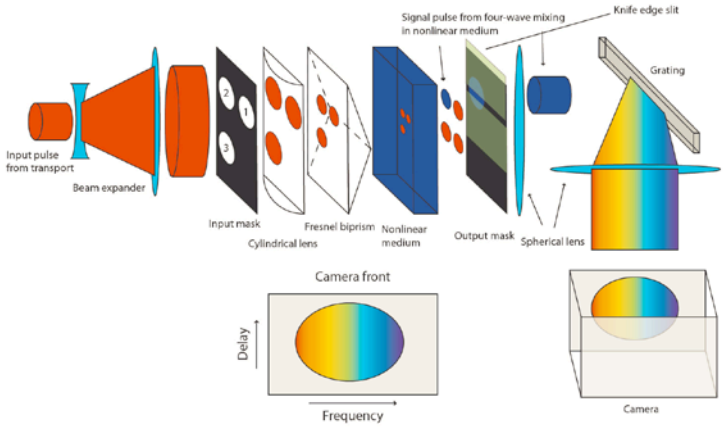

Fig. 2: FROG Diagnostic Layout (Courtesy of G. Marcus, UCLA)

A custom fabricated FROG diagnostic (see Fig. 2) was built and tested at UCLA that was designed with the unique capabilities and challenges of a FEL facility in mind, and was based off of a formerly proposed geometry.

The pulse obtained from transport from the end of the undulator is expanded to a relatively large diameter and is then passed through a mask, which serves to split the pulse into three identical copies (gate and probe pulses). The pulse expansion serves two purposes. FEL pulses may contain a transverse profile that is not uniform in intensity and that also carries transverse phase information. The degree to which these effects appear depends on what stage of the gain process the light pulse is in when it is extracted. These effects will transfer to any FROG trace, making a longitudinal reconstruction corrupt or, in the worst case, impossible. Therefore, selecting only the center of the transverse profile filters out these effects and leaves a uniform and

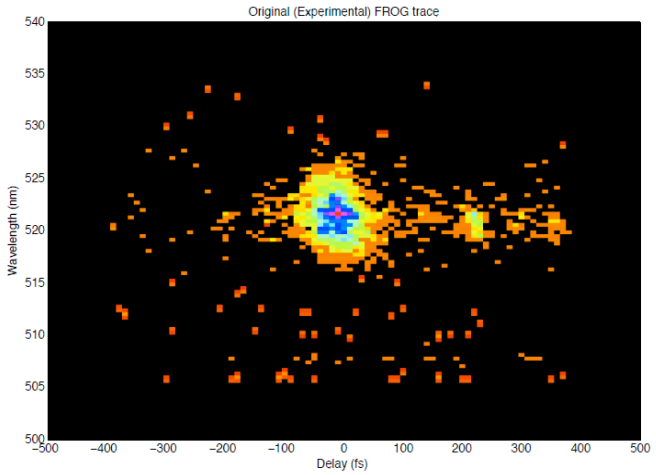

Fig. 3: Measures FROG trace

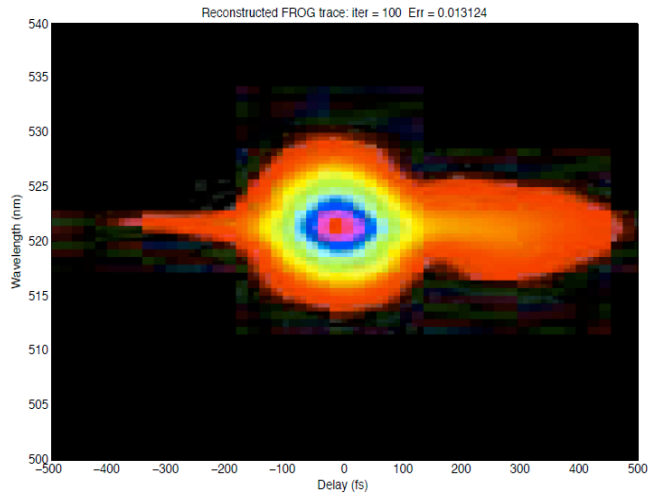

Fig. 4: Reconstructed FROG trace

transversely phase-constant wavefront. It also allows the creation of three identical beams without resorting to the use of multiple delay stages and beamsplitters, which would introduce more alignment degrees of freedom in an already position sensitive and complex diagnostic. These three beams are then passed through a cylindrical lens, which brings each pulse to a line focus within the nonlinear medium. Using a short focal length cylindrical lens allows for tighter focusing resulting in a smaller spot size and greater energy density at the point of interaction. Before reaching the nonlinear medium, however, the beams are passed through a fresnel bi-prism, which serves to cross these interfering beams at a large angle. This creates a variable delay between the probe and gate pulses that is mapped along a transverse dimension, here along the vertical axis. Therefore, this FROG geometry operates on a single shot basis, foregoing the need for an additional delay line. A major advantage of the bi-prism is that it is inherently aligned in space and time, thereby further simplifying the alignment. The interaction of the gate and probe pulses within the nonlinear medium produces an autocorrelation signal, which is selected by the output mask and knife edge slit. The mask also obstructs the probe and gate pulses, helping to reduce the noise in the trace. The autocorrelation signal is passed through a custom fabricated spectrometer consisting of a collimating lens, diffraction grating and focusing lens. The diffraction grating is oriented such that the pulse is spectrally dispersed along the transverse dimension orthogonal to the delay direction, here horizontally. Imaging the resulting pulse into a CCD camera yields the FROG trace.

While some of these properties are common to many FROG geometries, the TG FROG boasts some characteristics that make it ideal for FEL facilities. It utilizes a third order, rather than second order,

nonlinear optical process, which is at once its greatest strength and greatest weakness. While it does not suffer from the excitation bandwidth constraints that second order processes do, it requires more field intensity. It therefore phase matches a much larger bandwidth, which is ideal for a tunable laser source, while requiring a respectable amount of energy. This is a relatively minor concern, though, for most high-gain FEL amplifiers. It also works on a single-shot basis, which is necessary for investigations into SASE FEL pulses where the longitudinal shot to shot variability in the pulse is large. The FROG diagnostic transversely filters the input pulse by selecting only the center of the transverse profile. This ensures that no transverse intensity or phase information, which is certainly relevant in FEL pulses, corrupts the FROG trace.

The chirp/tapered configuration experiment was repeated under slightly different operating conditions, with the goal of measuring the longitudinal intensity profile of the FEL light. After extraction from vacuum and transport from the end of the undulator to the FROG diagnostic the FEL light produced the FROG trace found in Fig. 3.

A computer code was written to longitudinally reconstruct the FEL light using a reconstruction algorithm based on the "Vanilla" scheme. The reconstruction yields a FROG trace found in Fig. 4 and shows excellent overall agreement with the experimental trace with a FROG error of 0.013. The relatively small error and convergence to a FROG trace that strongly resembles the experimental trace are strong indications that the reconstruction is accurate. The reconstructed longitudinal intensity profile has a full width half max (FWHM) of 112 fs while the spectral FWHM is 1.3 nm. These two values combine to yield a time bandwidth product (TBP) ~ 2.06.

High-Gain Harmonic-Generation Free-Electron Laser Seeded by Harmonics Generated in Gas

Nonlinear harmonics generation is widely used to extend the operation of optical lasers to the UV-VUV spectral region, where research methods for the investigation of matter require ultra-short coherent pulses. Frequency up-conversion in the 10-100 nm range may be accomplished with high harmonics generated in Gas (HHG), where the active medium is a low density noble gas, but the emission of high-energy photons is inherently coupled with ionization, and the use of a non-linear optical medium poses severe limitations to the conversion efficiency at the shortest wavelengths. In the spectral region where ionization processes are dominant, harmonic generation may still be obtained in FELs. The mechanism of frequency up-conversion is based on the non-linear density modulation of an electron beam at a given seed wavelength. The frequency components of the

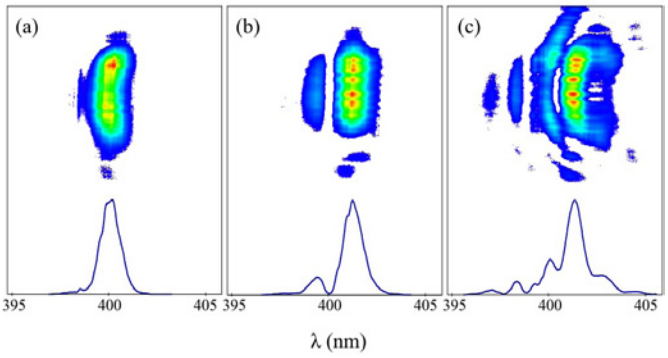

Fig. 5

modulated beam enforce the collective emission process at the resonant wavelength. The seed transfers its longitudinal coherence properties to the FEL pulse and schemes based on this principle

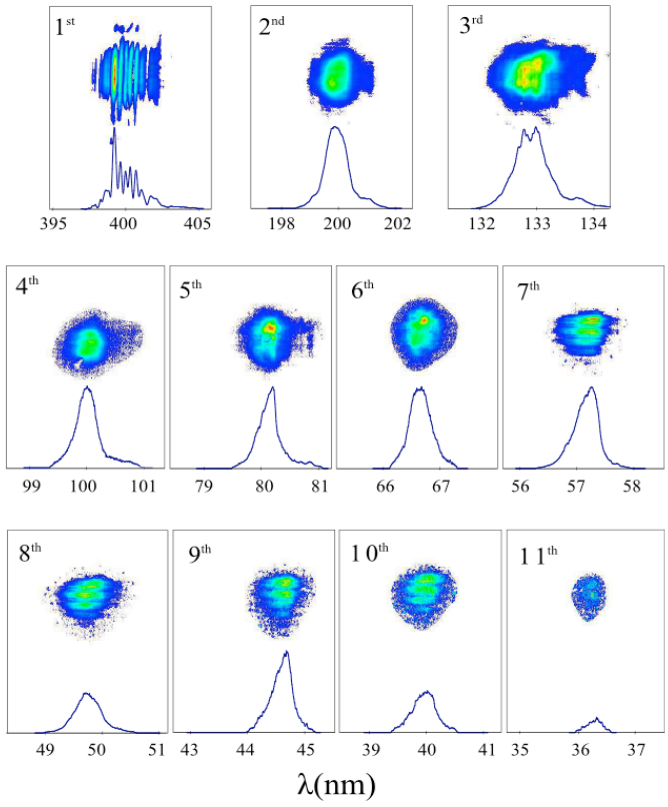

Fig. 6: spectra of the first 11 harmonics of the FEL in superradiance.

were proposed to improve the longitudinal coherence of FELs operating in Self Amplified Spontaneous Emission (SASE) mode where the temporal pulse structure is dominated by stochastic fluctuations associated to the initial shot noise. The seed amplification, combined with the generation of coherent harmonics, has been demonstrated first in the mid-infrared and then in the UV-VUV range. User facilities, as the FERMI free electron laser, based on the frequency up-conversion of a seed laser in the VUV-soft X-ray region of the spectrum are now in operation and provide radiation with unprecedented properties of longitudinal coherence. Coherent harmonics are observed when seeding a single-pass FEL amplifier, with generation of 3RD, 5TH and 7TH. The process is expected to extend to higher harmonics when the FEL operates in the regime of super-radiance, in which a short optical pulse slips over the electron beam and increases its energy while keeping a self-similar shape. In this regime, the radiation pulse has a peak power increasing with the square of the distance z along the undulator and a longitudinal width decreasing with the inverse square root of z. The front of the pulse presents a peculiar structure, characterized by a modulation of the longitudinal phase space density with high harmonics content. The self-similar nature of the radiation/particles system preserves this modulation while the pulse propagates through the undulator and a condition of phase matching is ensured by the fact that after saturation

the pulse shifts over the electron beam at the velocity of light.

Experimental results showed the generation of harmonics up to the 11th order in a seeded FEL operated in the super-radiant regime. The data were collected during two different shifts. The electron beam was injected in the undulator system. Super-radiance was induced by seeding the FEL as a single pass amplifier, with a short laser pulse of peak power comparable to the FEL saturation intensity.

Single shot spectra of the seeded FEL amplifier at increasing seed energies are shown in Fig. 5.

While at low seed energy (Fig. 5,(a)), the amplified signal has approximately the same spectral distribution as the seed, at higher energies ((b) and (c)), a sideband structure appears as an indication of saturation. In all the cases the FEL output is of the same order of magnitude and larger than the expected saturation energy. A further increase of the seed energy (9μJ) leads to the spectrum of the amplified signal as shown in Fig. 6. The spectra of the harmonics n=2,...,11 down to 36 nm were measured in the same conditions (Fig. 6, 2ND -11TH) .

4.3. Design of exotic PM undulator

Free Electron Lasers (FEL) are unique devices in their ability to produce coherent radiation at wavelengths and with characteristics of tunability not achievable with more conventional systems. One of the most limiting factors in short wavelength FEL is the need for electron beams of increasingly high energy. These difficulties can be overcome by creating devices that combine short period and very high magnetic field, as is obvious considering the expression of the resonant wavelength λ_r and undulator strength K:

$$\lambda_r = \frac{\lambda_u}{2\gamma^2}\left(1+\frac{K^2}{2}\right)$$

$$K = \frac{eB_0\lambda_u}{2\pi mc}$$

where λ_u the undulator period, γ is the relativistic electron beam energy parameter, B_o the peak magnetic field, *e* and *m* the electron's charge and mass respectively, and *c* the speed of light.

One of the goals of SPARX project is the design and construction of a short period, high field "exotic" magnetic undulator to be used as insertion device in future Free Electron Lasers. At an early stage the project focused on the definition of new design concepts like those (among others) displayed in Fig. 7

The program RADIA (see Fig. 8) was used to determine the performance of the

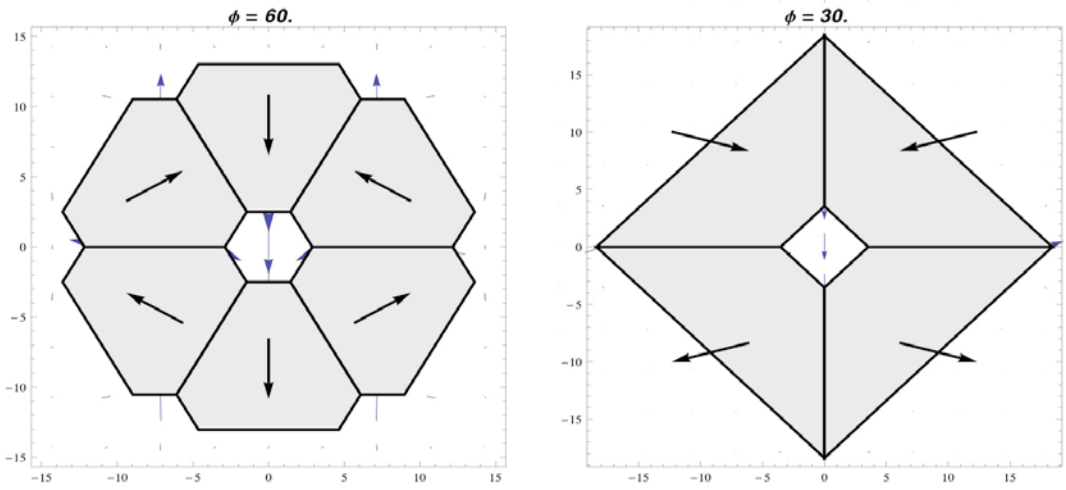

Fig. 7: different design of high on axis field undulators

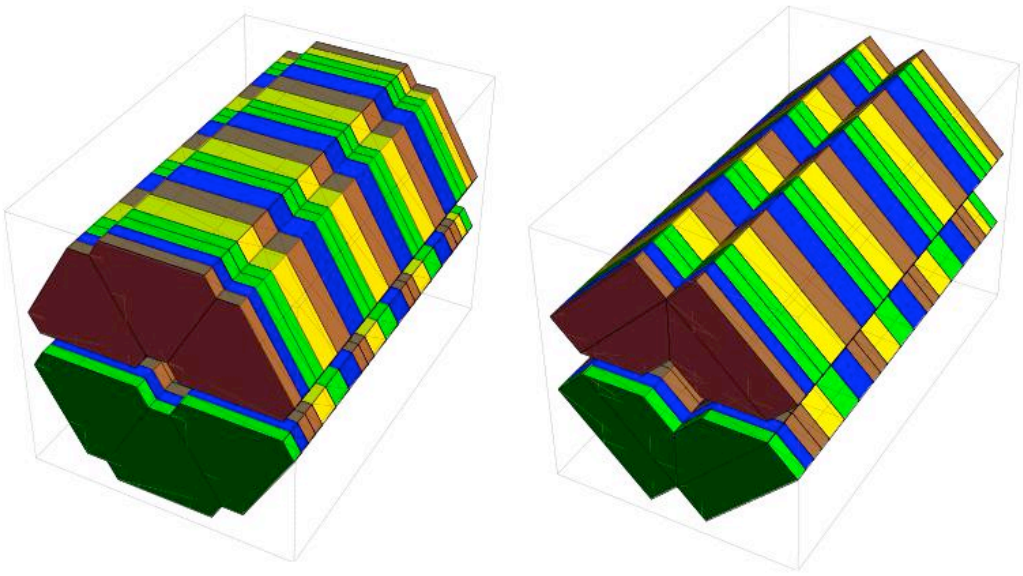

Fig. 8: Radia models of two high field undulator configurations

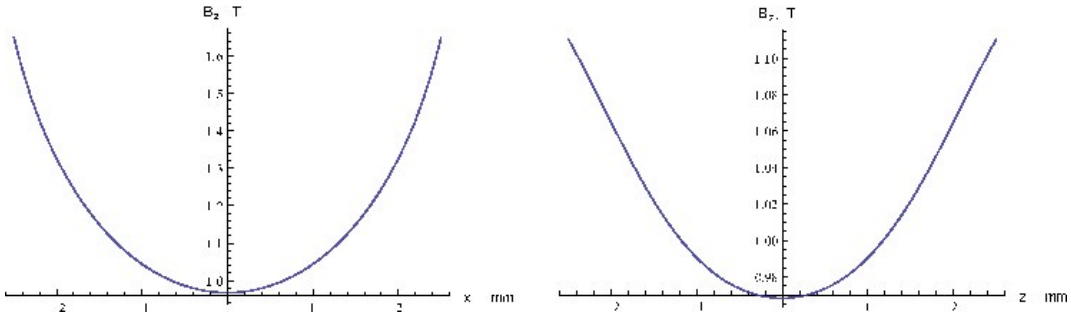

Fig. 9: Dependence of "BOLT" undualtor field on horizontal (left) and vertical (right) coordinates

undulator (field peak) as a function of variables such as the residual field to the surface of the magnets, size, gap.

The "cloverleaf" scheme Fig. 8 (right) was preferred to the "bolt" scheme (left) its greater simplicity of construction, although at the cost of a slightly lower field peak (see Fig. 9 and Fig. 10 for the main field component along the horizontal (left) and vertical (right) coordinates in the two cases.

The construction of the device was started during the winter of 2011 by the Kyma Technologies (Trieste), who participated actively also in the design phase. Delivery is scheduled for June 2012, putting into operation along the beam line of the FEL SPARC is scheduled for autumn 2012.

4.4. Oscillators with tapered undulators

FEL oscillators operating with tapered undulators have been discussed in the past, but the relevant theory and phenomenology require some clarifications because there are some not fully understood aspects, which deserve further consideration. Problems associated with the pulse propagation effects and non- linear harmonic generation here considered give rise to new and interesting dynamical features.

Originally the concept of undulator tapering was introduced for FEL amplifiers and its straightforward extension to the oscillator regime has been the source of some surprises, regarding the relevant consequences on the oscillator efficiency.

In the case of the amplifier the tapering is usually designed in such a way that the undulator field (and/or the undulator period as well) decreases in the forward direction, in order to compensate the effect of the energy losses of the e-beam and ensure an efficient trapping of the elec-

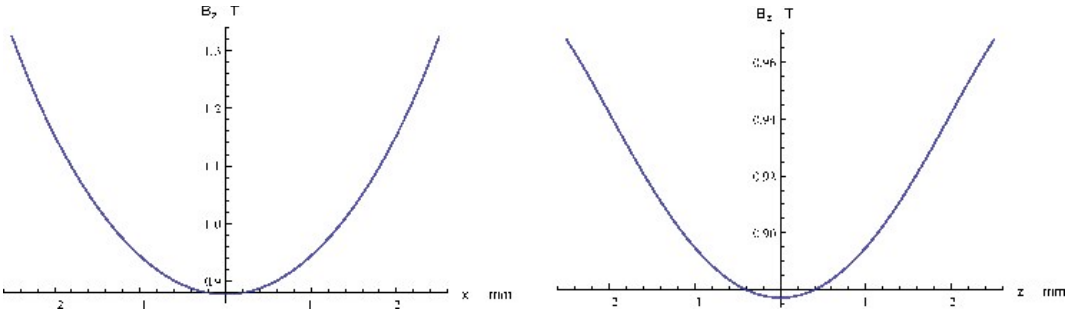

Fig. 9: Dependence of "CLOVERLEAF" undualtor field on horizontal (left) and vertical (right) coordinates

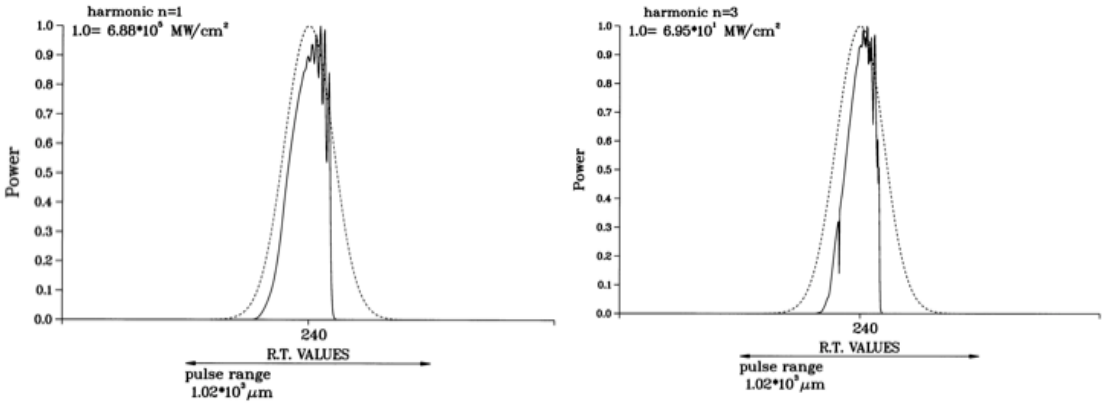

Fig. 11: 1ST and 3RD harmonics in deep saturationHigh Gain FEL and longitudinal phase space correlation

trons in a stable bucket. The increase of the undulator field in the forward direction, namely the reverse tapering, causes reduction in the FEL amplifier efficiency. On the hand side a mild reverse tapering may be a tool to enhance the efficiency in the case of FEL oscillators.

The results of this investigation on FEL oscillator with tapered undulators, carried on in cooperation with (ENEA UTFISSM-METINF) can be summarized as it follows:

- **a.** FEL oscillators operating with undulators having a uniform tapering exhibit an interesting behavior associated with the peculiar nature of the gain function.
- **b.** The uniform tapering guarantees an enhancement of the efficiency which is not the result of an optimization criterion as it happens in the case of the amplifier.
- **c.** The pulse propagation dynamics displays a very interesting phenomenology, which indicates that an interesting interplay may occur between tapering, slippage and lethargy.

In Fig. 11 we report the shape of the pulse in deep saturation along with the pulse of the third harmonic

The FEL high gain dynamics is affected by the characteristics of the electron beam phase space distribution. The effects of transverse phase space have been thoroughly investigated. Recently, new concepts, associated with the slice phase space distribution, have emerged as a consequence of the peculiar properties of the FEL SASE dynamics, characterized by the so called coherence length, associated with the slippage mechanism.

The FEL radiation, produced by a single electron bunch, slips, indeed, over the bunch itself, thus creating a kind of longitudinal mode-locking, responsible for a “local” coherence, due to the fact that radiation spans, during the interaction, over a small portion of the bunch only. Different, uncorrelated “local mode locked structures”, distributed all over the bunch, may interfere destructively during the interaction, thus giving rise to the spiking behavior characterizing the SASE FEL radiation. This is indeed one of the

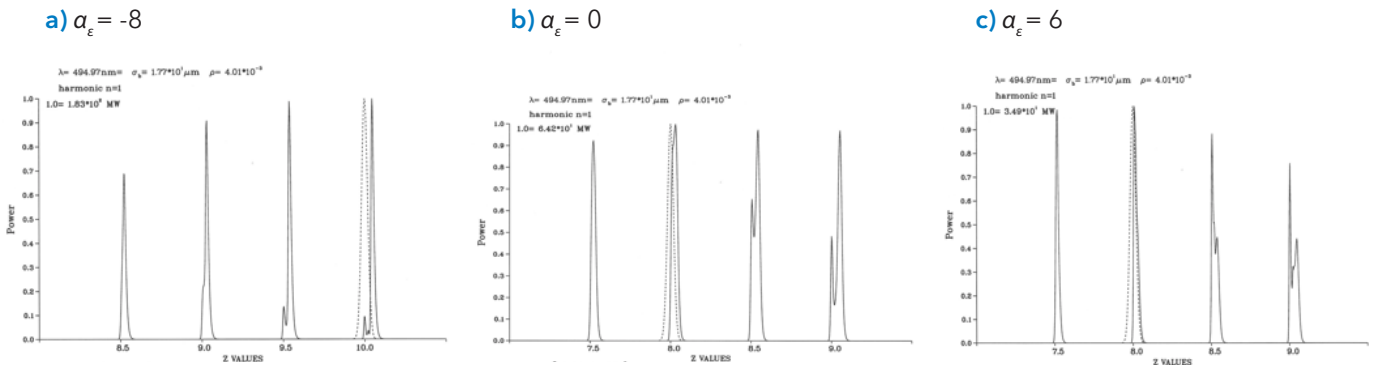

Fig. 12: Pulse shape evolution vs. the undulator longitudinal coordinate for the case σ_z = 17,67 μm , the dotted curve denotes the electron bunch distribution and specifies the position at which saturation.

main problems, which may hamper the use of the FEL radiation, for applications requiring a good deal of coherence.

It is evident that an electron bunch, with a length comparable to the coherence length, would provide the natural solution to this problem.

The FEL SASE operation with a beam exhibiting an energy phase correlation not only affects the maximum power, but also the laser pulse dynamics and shapes.

In fig. 12 we reported the evolution of the pulses in the region around the saturation point (before and after) for the cases with negative, positive and without correlation.

In the region above saturation the laser pulses exhibit the so called super-radiant behavior. They develop typical side bands in their rear part, because it interacts with the electron bunch, thus gaining more energy than the front part, which tends to escape outside the electron bunch. The presence of the side bands is a combination of slippage and finite length of the electron bunch.

The side band growth is smoothened by a non- vanishing correlation parameter, which controls the side band growth in a fairly efficient way. For negative values the pulse remains significantly narrower than the other two cases with a significantly larger peak of the power.

Note that the control of the side-band growth is essentially due to the fact that the correlation parameter affects the slippage mechanism. For positive values, the lethargic effect, namely the slowing down of the laser pulse velocity due to the interaction and consequent gain, is enhanced. The electron and optical bunches overlaps for most of the time and therefore the rear and front part of the bunch experiences nearly equal gain factors. In absence of the correlation the slippage is not sufficiently counteracted by the lethargy and the side band grows. For negative values the center of mass move faster, it is pulled outside abruptly

a) $\alpha_\varepsilon = -8$ **b)** $\alpha_\varepsilon = 0$ **c)** $\alpha_\varepsilon = 6$

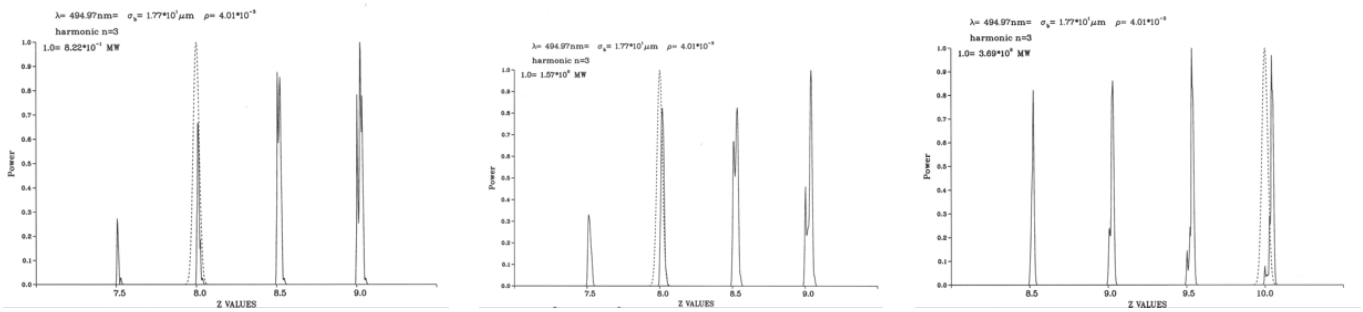

Fig. 13: Same as Fig. 12 for the third harmonics

and the side band has not sufficient time to grow.

It is interesting to understand the consequence of the above dynamics on the non- linear harmonic generation, which seems strongly enhanced for a beam with negative α_ε values (See Figs. 13).

The physical reasons determining this effect are just due to the fact that the shorter laser pulse emerging in the operation with negative correlation parameter determines a more efficient bunching, since a quite robust pulse interacts with almost fresh electrons, because the interaction occurs essentially on the border of the trailing edge of the electron bunch.

The effects we have pointed out appears quite remarkable and are peculiar of either the correlation factor and the shortness of the electron bunch. It is however interesting to consider the laser pulse shape evolution for larger values of the electron bunch length.

The pulse shape evolution for the fundamental harmonic are shown in Figs. 14. The same comments as before hold for this case too, and we find indeed that for negative correlation values the pulse re-

a) $\alpha_\varepsilon = -10$ **b)** $\alpha_\varepsilon = 0$ **c)** $\alpha_\varepsilon = 6$

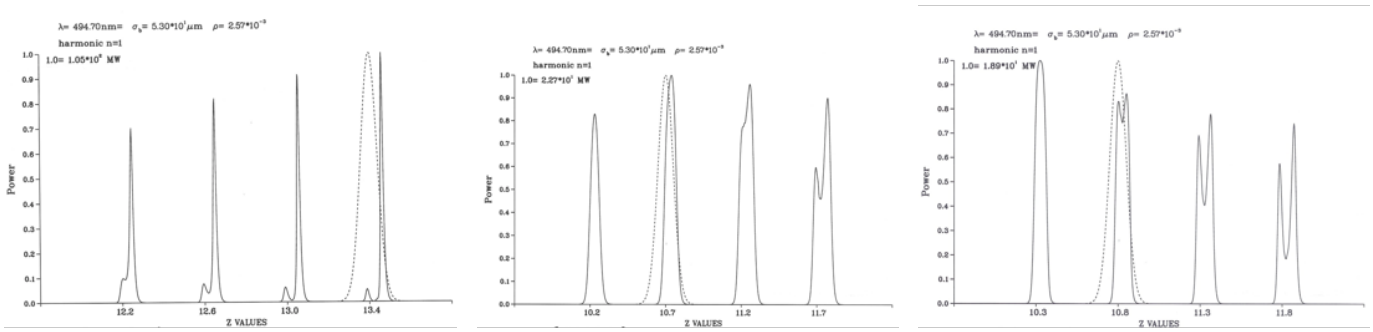

Fig. 14: Same as Fig. 12 for $\sigma_z = 17{,}67$ μm

mains narrow and does not develop any side band, even and remains on the front edge of the electron bunch even for large values of σ_z.

Note that the structure of the pulse of the fundamental determines the quality of the third harmonic.

Wigner distribution

The evolution of the free electron laser dynamics has been analyzed in terms of the so called Wigner distribution, accordingly an accurate analysis in this respect has been undertaken by the theory group. In particular the evolution of the FEL Wigner distribution has been systematically investigated with the inclusion of those associated with the non-linear harmonic generation.

The evolution of the Wigner distribution essentially reflects the FEL dynamics, in Fig. 15 we report the evolution of the FEL amplified power of a coherent seed for a set of parameters close to those of the SPARC experiment.

The input seed power has been chosen well below the saturation to avoid any distortion due to early saturation, induced by the seed itself.

We have included the evolution of the power of the first three harmonics and studied the evolution of the Wigner

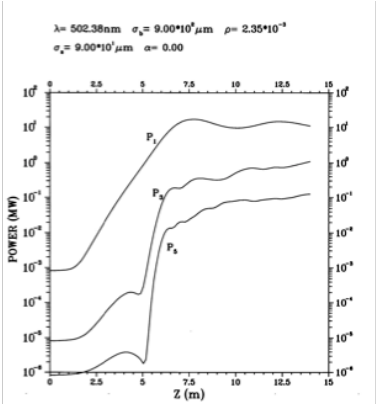

Fig. 15: Evolution of the first three harmonics for SPARC like parameters

distribution associated with the first, third and fifth harmonics, along the undulator.

The contour plots of the phase space distribution relevant to the fundamental harmonic are reported in Figs. 16 and 17. The evolution during the linear regime does not change significantly from the evolution obtained from the analytical solutions, the distribution even though initially uncorrelated acquires a small correlation during the linear growth. At the onset of the saturation the phase space curves become distorted (albeit not significantly), a consistent distortion with formation of island and filamentation occurs in the region above saturation, where the power undergoes substantial oscillations.

The behavior of the phase space evolution of the harmonics is very interesting, because the associated dynamics is more complicated than that of the fundamental. In this case we have essentially three regions of interest

a. The harmonics linear growth and the onset of the bunching, characterized by a “knee” in the power growth curve

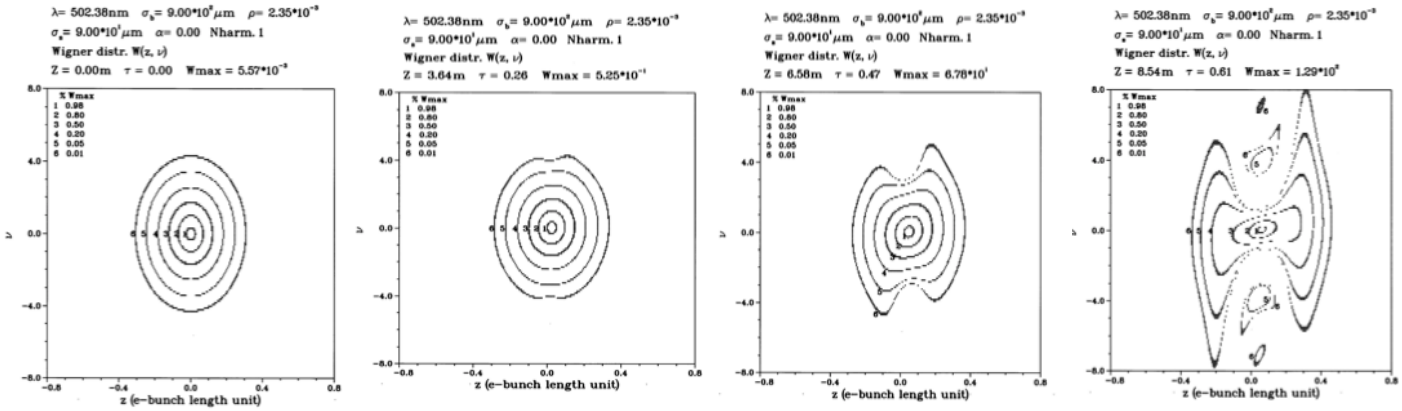

Fig. 16: Phase space distribution of the fundamental harmonic at different position inside the undulator

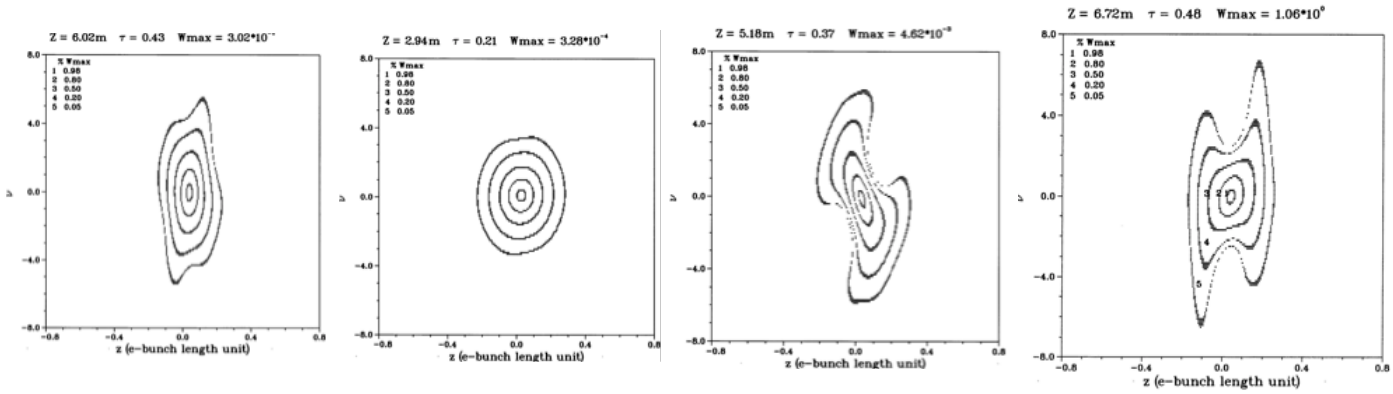

Fig. 17: Phase space contour plot for the third harmonic, a) linear growth, b) at the knee, c) nonlinear harmonic generation region, d) at the occurrence of the first peak.

b. The region of nonlinear coherent generation

c. The saturation

In the first region the harmonic undergoes the same behavior of the fundamental, however when the bunching induced by the fundamental occurs, the phase space is dominated by a significant distortion, in the region b) a kind of re-composition occurs, because the evolution is driven by the fundamental harmonic. Finally at the saturation the phase space plot become distorted and exhibit a kind of chirp, induced by the FEL interaction itself.

The evolution of the third and fifth harmonic is specified by the regions, I, II, III $k_{3,5}$ denote the knees where the transition to the nonlinear harmonic generation occurs, $p_{1,3,5}$ indicates the first peaks, used as reference for the onset of saturation.

5 LIST OF PERSONNEL

Technical Unit for the Development of Applications of Radiations (UTAPRAD)

Director Roberta Fantoni
roberta.fantoni@enea.it

Direction staff members

Fabio Avello, Emilia Batisti, Elisabetta Borsella, Paola Chiappini, Giorgio Fornetti, Anna Pagliardini, Luigi Picardi, Ilaria Sergi, Giulio Tuccinardi.

UTAPRAD-DIM (Diagnostics and Metrology Laboratory)

Director Antonio Palucci
antonio.palucci@enea.it

DIM staff members

Lorella Addari, Salvatore Almaviva, Paolo Aristipini, Florinda Artuso, Rodolfo Borelli, Luisa Caneve, Roberto Carletti, Dario Cataldi, Roberto Chirico, Francesco Colao, Luigi De Dominicis, Antonella De Ninno, Giovanni Dipoppa, Mario Ferri De Collibus, Luca Fiorani, Massimo Francucci, Gianfranco Giubileo, Massimiliano Guarnieri, Antonia Lai, Violeta Lazic, Giovanni Leggeri, Giacomo Lorenzoni, Salvatore Marullo, Ivano Menicucci, Marcello Nuvoli, Marco Pistilli, Roberto Ricci, Laura Teodori.

DIM research fellow

Valeria Spizzichino

UTAPRAD-MAT
(Mathematical Modelling Laboratory)

Director Giuseppe Dattoli
giuseppe.dattoli@enea.it

MAT staff members

Franco Ciocci, Emanuele Di Palma, Luca Gianessi, Marcello Quattromini, Elio Sabia, Ivan Panov Spassovsky, Amalia Torre.

MAT Co.Co.Co.

Marcello Artioli, Mario Del Franco, Alberto Petralia, Vincenzo Surrenti.

UTAPRAD-MNF
(Photonics Micro and Nano-structures Laboratory)

Director Rosa Maria Montereali
rosa.montereali@enea.it

MNF staff members

Francesca Bonfigli, Sabina Botti, Doriano Costantino Brogioli, Luciano Cantarini, Michele Arturo Caponero, Rosaria D'Amato, Roberto D'Imperio, Stefano Libera, Guido Martini, Valerio Orsetti, Salvatore Paolini, Alessandro Peloso, Andrea Polimadei, Antonino Santoni, Gaetano Terranova, Maria Aurora Vincenti, Alessandro Zini.

UTAPRAD-SOR
(Radiation Sources Laboratory)

Director Gian Piero Gallerano
gianpiero.gallerano@enea.it

SOR staff members

Alessandro Ampollini, Rosanna Balvetti, Maria Laura Bargellini, Marco Battaglia, Sarah Bollanti, Ezio Campana, Mariano Carpanese, Gemma Casadei, Domenico De Meis, Paolo Di Lazzaro, Andrea Doria, Antonio Fastelli, Alessandra Filippini, Francesco Flora, Emilio Franconi, Emilio Giovenale, Giovanni Messina, Luca Mezi, Daniele Murra, Gian Luca Orlandi, Loredana Puccia, Concetta Rosinvalle, Davide Vicca, Consuelo Zampetti.

UTAPRAD-STG
(Administration and Management Service)

Director Tiziana Giuli
tiziana.giuli@enea.it

STG staff members

Maria Luisa Mori, Tiziana Pigiani, Tiziana Vari.

6 RESEARCH PRODUCTS

6.1 Peer-reviewed papers and books

1. L. Fiorani, F. Colao, A. Palucci, D. Poreh, A. Aiuppa, G. Giudice, "First-time lidar measurement of water vapor flux in a volcanic plume", *Optics Communications 284*, 1295-1298 (2011).

2. V. Spizzichino, L. Fiorani, A. Lai, A. Palucci, K. Semyanov, E. Viaggiu, P. Albertano, "First studies of pico and nanoplankton populations by a laser scanning flow cytometer", *Journal of Quantitative Spectroscopy and Radiative Transfer 112*, 876-882 (2011).

3. L. Fiorani, F. Colao, A. Palucci, D. Poreh, "Lidar monitoring of anthropogenic pollution and natural phenomena", *Environmental Engineering and Management Journal 10*, 127-131 (2011).

4. L. Fiorani, F. Colao, A. Palucci "Environmental monitoring by laser radar", *Romanian Journal of Physics 56*, 448-459 (2011).

5. B. Perniconi, A. Costa, P. Aulino, L. Teodori (corresponding author) S. Adamo, D. Coletti, "The pro-myogenic environment provided by whole organ scale acellular scaffolds from skeletal muscle", *Biomaterials 32*, 7870–7882 (2011).

6. V. Lazic, A. Palucci, S. Jovicevic, M. Carpanese, "Detection of explosives in traces by laser induced breakdown spectroscopy: Differences from organic interferents and conditions for a correct classification", *Spectrochim. Acta Part B, 66 (2011)*, 644-655.

7. M. Cabalin, A. Gonzales, V. Lazic, J. Laserna, "Deep Ablation and Depth Profiling by Laser-Induced Breakdown Spectroscopy (LIBS) Employing Multi-Pulse Laser Excitation: Application to Galvanized Steel", *Applied Spectroscopy 65, No. 7 (2011)*, 797-805.

8. A. Lai, M. Sighicelli, "Indicatori gassosi per la qualità dei prodotti ortofrutticoli in postraccolta", *Italus Hortus 18 (2)*, 2011: 1-13 (Review)

9. S. Marullo, V. Artale, R. Santoleri, "2: The SST Multidecadal Variability in the Atlantic–Mediterranean Region and Its Relation to AMO", *J. Climate, 24*, 4385–4401, 2011. doi: http://dx.doi.org/10.1175/2011JCLI3884.1.

10. A. De Ninno, A. Congiu-Castellano, *Journal of Molecular Structure 1006 (2011)* 434–440

11. A. De Ninno, A. Congiu-Castellano, *Key Engineering Materials Vol. 495 (2012)* pp 347-350

12. M.F. Heringa, P.F. DeCarlo, R. Chirico, T. Tritscher, M. Clairotte, C. Mohr, M. Crippa, J.G. Slowik, L. Pfaffenberger, J. Dommen, E.

Weingartner, A.S.H. Prévôt, U. Baltensperger, "A new method to discriminate secondary organic aerosols from different sources using high-resolution aerosol mass spectra", *Atmos. Chem. Phys. Discuss., 11*, 29055-29091, 2011.

13. C. Mohr, P.F. DeCarlo, M.F. Heringa, R. Chirico, J.G. Slowik, R. Richter, C. Reche, A. Alastuey, X. Querol, R. Seco, J. Peñuelas, J.L. Jiménez, M. Crippa, R. Zimmermann, U. Baltensperger, A.S.H. Prévôt, "Identification and quantification of organic aerosol from cooking and other sources in Barcelona using aerosol mass spectrometer data", *Atmos. Chem. Phys. Discuss., 11*, 27383-27420, 2011.

14. T. Tritscher, Z. Juranyi, M. Martin, R. Chirico, M. Gysel, M.F. Heringa, P.F. DeCarlo, B. Sierau, A.S.H. Prévôt, E. Weingartner, U. Baltensperger, "Changes of hygroscopicity and morphology during aging of diesel soot", *Environ. Res. Lett., 6*, 2011, doi:10.1088/1748-9326/6/3/034026.

15. V. Zelenay, R. Mooser, T. Tritscher, A. Krepelova, M. Heringa, R. Chirico, A.S.H. Prévôt, E. Weingartner, U. Baltensperger, J. Dommen, B. Watts, J. Raabe, T. Huthwelker, M. Ammann, "Aging fingerprints in combustion particles", *Atmos. Chem. Phys. Discuss., 11*, 14455-14493, 2011.

16. R. Chirico, A.S.H. Prévôt, P.F. DeCarlo, M.F. Heringa, R. Richter, E. Weingartner and U. Baltensperger, "Aerosol and trace gas vehicle emission factors measured in a tunnel using an Aerosol Mass Spectrometer and other on-line instrumentation", *Atmos. Environ.*, doi:10.1016/j.atmosenv.2011.01.069.

17. A. Richard, M.F.D. Gianini, C. Mohr, M. Furger, N. Bukowiecki, M.C. Minguillon, P. Lienemann, U. Flechsig, K. Appel, P.F. DeCarlo, M.F. Heringa, R. Chirico, U. Baltensperger, A.S.H. Prévôt, "Source apportionment of size and time resolved trace elements and organic aerosols from an urban courtyard site in Switzerland", *Atmos. Chem. Phys. Discuss., 11*, 3727–3776, 2011.

18. T.W. Adam, R. Chirico, M. Clairotte, M. Elsasser, U. Manfredi, G. Martini, M. Sklorz, T. Streibel, M.F. Heringa, P.F. DeCarlo, U. Baltensperger, G. De Santi, A. Krasenbrink, R. Zimmermann, A.S.H. Prévôt and C. Astorga, "Application of modern online instrumentation for chemical analysis of gas and particulate phases of exhaust at the European commission heavy-duty vehicle emission laboratory", *Anal. Chem*., 83, 67–76, 2011.

19. M. De Angeli, C. Castaldo, S. Ratynskaia, G. Grosso, S. Almaviva, L. Caneve, F. Colao, G. Maddaluno, "Simultaneous electrical and optical detection of expanding dense partially ionized vapour clouds", *Review of scientific instruments 82*, 106101 (2011).

20. S. Almaviva, L. Caneve, F. Colao, R. Fantoni, G. Maddaluno, "Laboratory feasibility study of fusion vessel inner wall chemical analysis by Laser Induced Breakdown Spectroscopy" *Chemical Physics* (2011) ISSN: 03010104, CODEN CMPHC, DOI: 101016/jchemphys.2011.07.012 (article in press).

21. D. Babusci, G. Dattoli and M. Quattromini, "Relativic equation with fractional and pseudo-differential operators", *Phys. Rev.* A 83 062109 (2011)

22. D. Babusci, G. Dattoli, M. Quattromini and P. E. Ricci, "An extension of the Dirac Factorization method", *J. Appl. Comp. Math.* 54, 321 (2011)

23. D. Babusci, G. Dattoli and E. Sabia, "Operational methods and Lorentz Type equation", *J. Math. Phys.* (2011)

24. D. Babusci, G. Dattoli, E. Dipalma and E. Sabia, "Complex type numbers and generalizations of the Euler identity", *J. Clifford Algebras* (2011)

25. G. Dattoli and K. Zhukowsky, "Evolution of non-spreading Airy wave-pakets in time dependent potentials", *Applied Mathematics and Comp*. 217, 7966 (2011)

26. D. Babusci, G. Dattoli and D. Sacchetti, "The Lamb-Bateman integral equation and the fractional derivatives" (1006.0184) *Fract. Calc. Appl. Anal.* 14, n. 2, 317(2011).

27. Babusci, G. Dattoli and D. Sacchetti, "Special polynomials and elliptic integrals", *Appl. Math. Letters* 24, 1111 (2011).

28. Babusci, G. Dattoli and D. Sacchetti, "The Airy transform and the associated polynomials", *Cent. Eur. J. Phys.* 9 (6), 1381 (2011).

29. G. Dattoli, M. Labat, M. Migliorati, P. L. Ottaviani and S. Pagnutti, "The FEL SASE operation, bunch compression and the beam heater", *Opt. Commun* (2011)

30. L. Giannessi, D. Alesini, P. Antici, A. Bacci, M. Bellaveglia, R. Boni, M. Boscolo, F. Briquez, M. Castellano, L. Catani, E. Chiadroni, A. Cianchi, F. Ciocci, A. Clozza, M. E. Couprie, L. Cultrera, G. Dattoli, M. Del Franco, A. Dipace, G. Di Pirro, A. Doria, A. Drago, W. M. Fawley, M. Ferrario, L. Ficcadenti, D. Filippetto, F. Frassetto, H. P. Freund, V. Fusco, G. Gallerano, A. Gallo, G. Gatti, A. Ghigo, E. Giovenale, A. Marinelli, M. Labat, B. Marchetti, G. Marcus, C. Marrelli, M. Mattioli, M. Migliorati, M. Moreno, A. Mostacci, G. Orlandi, E. Pace, L. Palumbo, A. Petralia, M. Petrarca, V. Petrillo, L. Poletto, M. Quattromini, J.V. Rau, S. Reiche, C. Ronsivalle, J. Rosenzweig, A. R. Rossi, V. Rossi Albertini, E. Sabia, L. Serafini, M. Serluca, I. Spassovsky, B. Spataro, V. Surrenti, C. Vaccarezza, M. Vescovi, and C. Vicario, "Self-amplified spontaneous emission for a single pass free-electron laser", *Physical Review Special Topics - Accelerators and Beams* 14, 060712 (2011)

31. L. Giannessi, A. Bacci, M. Bellaveglia, F. Briquez, M. Castellano, E. Chiadroni,A. Cianchi, F. Ciocci, M. E. Couprie, L. Cultrera, G. Dattoli, D. Filippetto, M. Del Franco, G. Di Pirro, M. Ferrario, L. Ficcadenti, F. Frassetto, A. Gallo, G. Gatti, M. Labat, G. Marcus, M. Moreno, A. Mostacci, E. Pace, A. Petralia, V. Petrillo, L. Poletto, M. Quattromini, J.V. Rau, C. Ronsivalle, J. Rosenzweig, A. R. Rossi, V. Rossi Albertini, E. Sabia, M. Serluca, S. Spampinati, I. Spassovsky, B. Spataro, V. Surrenti, C. Vaccarezza, and C. Vicario, "Self-Amplified Spontaneous Emission Free-Electron Laser

with an Energy-Chirped Electron Beam and Undulator Tapering", *Physical Review Letters* 106, 144801 (2011)

32. M. Labat, M. Bellaveglia, M. Bougeard, B. Carre´, F. Ciocci, E. Chiadroni, A. Cianchi, M. E. Couprie, L. Cultrera, M. Del Franco, G. Di Pirro, A. Drago, M. Ferrario, D. Filippetto, F. Frassetto, A. Gallo, D. Garzella, G. Gatti, L. Giannessi, G. Lambert, A. Mostacci, A. Petralia, V. Petrillo, L. Poletto, M. Quattromini, J.V. Rau, C. Ronsivalle, E. Sabia, M. Serluca, I. Spassovsky, V. Surrenti, C. Vaccarezza, and C. Vicario, "High-Gain Harmonic-Generation Free-Electron Laser Seeded by Harmonics Generated in Gas", *Physical Review Letters* 107, 224801 (2011)

33. D. Filippetto, M. Bellaveglia, M. Castellano, E. Chiadroni, L. Cultrera, G. Di Pirro, M. Ferrario, L. Ficcadenti, A. Gallo, G. Gatti, E. Pace, C. Vaccarezza, and C. Vicario, A. Bacci, A. R. Rossi, and L. Serafini, A. Cianchi and B. Marchetti, L. Giannessi, M. Labat, M. Quattromini, and C. Ronsivalle, C. Marrelli, M. Migliorati, A. Mostacci, and L. Palumbo, "Phase space analysis of velocity bunched beams", *Physical Review Special Topics - Accelerators and Beams* 14, 092804 (2011)

34. F. Bonfigli, D. Brogioli, M. A. Vincenti, and R. M. Montereali, "Optical investigation of photo-bleaching effects in organic Alq_3 thin films", *Journal of Optical Technology* 78,7 (2011) 419-423.

35. E. Nichelatti, F. Bonfigli, M. A. Vincenti and R. M. Montereali, "Optical modelling of an Alq_3-based organic light-emitting diode", *Journal of Optical Technology* 78,7 (2011) 424-429.

36. A.P. Voitovich, V.S. Kalinov, G.E. Malashkevich, L.P. Runets, A.P. Stupak, R.M. Montereali, G. Baldacchini, "Luminescent Probe to Investigate Material Absolute Absorption", *Optical Materials* 33 (2011) 490-493.

37. A.P. Voitovich, M.V. Voitikova, V.S. Kalinov, E.F. Martynovich, A.N. Novikov, L.P. Runets, A.P. Stupak, R.M. Montereali, G. Baldacchini, "Aggregate Color Center Formation Processes in Lithium Fluoride Crystals after Irradiation", *J. Appl. Spectrosc.* 77,6 (2011) 857-868.

38. H.J. Kalinowski, I. Chiamenti, R.M. Montereali, M.A. Vincenti, F. Bonfigli, F. Michelotti, R.N. Nogueira, "Periodic Photonic Structures in Lithium Fluoride", in Manuel F.M. Costa, Ed., *Proceedings of SPIE Vol. 8001* (2011), pp.800114 (1-8).

39. M. Barbagallo, L. Cosentino, G. Greco, G. Guardo, R.M. Montereali, A. Pappalardo, C. Scirè, S. Scirè, M.A. Vincenti, P. Finocchiaro, "A Thermal Neutron Mini-Detector with SiPM and Scintillating Fibers", *Nuclear Instruments and Methods in Physics Research A 652* (2011) 355-358.

40. D. Hampai, S.B. Dabagov, G. Della Ventura, F. Bellatreccia, M. Magi, F. Bonfigli, and R.M. Montereali, "High-resolution X-ray imaging by polycapillary optics and lithium fluoride detectors combination", *Europhysics Letters* 96 (2011) 60010,1-4.

41. F. Loffredo, I. A. Grimaldi, A. De Girolamo, Del Mauro, F. Villani, V. Bizzarro, G. Nenna, Rosaria D'Amato and C. Minarini, "Poly(ethylenimine)/n-doped TiO2 nanoparticles based inks for ink-jet printing applications", *Journal Applied Polymer Science*,122 (2011)3630-3636.

42. E. Borsella, R. D'Amato, F. Fabbri, M. Falconieri, E. Trave, V. Bello, G. Mattei, Y. Nie, D. Wang, "On the role of non-bridging oxygen centers in the red luminescence emission from silicon nanocrystals", *Physica Status Solidi C, Vol. 8* (2011)974-978.

43. D. Donisi, L. De Sio, R. Beccherelli, M. A. Caponero, A. D'Alessandro, and C. Umeton, "Optical interrogation system based on holographic soft matter filter", *Appl. Phys. Lett.* 98 (2011) 151103-5

44. C. Ronsivalle, M.Carpanese, C. Marino, G. Messina, L. Picardi, S. Sandri, E.Basile, B. Caccia, D.M. Castelluccio, E. Cisbani, S. Frullani, F. Ghio, V.Macellari, M. Benassi, M. d'Andrea, L. Strigari, "The TOP-IMPLART Project", *Eur. Phys. J. Plus* (2011) 126:68

45. P. Antici, M. Migliorati, A. Mostacci, L. Picardi, L. Palumbo, and C. Ronsivalle, "A compact post-acceleration scheme for laser-generated protons", *Physics of plasmas 18*, 073103 (2011)

46. M. Ferrario, D. Alesini, A. Bacci, M. Bellaveglia, R. Boni, M. Boscolo, P. Calvani, M. Castellano, E. Chiadroni, A. Cianchi, L. Cultrera, G. DiPirro, L. Ficcadenti, D. Filippetto, A. Gallo, G. Gatti,L. Giannessi, M. Labat d, S. Lupi f, B. Marchetti b, C. Marrelli, M. Migliorati, A. Mostacci, D. Nicoletti, E. Pace, L. Palumbo, V. Petrillo, M. Quattromini, C. Ronsivalle, A.R. Rossi, J. Rosenzweig, L. Serafini, M. Serluca, B. Spataro, H. Tomizawa, C. Vaccarezza, C. Vicario,"Laser comb with velocity bunching:Preliminary results at SPARC", *Nuclear Instruments and Methods in Physics Research A 637* (2011) S43–S46

47. P. Di Lazzaro, S. Bollanti, F. Flora, L. Mezi, D. Murra, A. Torre, "A new anti-counterfeiting marking system", *Nanotec IT Newsletter,* N. 12 january-february, pp. 19-21, 2011.

6.2. Conference presentations and proceedings

1. L. Fiorani, F. Colao, A. Palucci, D. Poreh, "Laser remote sensing of Mount Stromboli's plume", *130 Convegno Nazionale delle Tecnologie Fotoniche – Fotonica 2011*, AICT-AEIT, Pisa, Italy (2011)

2. P. Ortiz, M. A. Gómez, F. Colao, R. Fantoni, L. Fiorani, L. Caneve, M. A. Vázquez, "A Database of pigments for laser-induced fluorescence: Application to the study of La Glorificacion de la Virgen", *Seville 10TH International Conference on Non-destructive Investigations and Microanalysis for the Diagnostics and Conservation of Cultural and Environmental Heritage Art'11*, AIPnD, Firenze (2011)

3. L. Fiorani, F. Colao, M. Guarracino, A. Palucci, "Bio-optical characterization of the water masses off the Svalbard Islands by laser-induced fluorescence", *5TH Workshop on Remote Sensing of the Coastal Zone*, EARSeL, Prague, Czech Republic (2011)

4. I. Iocola, D. Pittalis, M. Iannetta, A. Lugliè, B. Padedda, S. Pulina, N. Sechi, L. Fiorani, I. Menicucci, A. Palucci, "Bio-optical characterization of Asinara Gulf sea water in Sardinia (Italy) using both laser spectrofluorimeter and remote sensing data", *5TH Workshop on Remote Sensing of the Coastal Zone*, EARSeL, Prague, Czech Republic (2011)

5. L. Fiorani, F. Colao, A. Palucci, D. Poreh, "Chemicomorphological characterization of Stromboli's plume by atmospheric lidar", *31ST EARSeL Symposium*, EARSeL, Prague, Czech Republic (2011)

6. D. Pittalis, I. Iocola, M. V. Pinna, L. Fiorani, I. Menicucci, A. Palucci, M. Iannetta, G. Ghiglieri, "A compact laser spectrofluorimeter (CASPER) for groundwaters monitoring in an agricultural district of Sardinia", *International Conference on Dryland Ecosystem Functioning and Resilience: Integrating Biophisical Assessment with Socio-economic Issues*, Università di Sassari, Alghero, Italy (2011)

7. L. Fiorani, F. Colao, S. Marullo, A. Palucci, "Bio-optical characterization of the Arctic Ocean by laser-induced fluorescence and satellite radiometry", *VIII Forum Italiano di Scienze della Terra – Geoitalia 2011*, Geoitalia Fist Onlus, Torino, Italy (2011)

8. L. Fiorani, F. Colao, A. Palucci, "Lidar monitoring of volcanic clouds", *VIII Forum Italiano di Scienze della Terra – Geoitalia 2011*, Geoitalia Fist Onlus, Torino, Italy (2011)

9. I. Iocola, D. Pittalis, M. Iannetta, A. Lugliè, B. Padedda, S. Pulina, N. Sechi, L. Fiorani, I. Menicucci, A. Palucci, "Caratterizzazione ambientale delle acque del Golfo dell'Asinara (Sardegna) attraverso l'uso di spettrofluorimetria laser e immagini telerilevate" (in Italian), *15ª Conferenza Nazionale ASITA*, ASITA, Napoli, Italy (2011)

10. L. Fiorani, "Lidar monitoring of bomb factories", *5TH International Workshop on*

Optoelectronic Techniques for Environmental Monitoring, INOE, Bucharest, Romania (2011).

11. A. De Ninno, A. Congiu-Castellano, *9TH International Fröhlich's Symposium IOP Publishing, Journal of Physics: Conference Series 329* (2011) 012025 doi:10.1088/1742-6596/329/1/012025

12. L. De Dominicis, M. Ferri de Collibus, G. Fornetti, M. Francucci, M. Guarneri, M. Nuvoli, R. Ricci, "3D Color Laser Digitization for Oil and Gas Industry Inspection and Monitoring Applications", *3RD Annual Technical Meeting on Optoelectronic Technologies For the Oil and Gas Industry*, Bergen (Norway), November 8, 2011.

13. M. Guarneri, G. Fornetti, M. Ferri De Collibus, M. Francucci, R. Ricci, M. Nuvoli, "S. Peter Martyr (Rieti, Italy): a study case for 3D color laser scanner (RGB-ITR)", *Optics for Arts, Architecture, and Archaeology III*, (Optical Metrology Conference, Munich, Germany, 23 – 26 May 2011), Proceedings of SPIE Vol. 8084, 80840N (2011), 80840N-1 – 80840N-9 in O3A.

14. L. Teodori, D. Coletti, B. Perniconi, M. Fini, M. Barteri, A. Costa, D. Halicka, Z. Darzynkiwicz, "How to Guide Cell Direction and Orientation in Skeletal Muscle Progenitor Cells?", *International Congress of the International Society for the Advancement of Cytometry*, Baltimore, MA, USA, May 21-25, 2011.

15. D. Coletti, B. Perniconi, A. Costa, P Aulino, S. Adamo and L. Teodori, "Tissue engineered skeletal muscle: preliminary studies for in vivo tranplantation", *International Congress of the International Society for the Advancement of Cytometry*, Baltimore, MA, USA, May 21-25, 2011.

16. L. Teodori, B. Perniconi, P. Aulino, A. Costa, F. Cosmi D. Coletti, "Cell growth, differentiation and spatial orientatation in musculoskeletal tissue engineering" *Future Technologies for Health Care*, Allahabad, India, September 18-20, 2011.

17. L. Caneve, F. Colao, C. Giancristofaro, F. Persia, G. Ricci, A. Tatì, "LIF and ultrasound techniques to study thermal modification induced on white marbles. Lasers in the Conservation of Artworks", *Lacona IX* - London 7-10 september 2011.

18. V. Lazic, A. Palucci, S. Jovicevic, M. Carpanese, "Detection Of Explosives In Traces By Laser Induced Breakdown Spectroscopy", *EU Conference on the Detection of Explosives - EUCDE*, March 2011, Avignon (France)

19. S. Botti, L. Cantarini, V. Lazic, A. Palucci, "Surface Enhanced Raman Spectroscopy (SERS) for trace level detection of explosives", *EU Conference on the Detection of Explosives - EUCDE*, March 2011, Avignon (France)

20. V. Lazic, A. Palucci, S. Jovicevic, M. Carpanese, "Detection of explosives in traces by LIBS: differences from organic interferents and conditions for a correct classification", *EMS-LIBS Conference*, September 2011, Izmir (Turkey)

21. V. Lazic, S. Jovicevic, J. J. Laserna, "Insights in the laser ablation of samples underwater and in the LIBS signal generation using dual pulse excitation", *EMSLIBS Conf.*, 11-15/09/2011, Izmir (Turkey)

22. F. Lupi, L. Campanella, V. Lazic, "Characterization of archaeological ceramics and their decorations by LIBS technique", *EMSLIBS Conf.*, 11-15/09/2011, Izmir (Turkey)

23. A. De Ninno, "De-protonation of amino acids under ELF", *7TH ICEMS Rome-Florence Workshop*, 18/02/2011

24. A. De Ninno, A. Congiu-Castellano, "Effect of weal magnetic field on Glutamic Acid", *Symphosium on Quantum Physics in Living Matter*, Rome 14 July, 2011

25. R. Germano, E. Del Giudice, A. De Ninno et al., "Oxhydroelectric effect in bi-distilled water", *7TH Water Conference*, West Dover, Vermont, U.S. 18-21 October 2011

26. A. De Ninno, "Macroscopic phase coherence and the water bridge", *Water Bridge Mini Symphosium*, Oct. 5TH Wetsus, The Netherland.

27. L. Caneve, F. Colao, R.Fantoni, L. Fiorani, "Scanning hyperspectral lidar fluorosensor for remote diagnostic of surfaces", *2ND Int. Conf. Frontiers in Diagnostic Technologies*, Frascati, 28-20/11/2011.

28. R. Fantoni, L. Caneve, F. Colao, L. Fiorani, A. Palucci, Dell'Erba R., Fassina V. "LIF measurements on medieval frescos by Giusto de' Menabuoi in the Padua Baptistery", *5TH Int. Cong. Science and Technology for the Safeguard of Cultural Heritage in the Mediterranean Basin*, Instanbul (Turkey), 22–25/11/2011.

29. F. Colao, R. Fantoni, L. Caneve, M.P. Ortiz, M.A. Vasquez, M.A. Gomez, "Identification of pigments on frescoes by LIF", *5TH Int. Cong. Science and Technology for the Safeguard of Cultural Heritage in the Mediterranean Basin*, Instanbul (Turkey), 22–25/11/2011.

30. F. Bonfigli, G. Campurra, R.M. Montereali, M.A. Vincenti, "Fluoruro di Litio: anche l'imaging in fotoluminescenza oltre la dosimetria?" *G Ital Med Lav Erg*; 33:3, Suppl, (2011), 391-394, ISSN 1592-7830 (http://gimle.fsm.it).

31. H.J. Kalinowski, I. Chiamenti, R.M. Montereali, M.A. Vincenti, F. Bonfigli, F. Michelotti, R.N. Nogueira, "Periodic Photonic Structures in Lithium Fluoride", in Manuel F.M. Costa, Ed., *Proceedings of SPIE Vol. 8001* (2011), pp.800114 1-8.

32. C.Ronsivalle, M. Carpanese,G. Messina, L. Picardi,S. Sandri, C. Marino, M. Benassi, L. Strigari, E. Cisbani, S. Frullani, V. Macellari "The TOP-IMPLART Project", *Proceedings of IPAC2011*, San Sebastián, Spain,p. 3580

33. A.Mostacci, D. Alesini,P. Antici,A. Bacci,M. Bellaveglia,R. Boni,M. Castellano,E. Chiadroni,A. Cianchi,G. Di Pirro,A. Drago,M. Ferrario,A. Gallo,G. Gatti,A. Ghigo,B. Marchetti,M. Migliorati,E. Pace,L. Palumbo, V. Petrillo,C. Ronsivalle, A. R. Rossi,L. Serafini,B. Spataro,C. Vaccarezza, "Advanced beam manipulation techniques at SPARC",

Proceedings of IPAC2011, San Sebastián, Spain,p. 2877

34. S. Sandri, G. Ottaviano, C. Poggi, M. Carpanese, L. Picardi, C. Ronsivalle, "A proton therapy test facility: the radiation protection design", *Proceedings of IPAC2011*, San Sebastián, Spain,p. 3583

35. B. Marchetti,M. Boscolo, M. Castellano, E. Chiadroni, M. Ferrario, B. Spataro, C. Vaccarezza, A. Cianchi, C. Ronsivalle, "Novel schemes for the narrow band SPARC THz source using a comb like E-Beam", *Proceedings of IPAC2011*, San Sebastián, Spain,p. 3672

36. E. Chiadroni, M. Bellaveglia, M. Castellano, G. Di Pirro, A. Drago, M. Ferrario, G. Gatti, E. Pace, C. Vaccarezza, A. Bacci, A.R. Rossi, P. Calvani, O. Limaj, S. Lupi, A. Nucara,L. Catani, A. Cianchi, B. Marchetti, A. Mostacci, L. Palumbo, C. Ronsivalle, "Present and perspectives of the SPARC THz source", *Proceedings of IPAC2011*, San Sebastián, Spain, p.3669

37. G.P. Gallerano, A. Doria, E.Giovenale, G. Messina and I. Spassovsky, "Electromagnetic Pulser for the Investigation of Cell Membranes", *Proceedings 36TH International Conference on Infrared, Millimeter and Terahertz Waves*, IRMMW-THz2011, Houston (TX), 2-7 October 2011, ISBN: 978-1-4577-0510-6, 6105033 (2011)

38. G.P. Gallerano, A. Doria, E. Giovenale, G. Messina, I. Spassovsky, A.C. More, M. Seracini, "Reflectivity of Pigments in the THz Region", *36TH International Conference on Infrared, Millimeter and Terahertz Waves*, IRMMW-THz2011, Houston (TX), 2-7 October 2011, ISBN: 978-1-4577-0510-6, 6104091 (2011)

39. P. Di Lazzaro, "Laser produced plasmas for bio-photonics" in Biophotonics: Spectroscopy, Imaging Sensing and Manipulation, B. Di Bartolo and J. Collins Eds. NATO SPS Series B: Physics and Biophysics (Springer Netherlands, 2011) pp. 305 - 319. ISBN 978-90-481-9976-1 (print) 978-90-481-9977-8 (online).

40. P. Di Lazzaro, "L'immagine sindonica e la luce ultravioletta: alcune note riassuntive", *Quattro percorsi accanto alla Sindone*, a cura di D. Repice (Edizioni Radicequadrata 2011) pp. 41 - 48. ISBN 9788896862049

41. G.P. Gallerano, A. Doria, E. Giovenale, G. Messina, I. Spassovsky, A.C. More, M. Seracini, "Tecnologie THz per i beni culturali presso l'ENEA", Convegno *Diagnosis of Cultural Heritage* (Napoli, 15-16 Dicembre 2011)

42. S. Bollanti, P. Di Lazzaro, F. Flora, L. Mezi, D. Murra and A. Torre, "New technique for aberration diagnostics and alignment of an extreme ultraviolet Schwarzschild objective", *Proc. 2ND Int. Conf. Frontiers in Diagnostic Technologies*, submitted for publication in a special issue of Nucl. Instr. & Meth. A

43. R. Balvetti, M.L. Bargellini, M. Battaglia, A. Botticelli, G. Bozanceff, G. Casadei, A. Chiapparelli, A. Filippini,A. Grandinetti, A. Guidoni, B. Mussi, E. Pancotti, L. Puccia, L.

Rubini, C. Zampetti, Resentment as imaginative event", *On Resentment: An Interdisciplinary Workshop on The History of Emotions* (Università di Ginevra 26-28 Ottobre)

44. R. Balvetti, M.L. Bargellini, M. Battaglia, A. Botticelli, G. Bozanceff, G. Casadei, A. Filippini, A. Grandinetti, Guidoni A., B. Mussi, E. Pancotti, L. Puccia, L. Rubini, Tripodo A., C. Zampetti, "La visione è un processo mentale; Società Italiana di Fisica", *XCVII Congresso Nazionale* (L'Aquila 26-30 Settembre 2011)

45. H.J. Kalinowski, I. Chiamenti, R.M. Montereali, M.A. Vincenti, F. Bonfigli, F. Michelotti, R.N. Nogueira, "Periodic Photonic Structures in Lithium Fluoride", *International Conference on Applications of Optics and Photonics* (AOP'2011), Braga, Portugal (3-7 May 2011).

46. R.M. Montereali, F. Bonfigli, D. Brogioli, A. Santoni, M.A. Vincenti, E. Nichelatti, "Optical modelling, growth and characterization of thin films for OLED development", *International Conference on Organic Electronics, ICOE 2011*, June 22-24, 2011, P2.27.

47. F. Bonfigli, M.A. Vincenti, R.M. Montereali, H.J. Kalinowski, I. Chiamenti, R.N. Nogueira, F. Michelotti, "Guide d'onda e strutture periodiche otticamente attive nel LiF per dispositivi fotonici", *XCVII Congresso Nazionale Società Italiana di Fisica*, L'Aquila, 26-30 Settembre 2011, p.24.

48. M.A. Vincenti, G. Messina, R.M. Montereali, F. Somma, P. Aloe, S. Polosan, F. D'Acapito, "Caratterizzazione di difetti puntiformi in cristalli di fluoruro di litio drogati con piombo", *XCVII Congresso Nazionale Società Italiana di Fisica*, L'Aquila, 26-30 Settembre 2011, p.115.

49. S. Heidari Bateni, F. Somma, F. Bonfigli, A. Lai, R.M. Montereali, M.A. Vincenti, E. Nichelatti, P. Gaudio, I. Lupelli, M. Francucci, M. Richetta, "Risposta di rivelatori a film sottile di fluoruro di litio per microscopia-X a contatto con una sorgente laser plasma", *XCVII Congresso Nazionale Società Italiana di Fisica*, L'Aquila, 26-30 Settembre 2011, p.116.

50. R. Francini, R.M. Montereali, M.A. Vincenti, E. Nichelatti, F. Cavanna, "Misura delle proprietà ottiche nella regione spettrale uv-vis e vuv di film organici di TPB per wavelength shifting", *XCVII Congresso Nazionale Società Italiana di Fisica*, L'Aquila, 26-30 Settembre 2011, p.181.

51. F. Bonfigli and R.M. Montereali, P. Gaudio, I. Lupelli, and M. Richetta, S. Heidari Bateni and F. Somma, "Optical microscopy and spectroscopy for readout and characterization of lithium fluoride x-ray imaging detectors", *Fotonica 2011, 13° Convegno Nazionale delle Tecnologie Fotoniche*, Genova, 9-11 Maggio 2011 – ISBN 9788887237122, P29, B1_5.

52. S. Heidari Bateni, F. Bonfigli, A. Cecilia, D. Pelliccia, F. Somma, M.A. Vincenti and R.M. Montereali, "Optical characterization of lithium fluoride detectors for broadband X-ray imaging", *2ND International Conference Frontiers in Diagnostic Technologies*, Frascati, LNF-INFN, 28-30 November 2011, p.78.

53. D. Hampai, F. Bonfigli, S.B. Dabagov, R.M. Montereali, G. Della Ventura, F. Bellatreccia and M. Magi, "LiF detectors-Polycapillary Systems as a New Approach for Advanced X-Ray Imaging", *2ND International Conference Frontiers in Diagnostic Technologies*, Frascati, LNF-INFN, 28-30 November 2011, p.80.

54. F. Rondino, M. Falconieri, E. Borsella, R. D'Amato, "Measurements of thermal diffusivity by forced Rayleigh Light Scattering", *10TH European Conference on Nonlinear Optical Spectroscopy (ECONOS 2011)*, Enschede (The Netherlands) 23-25 maggio 2011.

55. E. Borsella, R. D'Amato, M. Falconieri, G. Terranova, "Laser synthesis of nanoparticles: from ceramic nanocomposites to nanofluids", *EuroNanoForum 2011, International Conference*, Budapest (Hungary), 30 maggio-1 giugno 2011.

56. F. Persia, L. Caneve, R. D'Amato, A. Tatì, C. Giancristofaro, G. Ricci, "Performance of nanocomposites as consolidants for artistic marbles", *5TH International Congress "Science and Technology for the Safeguard of Cultural Heritage in the Mediterranean Basin"*, Istanbul (Turkey), 22-25 November 2011.

57. F. D'Annibale, L. Ghidini, A. Mariani, L. Saraceno, E. Borsella, R. D'Amato, J. Cao, C. Schoolderman, "Heat Transfer Coefficient of Water-based SiC and TiO_2 Nanofluids", *NanotechItaly2011, International Conference, Promoting responsible innovation*, Venezia, 23-25 novembre 2011.

58. G. Saviano, F. Felli, S. Bianco, C. Lupi, M. A. Caponero, L. Benussi, D. Piccolo, C. Vendittozzi, "A novel optical fiber sensor for gas temperature monitoring in chemically pollutted environments", *ICST2011 - Fifth International Conference on Sensing Technology*, Palmerston North (New Zealand) 28 November – 1 December 2011

59. G. Saviano, F. Felli, S. Bianco, C. Lupi, M. A. Caponero, L. Benussi, D. Piccolo, C. Vendittozzi, "New magnetic connector for embedding of optical sensors in composite materials", *ICST2011 - Fifth International Conference on Sensing Technology*, Palmerston North (New Zealand) 28 November – 1 December 2011.

60. D. Rinaldis, P. Clemente, M. Caponero, G. Rossi, "Monitoring of a piling wall by means of FBG: Part 2", *SHMII 5 - 5TH International Conference on Structural Health Monitoring of Intelligent Infrastructure*, Cancún, México, 11-15 December 2011

61. D. Rinaldis, P. Clemente, M.A. Caponero, G. Rossi, "Monitoring of a piling wall by means of FBG", *SMAR 2011 - First Middle East Conference on Smart Monitoring, Assessment and Rehabilitation of Civil Structures*, Dubai, Emirates, 8 - 10 February 2011

62. L. Benussi, S. Bianco, M.A. Caponero, S. Colafranceschi, M. Ferrini, F. Felli, L. Passamonti, D. Pierluigi, A. Polimadei, A. Russo, G. Saviano, C. Vendittozzi, "A novel temperature monitoring sensor for gas-based detectors in large HEP experiments",

TIPP 2011 - 2nd International Conference on Technology and Instrumentation in Particle Physics, Chicago, Illinois USA, 8-14 June 2011.

63. C. Vendittozzi, F. Felli, A. Brotzu, G. Saviano, M. A. Caponero, "Use of FBG sensors for the monitoring of cultural heritage structures and monuments", *IGF XXI – XXI Congress of the International Group of Fracture*, Cassino, Italia, 13-15 Giugno 2011.

64. D. Rinaldis e G. Martini, "Seismic microzonation of the Conca di Roio", *4TH International Conference on Experimental Vibration Analysis for Civil Engineering Structures*, Varenna 3-5 Oct. 2011.

65. A. Colombi, E. Di Loreto, A. Orazi, G. Scarascia Mugnozza, S. Martino, L. Salvatori, M. Saroli, M. Albano, G. Martini, A. Paciello, S. Paolini, A. Peloso, V. Verrubbi, "Studi di microzonazione sismica in alcuni comuni del Lazio finanziati con l'OPCM 3907/2010: analisi della metodologia e prime considerazioni", *30° Convegno Nazionale del Gruppo Nazionale di Geofisica delle Terra Solida*, Trieste 14-17/11/2011.

66. A. Zini, D. Rinaldis, A. Pugliese, "Raggruppamento della pericolosità sismica del territorio nazionale attraverso parametri statistici", *12° Convegno Nazionale ANIDIS, Associazione Nazionale Ingegneria Sismica*, Bari 18-22 settembre 2011.

6.3. Invited papers and plenary talks

1. R. Fantoni, M. Ferri De Collibus, G. Fornetti, M. Guarneri, R. Ricci, L. Caneve, F. Colao, L. Fiorani, A. Palucci, M. P. Ortiz "High resolution laser remote imaging innovative tools for preservation of painted surface", *5TH International Congress on Science and Technology for the Safeguard of Cultural Heritage in the Mediterranean Basin*, Instanbul (Turkey), 22 – 25 November 2011.

2. R. Fantoni, S. Almaviva, L. Caneve, F. Colao, V. Spizzichino, M.P.Ortiz "Statistical Approaches in LIBS Data Analysis for Characterization of Cultural Heritage Surfaces" *EMSLIBS Conf.*, 11-15/09/2011, Izmir (Turkey)

3. G.P. Gallerano, "THz and mm-wave imaging as a diagnostic tool for art conservation and environmental studies", *6TH Optoelectroncs and Photonics Winter School - Physics and Applications of T-Rays*, Fai della Paganella, February 20-26, 2011

4. G.P. Gallerano, "Applications biologiques des rayonnements THz: Une revue de la littérature et des manifestations récentes puis un regard vers l'avenir", SFRP, Section Rayonnements Non Ionisants "Effets biologiques et sanitaires des Rayonnements Non Ionisants" 24 Janvier 2011

5. G.P. Gallerano, "Interaction of THz radiation with biological systems: toward a unifying view", Special Session "Terahertz Technologies and Biological Applications", *33RD Annual Meeting of the*

Bioelectromagnetics Society, Dalhousie University, Halifax, Nova Scotia, Canada, June 12 - 17, 2011

6. A. Doria, "Relativistic electrons based THz sources", *6TH Optoelectroncs and Photonics Winter School - Physics and Applications of T-Rays*, Fai della Paganella, February 20-26, 2011

7. R.M. Montereali, "Imaging radiation detectors for nano-bio-photonics based on luminescence of point defects in thin films", *Nanoforum 2011, Micro e Nanotecnologie, VII Edizione*, Università Sapienza, Roma, 14-15 settembre 2011.

8. A. Doria, "Relativistic electrons based THz sources", *6TH Optoelectroncs and Photonics Winter School - Physics and Applications of T-Rays*, Fai della Paganella, February 20-26, 2011

9. G.P. Gallerano, "Biological applications of THz radiation: A review of recent literature & events and a glance to the future", *2ND International THz-Bio Workshop*, Seoul University, 19-20 January 2011 – Plenary Talk

10. G.P. Gallerano, A. Doria, E. Giovenale, G. Messina and I. Spassovsky, "Development of high power mm-wave and THz sources at ENEA for novel biological applications and stand-off detection", *8TH International Workshop "Strong Microwaves and Terahertz Waves: Sources and Applications"*, N. Novgorod, Russia, July 9 - 17, 2011 - Plenary Talk

6.4. Workshops and seminars

1. R.M. Montereali, F. Bonfigli, D. Brogioli, M.A. Vincenti, "Fotodegradazione di film organici di Alq_3 e scrittura diretta in un microscopio confocale laser", *Fotonica 2011, 13° Convegno Nazionale delle Tecnologie Fotoniche*, Genova, 9-11 Maggio, 2011 – ISBN 9788887237122, P18.

2. E. Nichelatti, F. Bonfigli, M.A. Vincenti, R.M. Montereali, "Modello per emissione luminosa da multistrato otticamente attivo applicato a OLED", *Fotonica 2011, 13° Convegno Nazionale delle Tecnologie Fotoniche*, Genova, 9-11 Maggio, 2011 – ISBN 9788887237122, P07.

3. F. Bonfigli, M.A. Vincenti and R.M. Montereali, I. Chiamenti, L.N. Costa and H.J. Kalinowski, L. Dominici and F. Michelotti, A.S.L. Gomes, "Broad-band light-emitting waveguides written in LiF crystals by femtosecond laser", *Fotonica 2011, 13° Convegno Nazionale delle Tecnologie Fotoniche*, Genova, 9-11 Maggio, 2011 – ISBN 9788887237122, P29.

4. M.A. Vincenti, F. Bonfigli, D. Brogioli, and R.M. Montereali, "Confocal laser microscope writing of micro-patterns in broad-band light-emitting organic and insulating thin films", *Abstract 4TH EOS Topical Meeting on Optical Microsystems (OμS'11)*, 25TH-28TH September 2011, Capri, Italy, ISBN 978-3-00-033710-9.

5. D. Hampai, S.B. Dabagov, F. Bonfigli, R.M. Montereali, L. Allocca, L. Marchitto, S. Alfuso, G. Della Ventura, F. Bellatreccia and M.

Magi, "High resolution x-ray imaging based on Polycapillary Optics", *4TH International Workshop on Imaging Techniques with Synchrotron Radiation, ITSR2011*, Bordeaux (F), 24-27 Settembre 2011.

6. F. Bonfigli, T. Baumbach, A. Cecilia, S. Heidari Bateni, D. Pelliccia, F. Somma, P. Vagovic, E. Hamann, M.A. Vincenti and R.M. Montereali, "First white beam X-ray imaging experiments with lithium fluoride detectors at the TOPO-TOMO beamline of the ANKA synchrotron", *3RD ANKA/KNMF Joint Users' Meeting,* 13TH-14TH October 2011, p. 88.

7. F. Bonfigli and R.M. Montereali, "Confocal fluorescence imaging of light-emitting nano and micro photonic devices", *4TH Mediterranean Conference on Nano-Photonics, MediNano4* (Roma, 24-25 ottobre 2011), p.43.

8. E. Nichelatti, F. Bonfigli, R.M. Montereali, M.A. Vincenti, "Light emission from a volume source in a multilayer: analytical model", *4TH Mediterranean Conference on Nano-Photonics, MediNano4* (Roma, 24-25 ottobre 2011), p.43.

9. F. Bonfigli, G. Campurra, R.M. Montereali, M.A. Vincenti, "Fluoruro di Litio: anche l'imaging in fotoluminescenza oltre la dosimetria?", *Congresso Società Italiana di Medicina del Lavoro ed Igiene Industriale, SIMLII*, Torino, 16-19 Novembre 2011, Centro Congressi Lingotto, http://www.simlii.net/joomla_simlii/.

10. S. Righi, B. Salieri, A. Pasteris, E. Borsella, R. D'Amato, "The effect factor for nano TiO_2: preliminary toxicity tests on Daphnia magna and future developments", *SETAC Europe 21ST Annual Meeting, Ecosystem Protection in a Sustainable World: A Challenge for Science and Regulation*, Milano 15-19 may 2011.

11. R. Capobianco, M. Caponero, A. Polimadei, A. Caratelli, U. Iannıruberto, G. Puglisi, "Uso di sensori FBG per il monitoraggio della cura di getti di calcestruzzo", *Fotonica 2011, 13° Convegno Nazionale delle Tecnologie Fotoniche*, Genova, 9-11 Maggio, 2011 – ISBN 9788887237122,Genova, Italia,

12. M.A Caponero, "Controllo e verifiche statiche di strutture murarie con tecnologia in fibra ottica, *DNA. Italia – Tecnologia Cultura Economia per il Patrimonio*, Torino, Italia 3-5/nov/2011.

13. G. Martini, "Microzonazione sismica della Conca di Roio", *Seminario GLISS "Ricostruire L'Aquila in sicurezza con l'isolamento ed altri sistemi antisimici"*, Università dell'Aquila, 10-11 giugno 2011.

14. L. Teodori, "Disputationes on Tissue Engineering", India 2011.

6.5. Technical reports

1. D. Poreh, L. Fiorani, F. Colao, A. Palucci, "LIDENEA: a software tool for LIDAR data analysis Technical Reports of the Italian National Agency for New Technologies", *Energy and Sustainable Economic Development* (ISSN* 0393-3016), Rome, Italy (2011)

2. L. Fiorani, D. Poreh, M. Guarracino, F. Colao, A. Palucci, "Comparison between satellite and lidar data in the Arctic Sea Technical Reports of the Italian National Agency for New Technologies", *Energy and Sustainable Economic Development* (ISSN* 0393-3016), Rome, Italy (2011)

3. L. De Dominicis, M. Ferri de Collibus, G. Fornetti, M. Guarneri, M. Nuvoli, R. Ricci, L. Bartolini, M. Francucci, "Theoretical determination of total power backscattered by a Lambertian flat target with constant reflectivity immersed in a stratified homogeneous medium for an amplitude-modulated laser system", *ENEA*, RT/2010/47/ENEA, ISSN/0393-3016 (January 2011).

4. R. Ricci, M. Francucci, L. De Dominicis, M. Ferri de Collibus, G. Fornetti, M. Guarneri, M. Nuvoli, "Methods for optical noise rejection in an amplitude-modulated laser optical radars for underwater three-dimensional imaging". *Energia, Ambiente e Innovazione* (bimestrale ENEA), anno 57 (gennaio – aprile 2011), 67– 73.

5. L. Caneve, F. Colao, F. Arci, "Studio di marmi e consolidanti di interesse artistico mediante fluorescenza indotta da laser", *ENEA Report* RT/2011/13/ENEA, ISSN/0393-3016.

6. A. Lai, L. Addari, "The Phytoplankton biomass quantitative analysis by Spectrophotometric method" RT/2011/18/ENEA.

7. F. Colao, L. Caneve, L. Fiorani, A. Palucci, R. Fantoni, M. P. Ortiz, M. A. Gómez, M. A. Vázquez, "Report on LIF measurements in Seville - Part 1: San Telmo chapel", *ENEA RT 2011* (in press).

8. F. Colao, L. Caneve, L. Fiorani, A. Palucci, R. Fantoni, M. P. Ortiz, M. A. Gómez, M. A. Vázquez, "Report on LIF measurements in Seville - Part 2: Santa Ana church", *ENEA RT 2011* (in press).

9. M.A. Vincenti, F. Bonfigli, R.M. Montereali, A. Rufoloni, F. Basoli, E. Di Bartolomeo, S. Licoccia, E. Nichelatti, "Crescita e caratterizzazione di film sottili per diodi organici emettitori di luce", *Rapporto Tecnico ENEA* (2011), in stampa.

10. F. Bonfigli, M.A. Vincenti, R.M. Montereali, L. Caneve, S. Almaviva, "Caratterizzazione di film sottili di Alq_3 e LiF mediante misure LIBS e microscopia ottica", *Rapporto Tecnico ENEA* (2011), in stampa.

11. E. Borsella, R. D'Amato, F. Fabbri, M. Falconieri, G. Terranova, "Synthesis of nanoparticles by laser pyrolysis: from research to application", *Rivista ENEA Energia Ambiente e Innovazione*, luglio 2011.

12. De Blasi, S. Bollanti, P. Di Lazzaro, F. Flora, L. Mezi, D. Murra, A. Torre, F. Bonfigli, R.M. Montereali, M.A. Vincenti, C. Ricciardi, D. Tabuani, "Trattamenti per l'agroalimentare", *Trattamenti e Finiture, Nanotecnologie* (2011) 34-38.

13. P. Di Lazzaro, D. Murra, E. Nichelatti, A. Santoni, G. Baldacchini, "Colorazione similsindonica di tessuti di lino tramite radiazione nel lontano ultravioletto: riassunto dei risultati ottenuti presso il Centro ENEA di Frascati negli anni 2005 -2010" *RT/2011/14/ENEA* (2011)

The cover images were acquired and processed by the RGB-ITR system
at the Lodge of the Amore and Psyche at Villa Farnesina (Rome).

The activity was carried out by team UTAPRAD Metrology:
Mario Ferri De Collibus, Giorgio Fornetti, Massimo Francucci, Luigi De Dominicis,
Massimiliano Guarneri, Marcello Nuvoli, Roberto Ricci.

ITALIAN NATIONAL AGENCY FOR NEW TECHNOLOGIES,
ENERGY AND SUSTAINABLE ECONOMIC DEVELOPMENT

Unità Tecnica
di sviluppo
di Applicazioni
delle Radiazioni

utaprad